SANDIA REPORT
SAND2020-2609
February 2020

Sandia National Laboratories

Assessment of the MACCS Code Applicability for Nearfield Consequence Analysis

Daniel J. Clayton, Nathan E. Bixler

Prepared by
Sandia National Laboratories
Albuquerque, New Mexico
87185 and Livermore,
California 94550

Issued by Sandia National Laboratories, operated for the United States Department of Energy by National Technology & Engineering Solutions of Sandia, LLC.

Available to DOE and DOE contractors from
U.S. Department of Energy
Office of Scientific and Technical Information
P.O. Box 62
Oak Ridge, TN 37831

Telephone: (865) 576-8401
Facsimile: (865) 576-5728
E-Mail: reports@osti.gov
Online ordering: http://www.osti.gov/scitech

Available to the public from
U.S. Department of Commerce
National Technical Information Service
5301 Shawnee Rd
Alexandria, VA 22312

Telephone: (800) 553-6847
Facsimile: (703) 605-6900
E-Mail: orders@ntis.gov
Online order: https://classic.ntis.gov/help/order-methods/

ABSTRACT

Three codes are used for comparisons in this report to evaluate the adequacy of MACCS in the nearfield, AERMOD, ARCON96 and QUIC. Test cases were developed to give a broad range of weather conditions, building dimensions and plume buoyancy. Based on the comparisons of MACCS with AERMOD, ARCON96 and QUIC across the test cases, the following observations are made:

- MACCS calculations configured with point-source, ground-level, nonbuoyant plumes provide nearfield results that bound the centerline, ground-level air concentrations from AERMOD, ARCON96, and QUIC.
- MACCS calculations with ground-level, nonbuoyant plumes that include the effects of the building wake (area source) provide nearfield results that bound the results from AERMOD and QUIC and the results from ARCON96 at distances >250 m.
- If using a point-source is too conservative and it is desired to bound the results from all three codes, another alternative is to use area source parameters in MACCS that are less than the standard values, i.e., an area source intermediate between the standard recommendation and a point source.

All these options provide results from MACCS that are bounding for the test cases evaluated. Based on these observations, it appears that MACCS is adequate for use in nearfield calculations, given the correct parameterization.

This work was sponsored by the U.S. NRC's Office of Nuclear Regulatory Research under contract number NRC-HQ-60-15-T-0006.

This page left blank

CONTENTS

LIST OF FIGURES

LIST OF TABLES

ACRONYMS AND DEFINITIONS

Abbreviation	Definition
AERMOD	American Meteorological Society / Environmental Protection Agency Regulatory Model
AMS	American Meteorological Society
ARCON96	Atmospheric Relative Concentrations in Building Wakes
ATD	Atmospheric Transport and Dispersion
CFD	Computational Fluid Dynamics
X/Q	Normalized, ground-level, time-integrated air concentration
DOE	Department of Energy
EPA	Environmental Protection Agency
LES	Large Eddy Simulation
LWR	Light Water Reactor
MACCS	MELCOR Accident Consequence Code System
NRC	Nuclear Regulatory Commission
OpenFOAM	Open Source Field Operation and Manipulation
PNNL	Pacific Northwest National Laboratory
PRIME	Plume Rise Model Enhancements
QUIC	Quick Urban and Industrial Complex
RANS	Reynolds-Averaged Navier Stokes

This page left blank

1. INTRODUCTION

In the context of dispersion, nearfield is commonly defined as being over distance scales from those of individual buildings up to those of neighborhoods [1]. For this report, nearfield is defined to be distances for which the standard Gaussian plume and puff models have been questioned, and this is interpreted to be distances of less than about 0.5 km, as explained below.

The Nuclear Regulatory Commission (NRC) developed a non-Light Water Reactor (LWR) vision and strategy report that discusses computer code readiness for non-LWR applications [2]. The adequacy of the MELCOR Accident Consequence Code System (MACCS) [3] in the nearfield is discussed in that report. MACCS currently includes a simple model for building wake effects. The MACCS2 User's Guide [4] suggests that this simple building wake model should not be used at distances closer than 0.5 km. This statement raises the question of whether MACCS can reliably be used to assess nearfield doses, i.e., at distances less than 500 m. Nonetheless, the Department of Energy (DOE) uses MACCS to conservatively estimate doses to collocated workers at 100 m by assuming no building wake effects (point source release) and ground-level releases. Other codes based on Gaussian plume models are commonly used to estimate nearfield doses by using corrections that are intended to skew the results toward conservatism or at least toward a best estimate, depending on the purpose for the model.

Conservatism in the context of this report is based on centerline, ground-level air concentration, which translates to other results that are proportional to or depend directly on this concentration. Calculating higher centerline, ground-level air concentrations does not necessarily translate to higher values for other consequence metrics. For example, total population dose depends not only on the ground-level air concentration, but also the locations of population centers relative to the wind direction.

Methods to estimate atmospheric transport and dispersion (ATD) in the nearfield fall into four categories: (1) field measurements, (2) wind-tunnel measurements, (3) particle tracking based on computational fluid dynamics (CFD) or simplified models to estimate the wind flow around and between buildings, and (4) empirical models. Some models bridge these categories. This report focuses on modeling approaches, as opposed to experimental approaches, to estimate nearfield air concentrations and ground deposition. However, most of the models discussed in this report have been compared with nearfield measurements to provide a perspective on the accuracy and uncertainty of the modeling approaches.

A major focus of this report is to evaluate whether MACCS can be used to assess nearfield consequences. MACCS is a highly flexible tool and the user can choose whether to model a variety of physical phenomena, including such things as building wake effects, plume buoyancy, and plume meander. Furthermore, the user has flexibility in choosing how to model the Gaussian dispersion parameters. So, a second focus of this report goes beyond the question of whether MACCS can be used in the nearfield to the related question of how can MACCS be used to generate results that are bounding of other codes intended for nearfield analysis. How to best use MACCS in the nearfield is a more complex question that touches on the uncertainty inherent in ATD models and on the degree of conservatism that is desirable for regulatory applications. This report discusses the inherent uncertainties of ATD models in Section 2 by describing validation that has been performed against nearfield data. However, this report does not attempt to address the level of conservatism that is desirable for regulatory applications.

1.1. Background

The technical issue of nearfield modeling using a Gaussian plume model is not new. A summary of nearfield ATD models including building wake effects was documented for the NRC by Simpkins [5]. This summary shows results with different methods varying by multiple orders of magnitude. An evaluation of the technical bases for the atmospheric dispersion parameter, X/Q, used to calculate of onsite doses at 100 m was conducted by DOE [6]. They found that the current methodology provides a conservative estimate of X/Q at 100 m. A review of the ATD modeling for environmental radiation dose assessments at the Savannah River Site was conducted [7], which included a discussion of the validity of MACCS calculations at short distances. In the discussion of the validity of MACCS at short distances, a recommendation is made in [7] to use an area source rather than a point source to estimate doses.

1.2. Objective

To address the question of whether MACCS can reliably be used to assess nearfield doses, i.e., at distances less than 500 m, an evaluation of modeling approaches to estimate nearfield air concentrations and depositions was performed. Several candidate methods were ranked for comparison and potential incorporation into the MACCS code. In this report, it is assumed that the results from the selected codes are all adequate in the nearfield, which is reasonable because these codes are specifically intended to be used in the nearfield. Hence, by comparing the results of these codes to the results from MACCS, the adequacy of MACCS for assessing exposures in the nearfield can be evaluated.

1.3. MACCS Overview

MACCS has traditionally modeled dispersion during downwind transport using a Gaussian plume segment model. Thus, the crosswind and vertical extent of each plume segment is expressed in terms of crosswind (σ_y) and vertical (σ_z) standard deviations of the normal concentration distributions that characterize a Gaussian plume. The Gaussian equations implemented in MACCS are derived assuming that turbulent velocities are negligible compared with the mean wind speed.

During downwind transport, atmospheric turbulence causes plume segments to expand in all directions with the rate of expansion increasing when atmospheric turbulence increases. Vertical expansion of a plume is enhanced by larger values of surface roughness and constrained by the ground and by the temperature structure of the atmosphere (location of inversion layers). Crosswind spreading of the plume along the y-direction is unconstrained. The effective crosswind dimensions of a plume segment are increased by lateral meander of the plume about its centerline trajectory. Because turbulent velocities are almost always small compared to the mean wind speed that transports the bulk plume, expansion in the wind direction can be neglected.

Several parameterizations are available for estimating dispersion coefficients for use with MACCS. The dispersion model parameters in MACCS are under the control of the user. MACCS should be configured by the user in an appropriate manner. For the analyses in this report, the parameterization of Eimutis and Konicek [8] is used for σ_y and σ_z and implemented via a lookup table. The lookup table parameters are documented in Napier et al. [7] and are also shown in the MACCS input files in Appendix C.

Wind shifts that can occur at time intervals less than that of the recorded weather data can result in an apparent dispersion that is greater than would be computed using dispersion curves based on

measurements over a shorter time period. The apparent increase in crosswind dispersion can be significant under stable, low-wind speed conditions. This effect is known as plume meander. Adjustment of the crosswind plume dimensions to account for plume meander can be handled in a variety of ways in MACCS. The model used in the analyses in this report is based on NUREG/CR-2260 [9] and Regulatory Guide 1.145 [10] and accounts for the observation that the impact of plume meander depends on stability class and wind speed. This model is selected by setting the value of the MACCS parameter MNDMOD to "NEW", as shown in the MACCS input files in Appendix C.

The model for building wake effects included in MACCS scales the initial dimensions of the plume based on the dimensions of the building or complex of buildings from which the pollutants are emitted. The standard guidance is to assume that ground-level concentrations at the edges of the building and the concentration directly above the centerline at the top of the building are 10% of the centerline plume concentration. This guidance translates into assuming σ_y = 0.23 x building width and σ_z = 0.47 x building height immediately downstream of the building. This model is selected by setting the values of σ_y and σ_z based on the building dimensions and is shown in the MACCS input files in Appendix C.

This page left blank

2. RANKING OF CANDIDATE MODELS

A basis for ranking candidate methods is described in this section. Subsequently, a set of candidate methods, CFD models (Open Source Field Operation and Manipulation (OpenFOAM) [11]), simplified wind-field models (Quick Urban and Industrial Complex (QUIC) dispersion modeling system [12]), and modified Gaussian models (Atmospheric Relative Concentrations in Building Wakes (ARCON96) program [13] and American Meteorological Society / Environmental Protection Agency Regulatory Model (AERMOD) program [14]) are evaluated against the criteria. The candidate models are not exhaustive but include a set of options that span the range from complex to simple. The results from the ranking are described subsequently.

2.1. Criteria

A set of ranking criteria are shown in Table 2-1. Following the table, each criterion is discussed in turn along with a numerical scale to evaluate the criterion.

Table 2-1. Criteria for Ranking Candidate Models for Nearfield ATD

	Model Characteristics					
Model	**Simplicity**	**Efficiency**	**Validation**	**Conservative Bias**	**Community Acceptance**	**Ease of Implementation**

Each of the model characteristics and evaluation criteria are defined as follows:

- Simplicity is a measure of the time and effort required to set up a model for a specific application. A score of 1 is simplest; 3 is most complicated.
- Efficiency is a measure of the computing resources required to run a problem once it has been set up. A score of 1 is most efficient; 3 is least efficient.
- Validation is a measure of the magnitude of errors between the model and either experimental data or a state-of-the-art analysis method, as established by documented evidence. A score of 1 is most accurate compared with data; 3 is least accurate. Lack of documented evidence of validation is not acceptable and disqualifies the candidate model. (It would require a significant effort to validate a model for which no documentation exists, but this could be done if a model is otherwise highly ranked but lacks adequate documented validation.)
- Conservative bias is a measure of the likelihood that results are on the higher side of experimental data or state-of-the-art analysis, i.e., predicts higher peak doses. A score of 1 means a model is usually conservative; 2 means it is neither conservative nor nonconservative; 3 means it is usually nonconservative.
- Community acceptance is a measure of whether a method is commonly used and accepted for applications that support decision making. A score of 1 means highly accepted by the community; 3 means few or no precedents of use and acceptance by the community.
- Ease of implementation is a measure of the effort required to integrate the model with MACCS. A score of 1 means relatively little effort is required to implement; 3 means a significant effort is required to implement.

A score of 1 for each model characteristic is best; a score of 3 is worst. Likewise, a method that scores mostly 1s is ranked highest while a method that scores mostly 3s is ranked lowest.

2.2. CFD Models

CFD models are generally considered to be the gold standard in terms of accuracy; however, accuracy comes at a significant price in terms of simplicity, efficiency, and ease of implementation. CFD models are commonly divided into two categories: (1) Reynolds-averaged Navier Stokes (RANS) and (2) large eddy simulation (LES) [1]. RANS-based CFD calculations usually employ the k-ε model for turbulence, which is known for its robustness, economy, and reasonable accuracy. LES is generally considered superior in terms of accuracy but requires more computing time than RANS. LES is especially advantageous for modeling flow around bluff bodies, like most buildings, that tend to shed large vortices. A commonly used code that implements both RANS and LES models is OpenFOAM [11].

For either of these CFD models, a grid and boundary conditions must be established for each facility. Furthermore, a large set of wind directions, speeds, and turbulence characteristics must be evaluated to determine nearfield air concentrations for the variety of weather situations that could occur. The effort required to perform the CFD calculation must be repeated for each unique facility requiring a consequence analysis.

CFD models are mechanistic models (based on first principles) that should accurately represent real wind flows. However, CFD models of wind fields suffer from two major types of approximation error: (1) discretization error from finite grid dimensions and (2) model error from the use of a turbulence model. Other parameter choices also contribute to uncertainty in the results. Because of this, best practice is to validate a CFD model against experimental wind-field measurements for a specific building configuration [1]; however, in practice, such experimental data are rarely available. Short of experimental data for validating a CFD model, discretization error can be evaluated by refining the computation grid. Errors introduced by a specific choice of turbulence model and other input parameters are more difficult to quantify. Nonetheless, a careful calculation based on CFD is generally considered to provide reasonably accurate results.

2.3. Simplified Wind-Field Models

Simplified wind-field models employ various techniques to generate wind fields quicker than CFD models. QUIC is a code with two options to generate a wind field. Either option can be used to estimate concentrations via particle tracking. The first option, called QUIC-URB, is an empirical method that generates a mass-consistent wind field and accounts for upwind recirculation zones, downwind cavities and wakes, and canyon areas between buildings. The second option, called QUIC-CFD, is a RANS CFD model using a simple (algebraic) turbulence formulation based on Prandtl's mixing length theory. Following estimation of the wind field via QUIC-URB or QUIC-CFD, QUIC-PLUME is used to estimate air concentrations using a Lagrangian, random-walk, dispersion model.

Like the CFD approaches described above, QUIC requires a model of each unique facility to be developed. For each facility, a large set of wind directions and speeds need to be evaluated to characterize the variety of weather situations that could occur.

QUIC has been evaluated against two sets of experimental measurements: Salt Lake City URBAN 2000 Tracer Experiment [15] and the Joint Urban 2003 field experiment in Oklahoma City [16]. Both references employ the QUIC-URB empirical model for estimating the wind field combined with QUIC-PLUME for evaluating dispersion. Reference [15] shows that the original version of QUIC-URB combined with QUIC-PLUME generates concentrations that are usually within a factor of 5 and almost always within a factor of 10 of the nearfield measurements from the URBAN 2000

tracer experiment. Reference [16] shows that the updated version of QUIC-URB provides a noticeable improvement over the original version, but the predicted concentrations can still differ by more than a factor of 5 from the observations. No report was found that shows a validation of the results using a combination of the QUIC-CFD and QUIC-PLUME models. In principle the QUIC-CFD model should be more accurate than the QUIC-URB model.

2.4. Modified Gaussian Models

Straight-line Gaussian plume models have been used extensively to model ATD. Over the years, researchers have proposed modifications to the Gaussian models to account for various phenomena. Two codes that use modified equations for a Gaussian plume are described in this subsection. The first is ARCON96, which was developed by Pacific Northwest National Laboratory (PNNL) for the NRC to be used for estimating air concentrations at ventilation intakes for control room habitability during a design basis accident. The second is AERMOD, which was developed by the American Meteorological Society (AMS) and the Environmental Protection Agency (EPA) for estimating environmental pollution levels.

2.4.1. ARCON96

ARCON96 is a straight-line Gaussian plume model (like MACCS) but with modifications to account for enhanced dispersion near a building at low and high wind speeds [13]. At low wind speeds, building wakes have a minimal effect and the major contributor to enhanced dispersion is plume meander. At high wind speeds, building wakes are the major contributor to enhanced dispersion. The modifications to the standard equations for Gaussian dispersion and their basis are described in Ramsdell and Fosmire [17]. The basic concept is to replace the standard formulation for the Gaussian dispersion parameters by a three-term equation:

$$\Sigma = (\sigma_0{}^2 + \Delta\sigma_1{}^2 + \Delta\sigma_2{}^2)^{1/2}$$

Where

σ_0 = standard function for Gaussian dispersion

$\Delta\sigma_1$ = additional dispersion from low-wind-speed phenomena, primarily plume meander

$\Delta\sigma_2$ = additional dispersion from high-wind-speed phenomena, primarily wake effects

Σ = combined dispersion parameter to be used in Gaussian plume equation

The equation above represents both crosswind (y) and vertical (z) dispersion parameters, which are usually represented with an additional subscript of y or z that are not shown.

Reference [17] shows a comparison of the ARCON96 model predictions (shown as Revised Model) with observations in Figure 7. Table 1 of Reference [17] summarizes the statistics as follows:

- Median ratio of predicted to measured concentrations 1.51
- Minimum ratio 0.010
- Maximum ratio 166.
- Predicted concentrations within a factor of 2 of measured value 27.4%
- Predicted concentrations within a factor of 4 of measured value 53.8%
- Predicted concentrations within a factor of 10 of measured value 84.2%

The first statistic indicates that the model has a modest conservative bias, but the second and third statistics indicate that the error is similar in both the conservative and anticonservative directions. Predicted values can be about a factor of 100 above and below measured values and are clearly significantly larger than those for the QUIC model, which are more like a factor of 10, as discussed below. On the other hand, the ARCON96 model is very simple and easy to implement compared with the QUIC model. Unlike the OpenFOAM and QUIC approaches described above, the ARCON96 approach does not require that each individual facility be modeled to assess building wake effects. Instead, algebraic equations are used that apply to all sites over the full range of weather situations.

2.4.2. AERMOD

AERMOD [14] uses a simple approach for plume meander, which involves a weighted average of uniform dispersion in all directions (for an average wind velocity of zero) and the standard Gaussian dispersion equation. The weighting fractions for the two terms depends on mean wind speed and the random component of wind speed.

AERMOD contains a treatment of building downwash to account for wake effects that is significantly more complex than the one in ARCON96. Similar to the AERMOD equations for plume meander, the equations for building downwash use a weighted average of concentrations within the building wake and a standard Gaussian plume concentration. The weighting factor depends on the ratios of distance from the downwind edge of the building to the downwind extent of the building wake, of distance from the centerline of the building to the width of the building wake, and of the distance above ground to the height of the building wake. The reader is referred to Schulman et al. [18] for a detailed description of the building downwash model.

Reference [18] provides several validation results for the AERMOD building downwash model. The first is for a neutrally-buoyant release into a building wake performed in a wind tunnel. Beyond 1.5 building heights downwind, the AERMOD prediction follows the wind-tunnel results. Two other comparisons are provided based on field tests, the Alaska North Slope and the Bowline Point Power Plant Field Studies. Both are for releases from stacks above the buildings. Results are provided on a quantile-quantile plot, so the data points may correspond to different prediction and observation times. In one case, the agreement is within about 25%; in the other case, the agreement is within about a factor of 5.

Reference [19] compares AERMOD, with and without the building wake option (called PRIME, Plume Rise Model Enhancements), along with two other dispersion codes, against a set of field data from a tracer experiment at the CE-CERT facility. The main results are presented as quantile-quantile plots and show that AERMOD using the PRIME model tends to overpredict, by up to a factor of about 3, at higher concentrations and under predict, by up to a factor of about 5, at lower concentrations. On the other hand, AERMOD using a simple area source without the PRIME model falls within a factor of 2 of the observations over nearly the entire range of concentrations. The authors point out that one source of error at higher concentrations is that AERMOD switches off its plume meander model when the PRIME model is used. (This deficiency may have been addressed in AERMOD after this article was published, but in any case, it could be addressed in MACCS if it were implemented there.)

Either with or without the PRIME model, AERMOD results appear to be significantly more accurate than those for ARCON96; however, the apparent accuracy of the AERMOD results may be enhanced by the quantile-quantile plots used to display the results as opposed to the direct

comparison of results used to display the results for ARCON96. Like ARCON96, the AERMOD models for plume meander and building wake effects are algebraic and can be applied to all sites under all weather conditions without significant, additional computational effort.

2.5. Ranking Results

The ARCON96 models for plume meander and wake effects would be easy to implement in the current MACCS framework since both models are very simple and the underlying Gaussian models are essentially the same in the two codes. Validation of the ARCON96 model shows that most of the results are within a factor of 10 of observations but some results differ by as much as a factor of 100. ARCON96 has a modest conservative bias, but it is not obvious that average results over a year of weather data would necessarily be conservative using the ARCON96 model.

AERMOD uses a distinctly different treatment for both plume meander and building wake effects than ARCON96. The plume meander model is relatively simple to implement but the building downwash model is more complex. Nonetheless, the model is entirely algebraic and could be implemented within the MACCS code rather than requiring any preprocessing outside of MACCS, as would be needed for the OpenFOAM and QUIC options. Validation of the AERMOD models indicates that its accuracy is within a factor of 5 compared with wind tunnel and field experimental data. However, it may be misleading to compare the quantile-quantile presentation of results for AERMOD with the direct presentation of results for ARCON96.

Table 2-2 contains a set of quantifications for each of the model characteristics of the four models discussed above. Two of the model options, OpenFOAM and QUIC, would be relatively difficult to implement and would place considerable burden on the user to evaluate nearfield consequences at a specific site. The other two model options are simpler to implement and place a relatively small burden on the user to evaluate a specific site. The AERMOD model appears to fit experimental results closer than ARCON96, but it would be more difficult to implement. Nonetheless, it would be much simpler to implement than either the OpenFOAM or QUIC option.

Table 2-2. Evaluation of Model Characteristics for Four Model Options

	Model Characteristics					
Model	**Simplicity**	**Efficiency**	**Validation**	**Conservative Bias**	**Community Acceptance**	**Ease of Implementation**
OpenFOAM	3	3	1	2	1	3
QUIC	3	2	1	2	2	3
ARCON96	1	1	2	2	1	1
AERMOD	1	1	1	2	1	2

Based on these rankings, three codes are used for comparisons in this report to determine the adequacy of MACCS in the nearfield, ARCON96, AERMOD and QUIC. ARCON96 and AERMOD were selected due to the results of the ranking and ease of implementation. QUIC, using the QUIC-URB method, was also selected for use in the comparison due to its validation and intermediate computational cost. OpenFOAM was not selected due to the high computational cost and difficulty in implementing into MACCS. In this report, it is assumed that the results from ARCON96, AERMOD and QUIC are all adequate in the nearfield. This assumption is based on the fact that each of these codes are intended to be used in the nearfield and also that each has been validated at short downwind distances. Hence, by comparing the results of these codes, the adequacy

of MACCS for assessing exposures in the nearfield can be evaluated, which is the objective of this report.

3. TEST CASES

Test cases were developed to provide a broad range of conditions for this evaluation. The highlighted characteristics of the test cases are weather conditions, building dimensions and plume buoyancy. The test cases are not intended to be exhaustive, but rather to represent the range of potential conditions.

3.1. Assumptions and Limitations

The test cases consider isolated, simple buildings. This report does not attempt to discuss the application of MACCS to clusters of buildings or complex building shapes. For more information on idealized clusters of buildings and potential models, the reader is directed to Hosker and Pendergrass [20]. It is assumed that the comparison of the results for the test cases with isolated simple buildings provides a basis for determining the adequacy of MACCS in the nearfield.

For all the test cases, a surface roughness of 3 cm is used to represent grassy fields surrounding the building. This was selected to reduce potential dispersion in the vertical direction and potentially highlight differences between models. Winds are assumed to be perpendicular to the building face of larger dimension. The release location is assumed to be the top center of the downwind face of the building (20 m).

Two weather conditions were chosen. The first condition is a constant wind field of 4 m/s with neutral stability (Pasquill-Gifford stability class D). This condition was selected as a typical weather condition for comparison. The second condition is a constant wind field of 2 m/s with stable conditions (Pasquill-Gifford stability class F). This weather condition was selected as a reduced dispersion condition that would result in higher ground-level concentrations and potentially highlight differences between models. Because nearfield doses are commonly evaluated at the 95th percentile for licensing applications, the weather conditions that were chosen are biased toward the stable end of the range to represent the ones more likely to represent a 95th percentile exposure.

For building dimensions, three configurations were chosen. The first configuration includes a building 20 m tall, 40 m wide and 20 m deep and was selected to represent a typical building size. The second configuration includes a building 20 m tall, 100 m wide and 20 m deep and was selected to represent a building with a more extreme width to height ratio. The third configuration has no building, but rather is an elevated point source (20 m) and was selected to evaluate basic differences in dispersion models between the codes in the absence of confounding factors.

For the buoyancy condition, two variations were chosen, with and without buoyancy. For the cases with buoyancy, a plume energy content of 5 MW is used. These variations were chosen to evaluate the interactions between plume rise models and building wake models used in the four codes.

The combination of the two weather conditions, three building configurations and two buoyancy variations results in twelve test cases. Each of the codes are evaluated to determine how to best analyze each of the test cases based on the modeling options available with each code. The twelve test cases are shown below in Table 3-1.

Table 3-1. Test cases used for comparison with MACCS

Weather/Energy Content	Building HxWxL (m)		
	20x100x20	20x40x20	None
4 m/s, D stability, 0 MW	Case01	Case05	Case09
2 m/s, F stability, 0 MW	Case02	Case06	Case10
4 m/s, D stability, 5 MW	Case03	Case07	Case11
2 m/s, F stability, 5 MW	Case04	Case08	Case12

The native treatment of the weather, building, and buoyancy differs between the codes. The following sections discuss how the variations were implemented in each code. The discussions include the techniques used to ensure consistency in the implementation. Example input files for AERMOD, ARCON96, MACCS and QUIC are provided in Appendices A through D for reference.

3.2. Weather Conditions

ARCON96 and MACCS require a specification of the mean wind speed and direction and Pasquill-Gifford stability class. Thus, implementation of the specified weather conditions is straightforward for these two codes. These values are shown in the input files for ARCON96 and MACCS in Appendices B and C.

For AERMOD, the specification of weather conditions is through both a surface-weather parameter file and a vertical-profile weather parameter file. Specification of the wind speed and direction is straightforward, but there is no direct method for specifying a stability class. The weather parameters in the AERMOD input weather files related to stability class are the friction velocity (u*) and Monin-Obukhov length (L). Golder [21] contains a figure relating Pasquill-Gifford stability class and Monin-Obukhov length (see Figure 4 in [21]). This figure shows a range of values for 1/L that correspond to each stability class. The estimated value for D stability class was chosen to be near the center of the range, while the estimated value for F stability was chosen to be a similar distance from the line separating class E and F as the center of the range for class E. These estimates were selected in this manner to represent a nominal value of the range of values. Using a surface roughness (z_0) of 3 cm, values for 1/L were estimated for stability classes D and F to be 0.002 m^{-1} and 0.08 m^{-1}, respectively, which corresponds to values of 500 m and 12.5 m for L, respectively.

Hanna et al. [22] provide equations for calculating friction velocity (u*) from wind speed (u), surface roughness (z_0) and Monin-Obukhov length (L) for neutrally-stable and stable conditions, shown below.

$$u^* = k\,u / \ln(z/z_0) \qquad \text{for neutral stability}$$

$$u^* = k\,u / [\ln(z/z_0) + 5\,z/L] \qquad \text{for stable conditions}$$

Where

k = empirical constant (0.4 unitless), and

z = height that correlates to wind speed determination (10 m).

Using the above equations, the friction velocities for the 4 m/s with D stability class and 2 m/s with F stability class are calculated to be 0.275 m/s and 0.082 m/s, respectively. These values for Monin-Obukhov length and friction velocity were used in the AERMOD weather files for the analyses and are shown in Appendix A.

For QUIC, weather conditions are specified by setting wind speed and direction, with a wind speed profile as a function of height, and setting a value for 1/L. The wind speed profile was selected by using the values obtained from Golder [21] of 1/L (0.002 m^{-1} and 0.08 m^{-1}) and setting the wind speed at a 10 m to 4 m/s or 2 m/s, respectively. For comparison with the values calculated with the equations from Hanna et al. [22], an average friction velocity is calculated during QUIC execution. Using the values above for the weather conditions, friction velocity values of 0.271 m/s and 0.083 m/s were calculated by QUIC. Note that the friction velocity values calculated by QUIC are very similar to those calculated with the equations from Hanna et al. [22]. The weather parameters used for QUIC are shown in Appendix D.

A ground-level, point-source release for each weather condition was evaluated with each code. This was done to ensure weather conditions were implemented correctly, as well as to evaluate differences in dispersion modeling in the four codes. Figure 3-1 and Figure 3-2 show the normalized, ground-level, time-integrated air concentrations (X/Q) for the neutrally stable (4 m/s, D stability class) and stable (2 m/s, F stability class) weather conditions, respectively, using the weather parameters specified above and the nominal dispersion mode for each code.

Examining Figure 3-1 and Figure 3-2 shows that the results differ significantly between the four codes. The trends are that the concentrations predicted by QUIC are largest (least dispersive) and those predicted by ARCON96 are smallest (most dispersive) for both weather conditions. QUIC can also generate concentration profiles along specified planes. The time-averaged air concentrations at a height of 1 m for the neutrally-stable and stable weather conditions are shown in Figure 3-3, which shows that the concentrations at the center of the plumes appear well defined. Based on the results in Figure 3-3, the differences between the QUIC results and those of the other codes does not appear to be due to the setup of the QUIC calculations.

One possible cause for the differences is the treatment of meander in the codes. To investigate this possibility, the meander model for each code was examined. Both ARCON96 and MACCS allow for calculations without including a meander model. The meander model in AERMOD is fully integrated and cannot be disabled without code modifications. The QUIC code does not appear to have a meander model.

Analyses with the meander models disabled for ARCON96 and MACCS were performed. The results for the ground-level point release for ARCON96 and MACCS with meander models disabled compared with the results for AERMOD and QUIC are shown in Figure 3-4 and Figure 3-5 under the neutrally-stable and stable weather conditions, respectively.

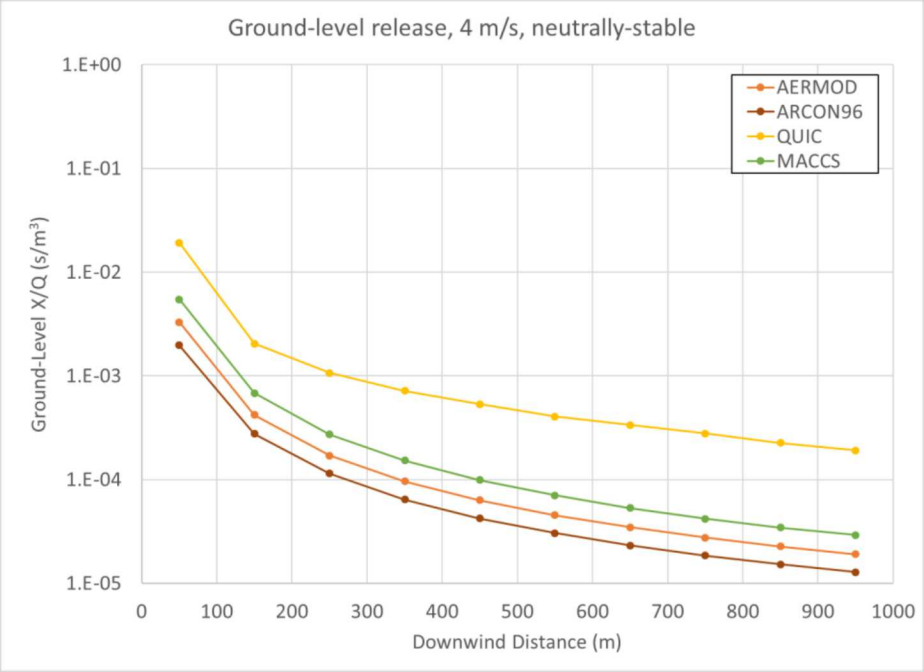

Figure 3-1. Ground-level, time-integrated X/Q versus distance for a ground release under the neutrally-stable weather condition and the nominal dispersion mode for each code.

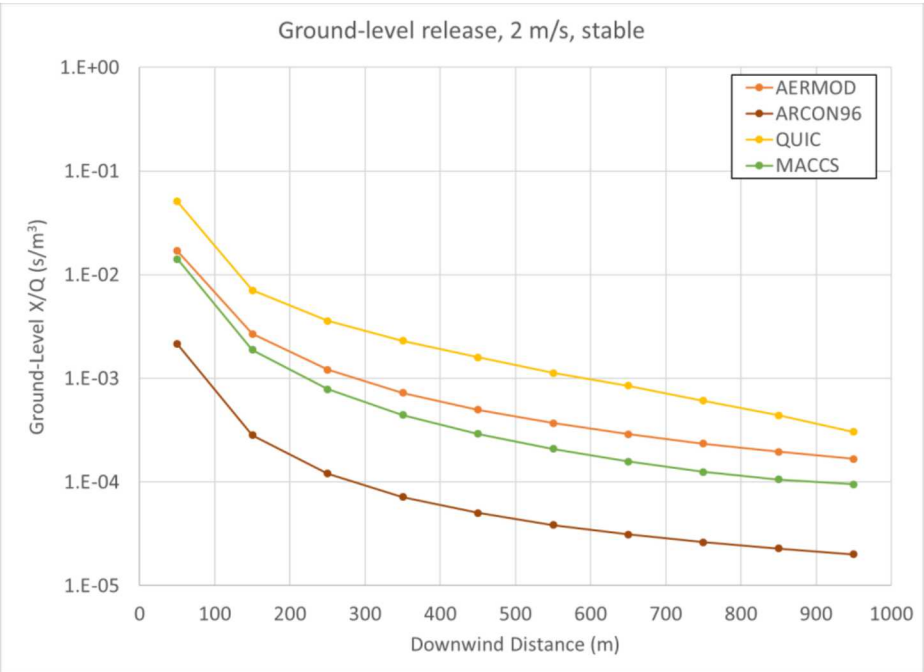

Figure 3-2. Ground-level, time-integrated X/Q versus distance for a ground release under the stable weather condition and the nominal dispersion mode for each code.

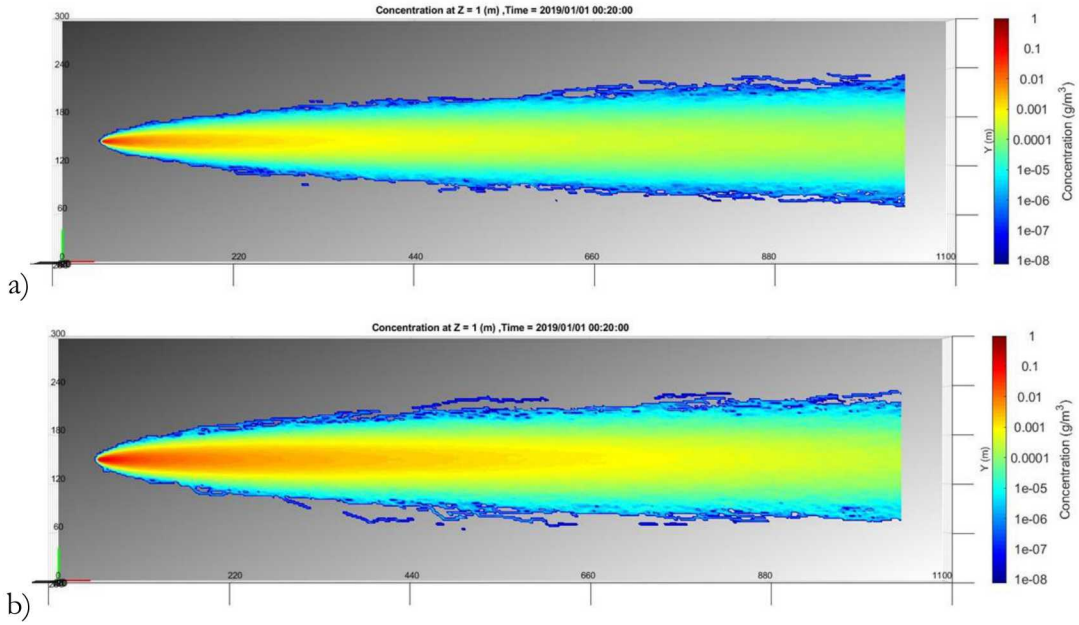

Figure 3-3. Time-averaged air concentration profiles at 1-m elevation for a ground release under a) neutrally-stable and b) stable weather conditions with QUIC using its nominal dispersion mode.

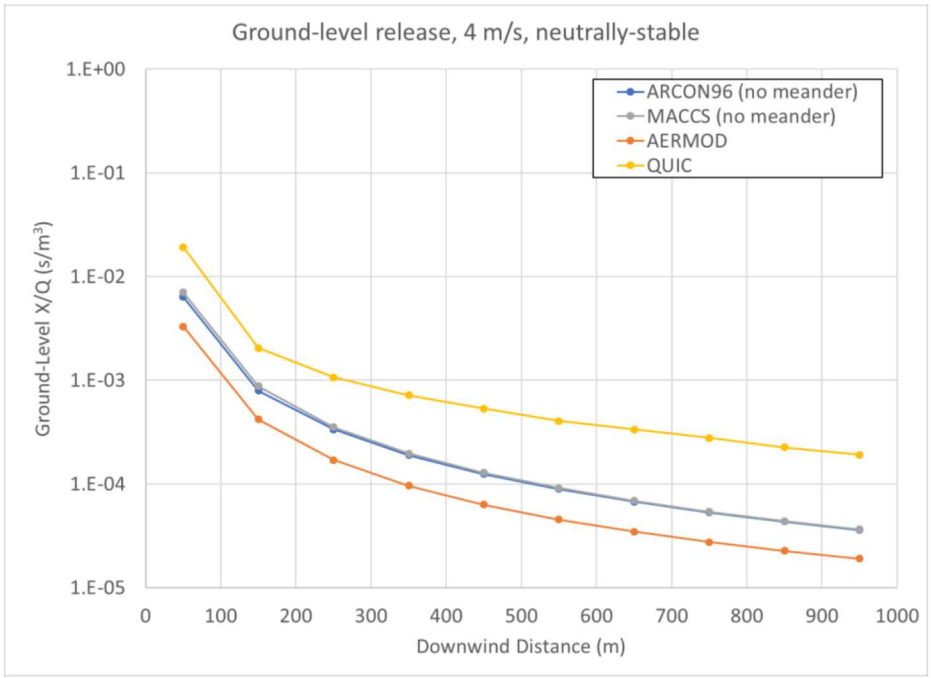

Figure 3-4. Ground-level, time-integrated X/Q versus distance for a ground release under the neutrally-stable weather condition and the nominal dispersion mode for each code with meander model disabled for ARCON96 and MACCS.

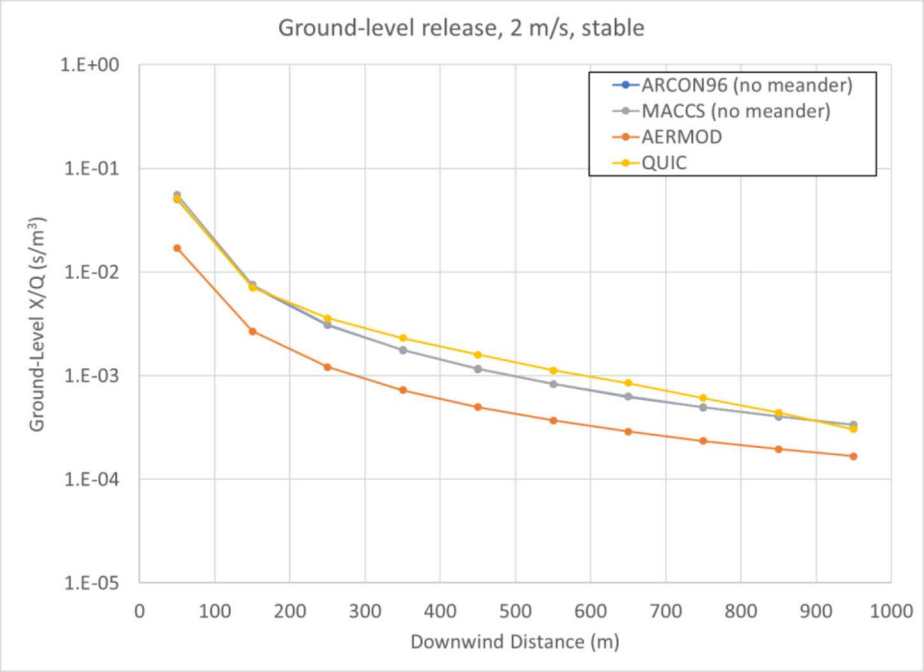

Figure 3-5. Ground-level, time-integrated X/Q versus distance for a ground release at the stable weather condition and the nominal dispersion mode for each code with meander model disabled for ARCON96 and MACCS.

As seen in Figure 3-4 and Figure 3-5, the results from ARCON96 and MACCS without their meander models enabled are nearly identical for both weather conditions. In addition, the results match those of QUIC for the stable weather condition. The AERMOD results are more dispersive than those of the other three codes in Figure 3-4 and Figure 3-5, as might be expected since plume meander is inherent in the AERMOD calculation. These results indicate that the differences between ARCON96 and MACCS in Figure 3-1 and Figure 3-2 are due to differences in plume meander model, since with the meander model disabled, the results match. Furthermore, this indicates that the QUIC results do not include the effects of plume meander. To account for plume meander in the QUIC calculations, the wind speed profile can be modified to increase the dispersion.

Additional QUIC calculations were performed with the weather parameters adjusted to increase the dispersion to emulate the effects of meander. The QUIC weather parameters were adjusted such that the resulting normalized, ground-level, time-integrated air concentrations (X/Q) over the 1000 m distance from the release location were similar to the results from the other codes with their meander models active, while still trending towards less dispersion.

To increase the dispersion in the QUIC calculations, both the inverse Monin-Obukhov length (1/L) and the wind speed profile as a function of height were modified. For a neutrally stable condition, the inverse Monin-Obukhov length was reduced to -0.025 m^{-1} and the wind speed profile was modified to a power-law function with an exponent of 0.35. These modifications resulted in a calculated average friction velocity was 0.385 m/s. For the stable weather condition, the inverse Monin-Obukhov length was reduced to -0.01 m^{-1} and the wind speed profile was modified to a power-law function with an exponent of 0.30. These modifications resulted in a calculated average friction velocity was 0.159 m/s. The updated input files for the QUIC weather conditions are

shown in Appendix D. These parameter values are used in the QUIC calculations shown in the subsequent sections.

The results from the three codes with the plume meander models enabled and the increased dispersion for the QUIC results to account for plume meander for the ground-level, point release are shown in Figure 3-6 and Figure 3-7 for the neutrally-stable and stable weather conditions, respectively. These figures show that the updated normalized, ground-level, time-integrated air concentrations for QUIC are similar to the results from the three other codes, while still trending towards less dispersion. The weather condition parameters used to generate the results in Figure 3-6 and Figure 3-7 are used in the other test cases, which include the effects of buildings and buoyancy and are discussed below.

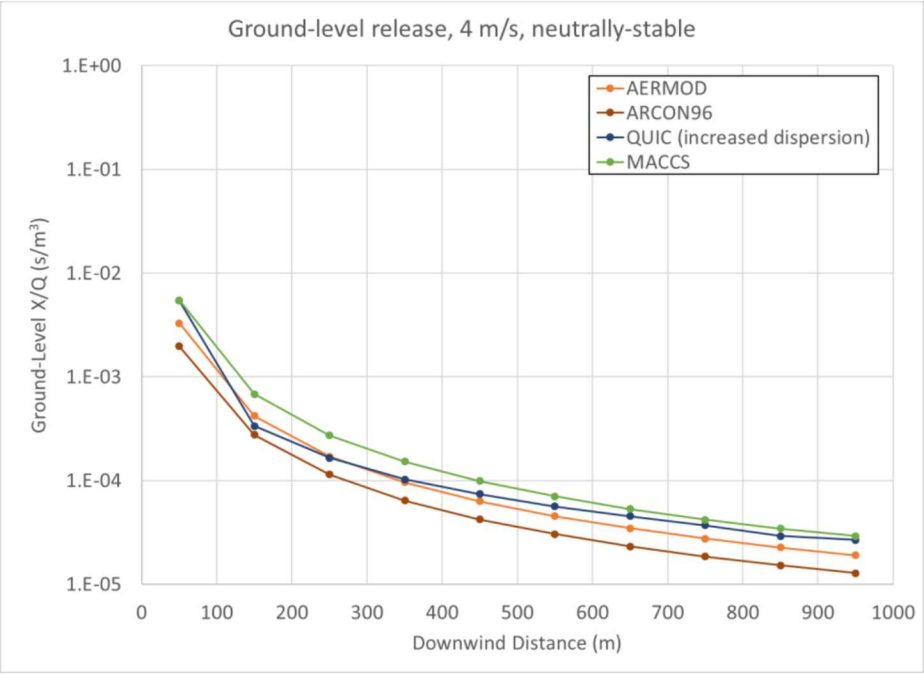

Figure 3-6. Ground-level, time-integrated X/Q versus distance for a ground release under the neutrally-stable weather condition and the nominal dispersion mode for each code and increased dispersion for QUIC.

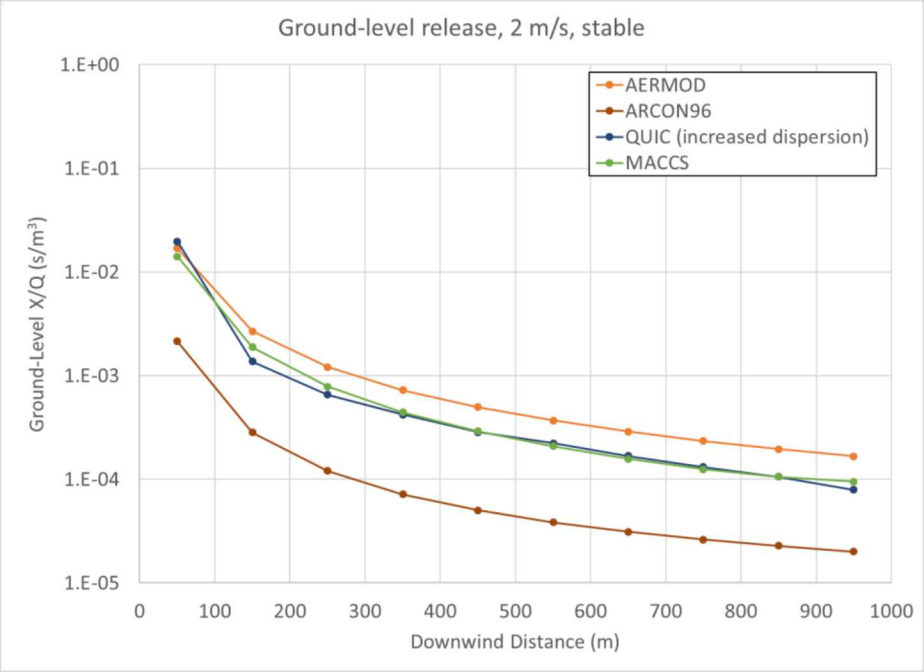

Figure 3-7. Ground-level, time-integrated X/Q versus distance for a ground release at the stable weather condition and the nominal dispersion mode for each code and increased dispersion for QUIC.

3.3. Building Effects

Incorporating the building configurations into the analyses was straightforward. For the AERMOD code, preprocessing software is used in which the full dimensions of the building are entered. The outputs from the preprocessor are the parameters to be used in the AERMOD building downwash model. For the calculations without a building, removing the downwash model parameters removes the effect of the building. The input and output from the preprocessor for the two building configurations are shown in the input files in Appendix A.

For the ARCON96 code, the building dimensions are accounted for by entering a building area in the input file. For this analysis, the projected area was used assuming that the wind was perpendicular to the building face with larger dimension. Therefore, the projected area was calculated as the building height times the building width. For the 20 m x 100 m x 20 m building, the projected area is 2,000 m^2; for the 20 m x 40 m x 20 m building, the projected area is 800 m^2. For the calculation with no building, a projected area of 0 m^2 was used. These projected areas can be seen in the ARCON96 input files in Appendix B.

In the MACCS calculations, building height is only used to determine whether the plume is trapped in the building wake. The building wake size is defined by the initial dispersion parameters. The initial dispersion parameters (σ_y and σ_z) are calculated based on the building width and height. The typical equations are that the initial σ_y = 0.23 x building width and the initial σ_z = 0.47 x building height. For the 20 m x 100 m x 20 m building, an initial σ_y of 23 m and an initial σ_z of 9.4 m were used; for the 20 m x 40 m x 20 m building, an initial σ_y of 9.2 m and an initial σ_z of 9.4 m were used. For the calculations with no building, an initial σ_y and σ_z of 0.1 m were used. These initial dispersion values can be seen in the MACCS input files shown in Appendix C.

In the QUIC code, buildings are defined graphically by entering all three dimensions of the building, along with its location. Buildings with the dimensions of 20 m x 100 m x 20 m and 20 m x 40 m x 20 m were included in two separate computational domains. All domains had overall dimensions of 1,100 m x 300 m x 200 m. The graphical representations of the computational domains for the QUIC analyses are shown in Appendix D.

3.4. Buoyancy

For MACCS, the buoyancy flux can be calculated from the rate of release of sensible heat. A rate of sensible heat release of 0 and 5 MW is used for the test cases and is shown in the MACCS input files in Appendix C. In MACCS, the buoyancy flux (F) is the calculated as 8.69 x 10-6 $m^4/s^3/W$ times the rate of release of sensible heat. For the 5 MW cases, this results in a buoyancy flux of about 43 m^4/s^3. MACCS checks whether the plume is trapped in the building wake based on the wind speed (u), buoyancy flux and building height (H_b) based on the following inequality.

$$u > \left(\frac{9.09F}{H_b}\right)^{1/3}$$

If the wind speed is greater than the expression, the plume is trapped in the building wake and no plume rise model is used. For the 4 m/s weather condition, the 5 MW plume is calculated to be trapped in the building wake, while for the 2 m/s weather condition, the 5 MW plume is calculated to escape the building wake.

For AERMOD, the buoyancy flux (F) is calculated from a stack diameter (d), exit velocity (V_s) and gas temperature (T_s) according to the equation below.

$$F = \frac{g \,.\, V_s \,.\, d^2 \,.\, \Delta T}{4 \,.\, T_s}$$

Where

g = gravitation constant (9.8 m/s^2), and

ΔT = temperature difference between the plume and the ambient temperature.

A stack diameter, exit velocity, and gas temperature were chosen to generate the same buoyancy flux as calculated for MACCS from heat content (43.45 m^4/s^3). In determining the values, minimizing the calculated momentum flux was also considered to be consistent with the MACCS model, which does not treat momentum flux. Momentum flux was minimized by specifying a large-diameter exit, a high-temperature gas and a low exit velocity (6.22 m, 4000 K, 0.5 m/s). These parameters appear in the AERMOD input files shown in Appendix A.

ARCON96 does not have a plume rise model. The code documentation recommends increasing the initial release height to account for plume buoyancy. Thus, the test cases that include buoyant plumes were not analyzed with ARCON96.

QUIC does not model steady processes but rather is a transient code based on a short release duration. To compensate, reported results are based on time averages or time integrals to represent a steady state. Hence, the test cases that include buoyant plumes were not able to be analyzed with QUIC because there is no straightforward way to represent a continuous buoyancy flux.

This page left blank

4. CODE RESULTS

The six test cases without buoyancy were run with AERMOD, ARCON96, MACCS and QUIC. The six test cases that include buoyancy were only run for AERMOD and MACCS, for reasons explained previously. The results from these test cases are discussed below. In this section, the trends observed for each code related to building configuration, weather condition and buoyancy (if applicable) are discussed. Comparisons between codes are discussed in the next section.

4.1. AERMOD

All twelve test cases were run with AERMOD. Comparing the results of these test cases shows the dependence of centerline ground-level, air concentration on weather condition, building size, release elevation and buoyancy.

Figure 4-1 shows cases for a neutrally-stable atmosphere; Figure 4-2 shows the same cases but for a stable atmosphere. The observed trends for the two figures are as follows:

- The ground-level release gives the highest concentrations at all downwind distances, although the concentrations for the other cases approach these values as distance increases.
- As expected, the curves for stability class F in Figure 4-2 are consistently higher than the corresponding curves for stability class D in Figure 4-1.
- The cases with no building (release locations are at 20 m elevation) have low concentrations at short distances but approach the curves for ground-level point sources as distance increases.
- Adding a building significantly increases dispersion at short distances, but the building effects are greatly diminished at 1 km downwind.
- A larger building results in lower concentrations, especially at short distances.
- The effect of buildings is more pronounced when atmospheric stability is greater, i.e., for stability class F.

Figure 4-3 shows results for four combinations of weather condition and buoyancy for the wider building. For each of the weather conditions, the initial concentrations are lower for the cases with buoyancy; however, the effect essentially disappears by about 150 m downwind. For reasons that the authors do not understand, these curves diverge again at 600 to 700 m downwind, although the divergence in not great. The trends are similar but slightly more exaggerated for the narrower building, as shown in Figure 4-4. Figure 4-5 shows similar results for AERMOD but for an elevated release (20 m) with no building. X/Q for the cases without buoyancy behave as expected, the ground-level values are very low at short distances, increase over several hundred meters because higher concentrations near the centerline disperse toward the ground, then diminish again as additional dispersion dilutes the concentrations at ground level. For the cases with buoyancy, the values of X/Q are nearly constant over the entire distance range shown in the figure; the trends are that X/Q decreases out to about 500 m then increases again. A possible explanation for this behavior is that AERMOD models the plume as something like a vertical line or cylindrical source rather than as a rising plume. In other words, it appears that AERMOD assumes mixing between the plume and the surrounding air during plume rise, causing a significant portion of the plume content to be left behind as it rises.

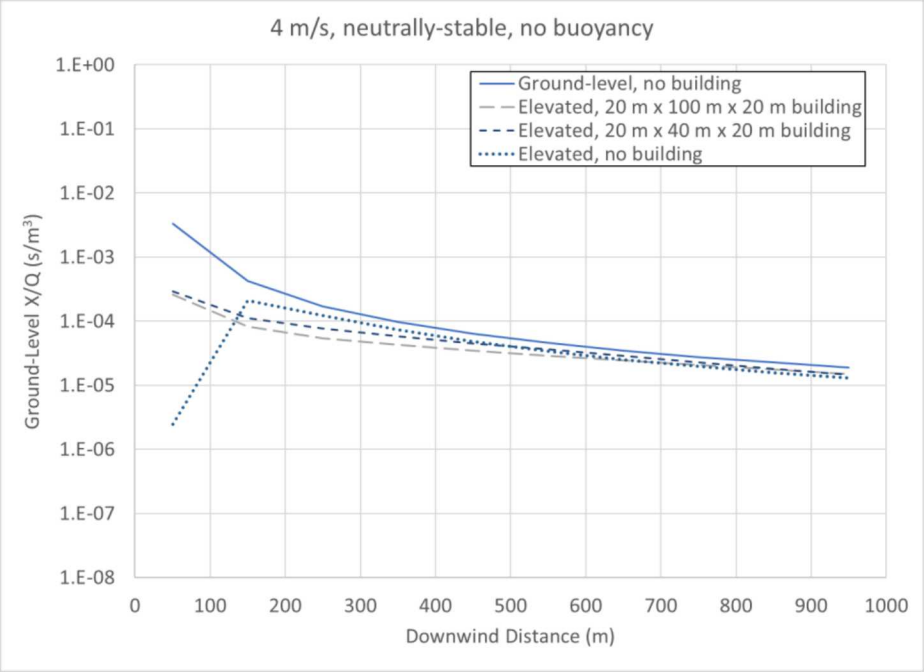

Figure 4-1. Ground-level, time-integrated X/Q versus distance for various release location/building configurations under the neutrally-stable weather condition calculated with AERMOD

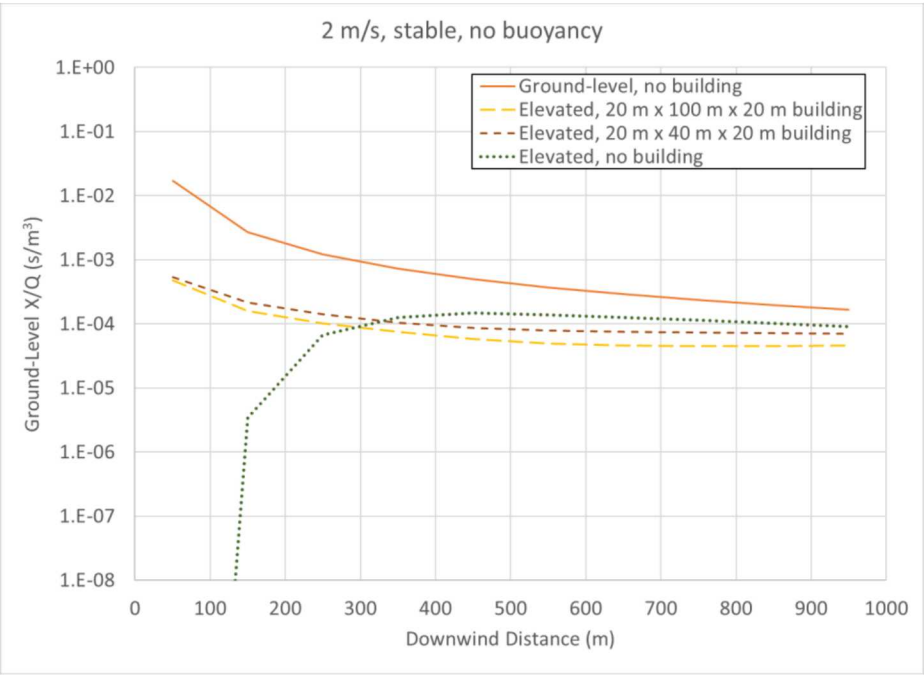

Figure 4-2. Ground-level, time-integrated X/Q versus distance for various release location/building configurations at the stable weather condition calculated with AERMOD

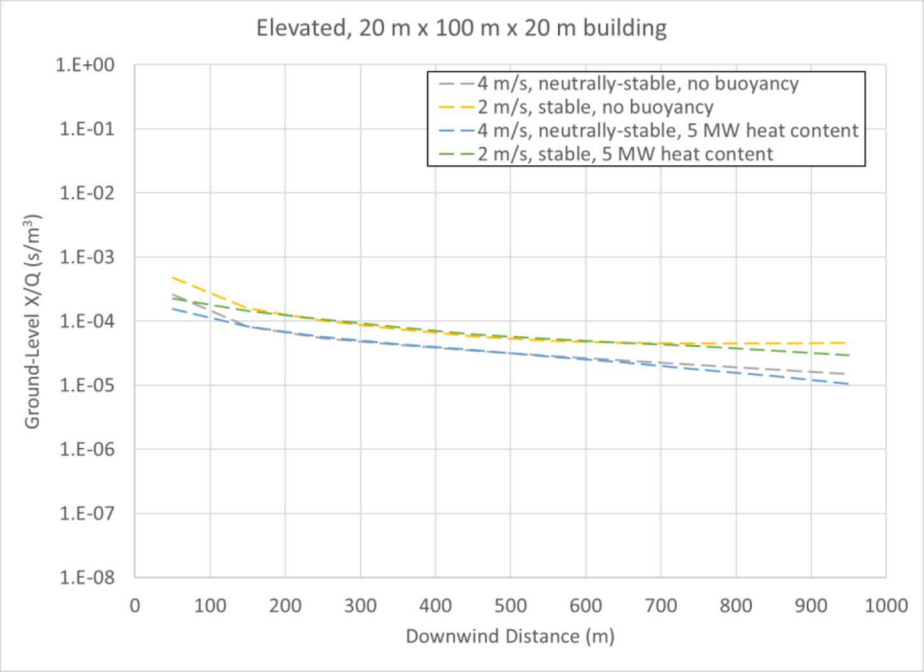

Figure 4-3. Ground-level, time-integrated X/Q versus distance for various weather and plume conditions with a 20 m x 100 m x 20 m building calculated with AERMOD

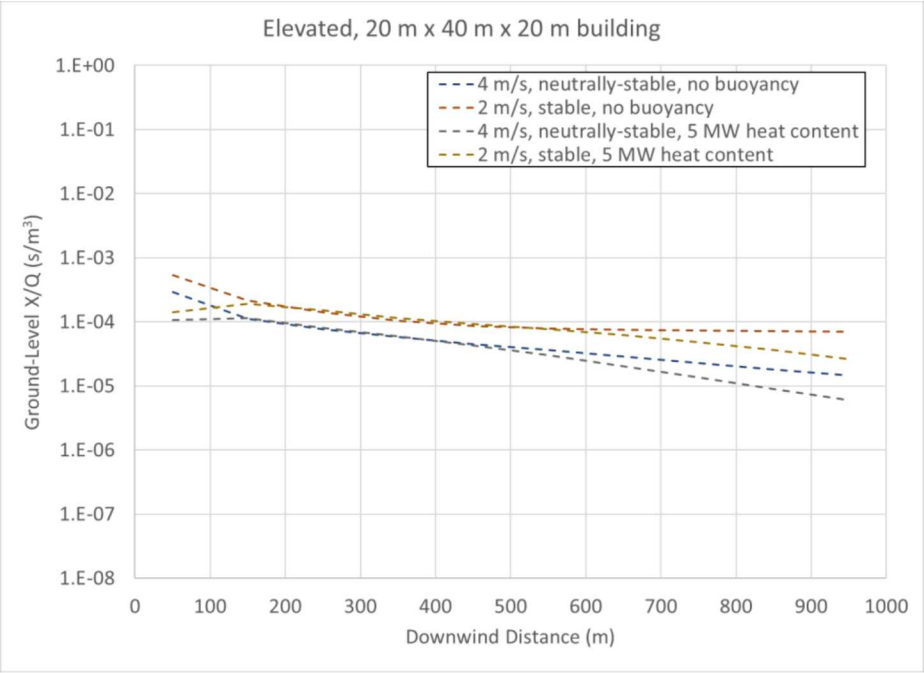

Figure 4-4. Ground-level, time-integrated X/Q versus distance for various weather and plume conditions with a 20 m x 40 m x 20 m building calculated with AERMOD

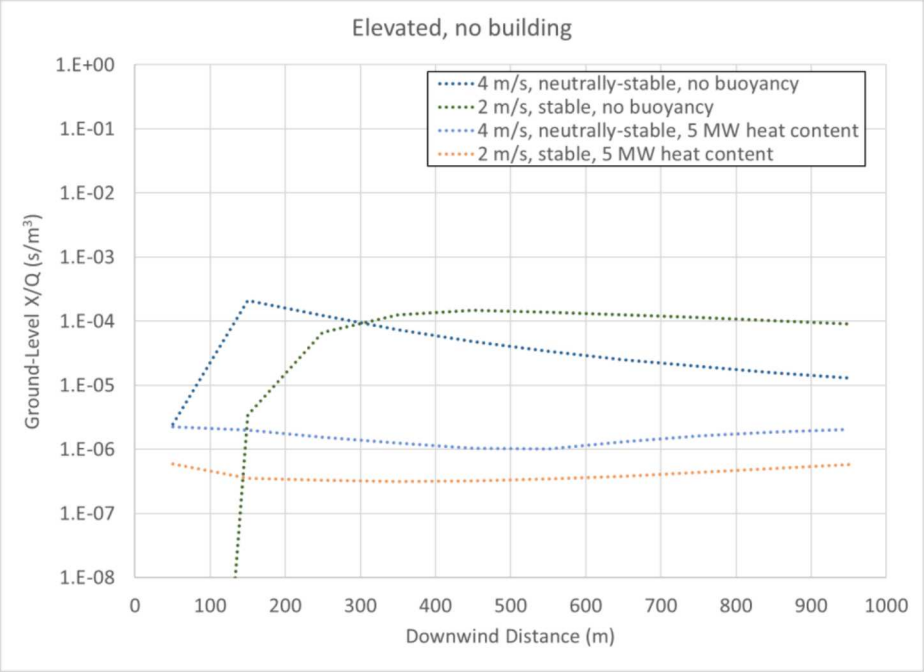

Figure 4-5. Ground-level, time-integrated X/Q versus distance from AERMOD for various weather and plume conditions for an elevated release with no building

4.2. ARCON96

Six of the twelve test cases were run with ARCON96. The six test cases that included buoyant plumes were not run because ARCON96 does not include a plume rise model. Comparing the results of these test cases run with ARCON96 shows the dependence on weather condition and building size in the ARCON96 models. The results from the ARCON96 test cases with no buoyancy for the neutrally-stable and stable weather conditions are shown in Figure 4-6 and Figure 4-7, respectively. As seen in Figure 4-6 and Figure 4-7, inclusion of a building and elevation of the source results in a minimal change in the predicted ground-level X/Q within the first 1000 m. For both neutrally-stable and stable conditions, predicted X/Q for the elevated release is slightly (~8%) higher compared with a ground-level release, but the differences diminish with downwind distance. The stable weather condition results are slightly (~8%) higher between 100 m and 500 m. Little difference is observed between the results with the larger building (20 m x 100 m x 20 m) compared with the smaller building (20 m x 40 m x 20 m). Based on these results, buildings and elevated release appear to have a minimal effect on dispersion under the tested conditions. The buildings sizes in the test cases are not different enough to significantly affect the results.

The results from the two test cases that included a 20 m x 100 m x 20 m building are shown in Figure 4-8. The results show that the ARCON96 models predict more dispersion under neutrally-stable conditions compared with the corresponding predictions under stable conditions. Figure 4-9 shows the results from the two test cases that included a 20 m x 40 m x 20 m building showing the same trend as for the 20 m x 100 m x 20 m building. The ARCON96 calculations for an elevated release with no building are shown in Figure 4-10. As seen in Figure 4-10, the trends are similar to those in the previous figures. Based on these results it appears that the ARCON96 model predicts more dispersion in the neutrally-stable condition compared with the stable condition, as expected, but that the results are substantially the same for ground-level and elevated releases with or without a building present.

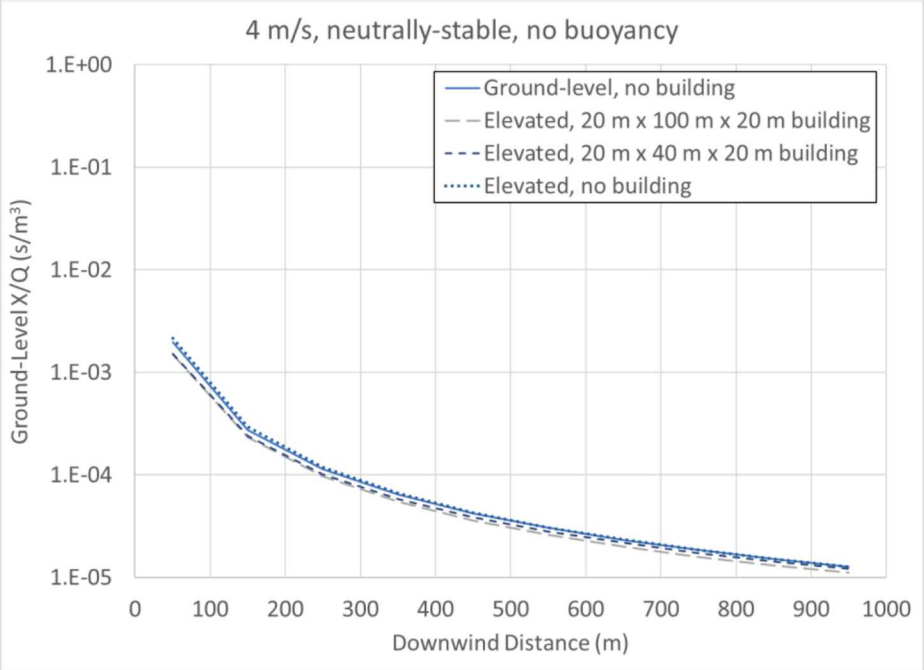

Figure 4-6. Ground-level, time-integrated X/Q versus distance for various release location/building configurations under the neutrally-stable weather condition calculated with ARCON96

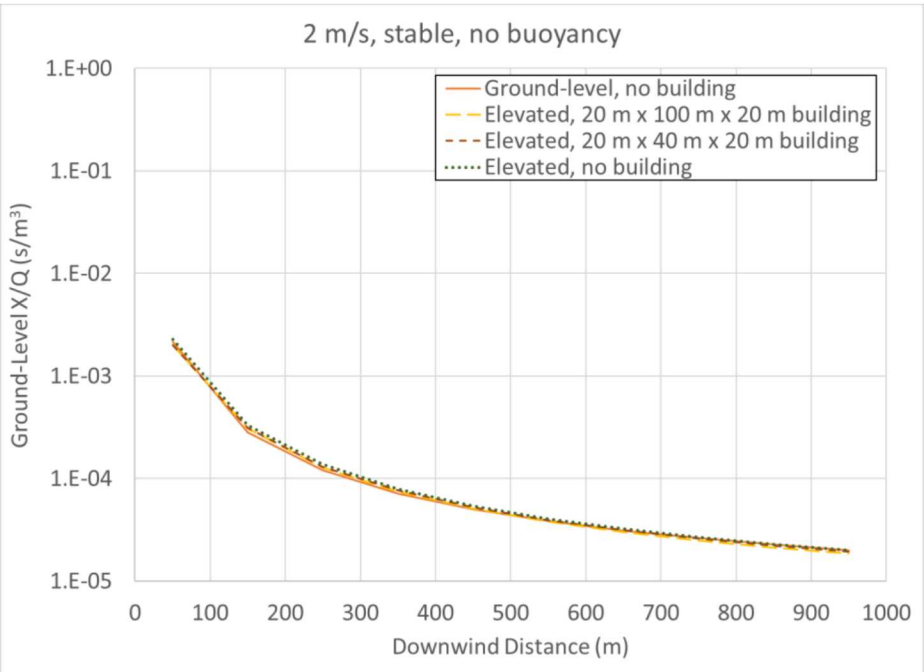

Figure 4-7. Ground-level, time-integrated X/Q versus distance for various release location/building configurations at the stable weather condition calculated with ARCON96

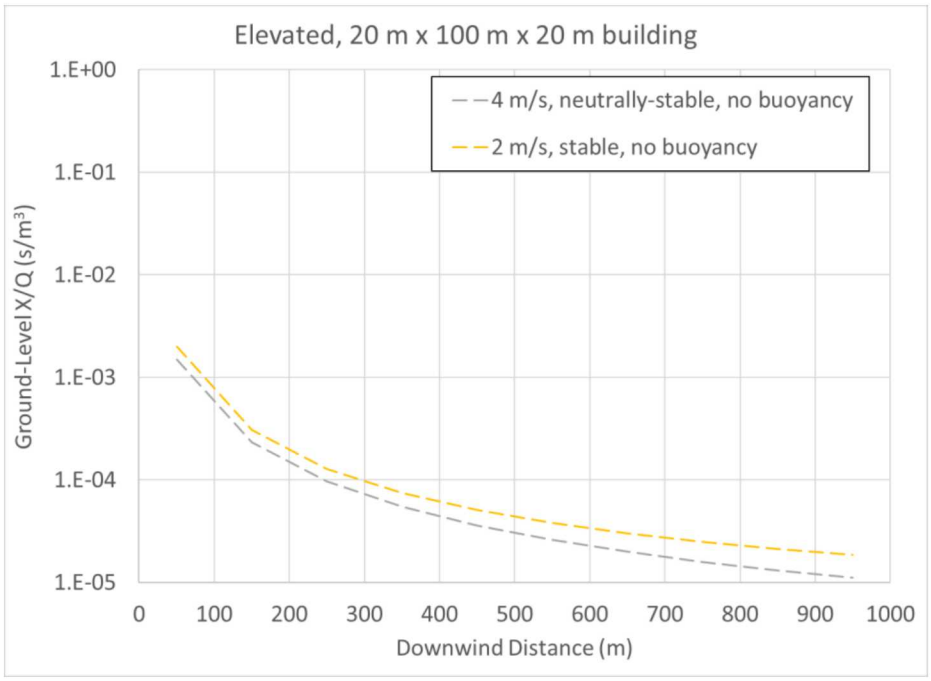

Figure 4-8. Ground-level, time-integrated X/Q versus distance for various weather conditions with a 20 m x 100 m x 20 m building calculated with ARCON96

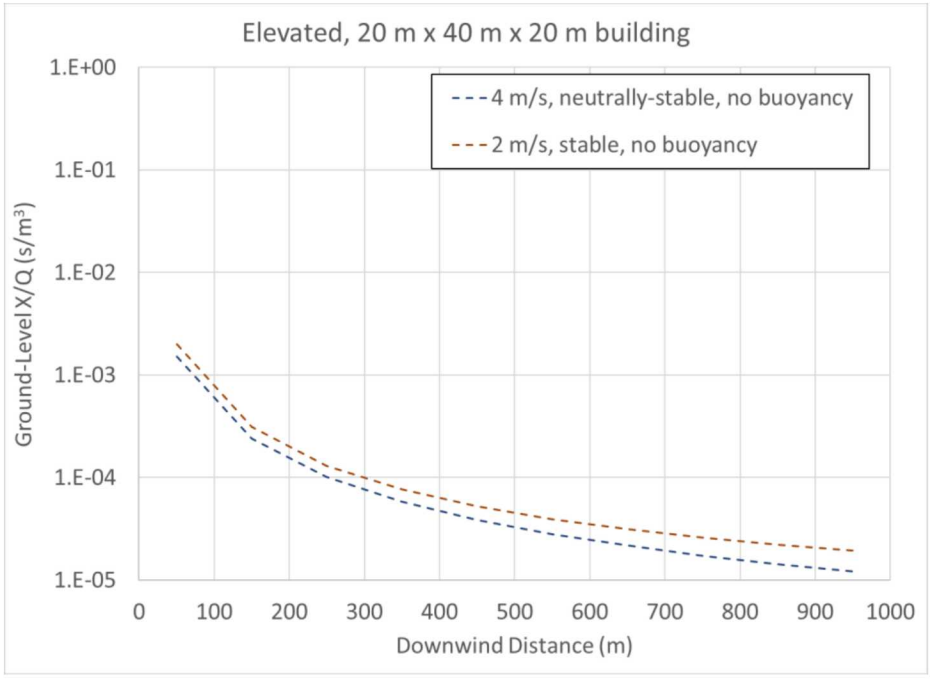

Figure 4-9. Ground-level, time-integrated X/Q versus distance for various weather conditions with a 20 m x 40 m x 20 m building calculated with ARCON96

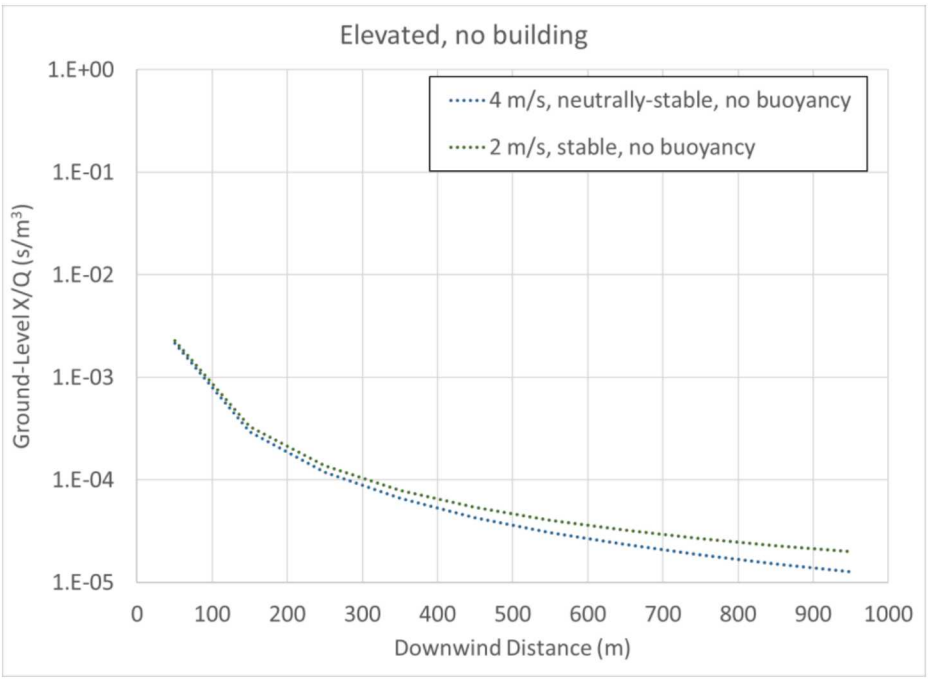

Figure 4-10. Ground-level, time-integrated X/Q versus distance from ARCON96 for various weather conditions for an elevated release with no building

4.3. MACCS

All twelve test cases were run with MACCS. Comparing the results of these test cases run with MACCS shows the dependence on weather condition, building size and buoyancy in the MACCS models. The four cases with no buoyancy for the neutrally-stable and stable weather conditions are shown in Figure 4-11 and Figure 4-12, respectively. The observed trends for the two figures are as follows:

- The ground-level point release gives the highest values of ground-level X/Q at all downwind distances, although the values of X/Q for the other cases approach these values as distance increases.
- As expected, the curves for stability class F in Figure 4-12 are generally higher than the corresponding curves for stability class D in Figure 4-11 except for the elevated release with no building at shorter distances.
- The cases with elevated release (20 m) and no building have low values of X/Q at short distances but approach the curves for ground-level point sources as distance increases. For these cases, the ground-level X/Q initially rises as the plume content disperses toward the ground, then diminishes as further dispersion causes the plume to be diluted. For stability class F, this last feature occurs beyond 1000 m downwind.
- Adding a building significantly increases dispersion at short distances, but the building effects are greatly diminished at 1 km downwind.
- A larger building results in lower concentrations, especially at short distances.
- The effect of buildings is relatively independent of atmospheric stability.

The results from the four test cases that included a 20 m x 100 m x 20 m building are shown in Figure 4-13. The MACCS plume rise model predicts that the 4 m/s wind speed is high enough that

the 5 MW plume remains trapped in the building wake and hence the results with and without buoyancy under neutrally-stable conditions are indistinguishable in the figure. The results also show that the MACCS models predict lower values of X/Q under neutrally-stable conditions compared with X/Q under stable conditions when the releases are nonbuoyant. Figure 4-13 shows that for the buoyant plume that does escape the building wake (for F stability), MACCS predicts much lower values of X/Q within 1000 m. This is due to the calculation of the plume rising faster than it is dispersing, which results in a reduction of the ground-level air concentration until the plume stop rising. Figure 4-14 shows the results from the four test cases that included a 20 m x 40 m x 20 m building. Similar trends are observed as for the 20 m x 100 m x 20 m building. The MACCS calculations for an elevated release with no building are shown in Figure 4-15.

Figure 4-15 shows that significantly lower ground-level values of X/Q are observed near the release location for a stable condition relative to a neutrally-stable condition. Ground-level values of X/Q for the buoyant cases are significantly lower than for the nonbuoyant cases because plume rise is predicted to be significant and time is required for concentrations to disperse down to the ground level.

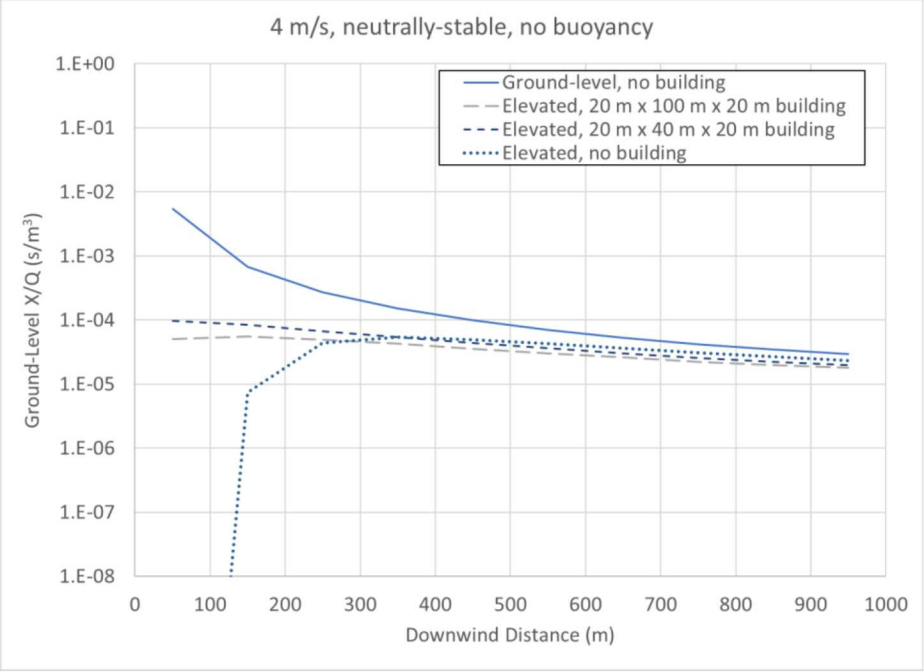

Figure 4-11. Ground-level, time-integrated X/Q versus distance for various release location/building configurations at the neutrally-stable weather condition calculated with MACCS

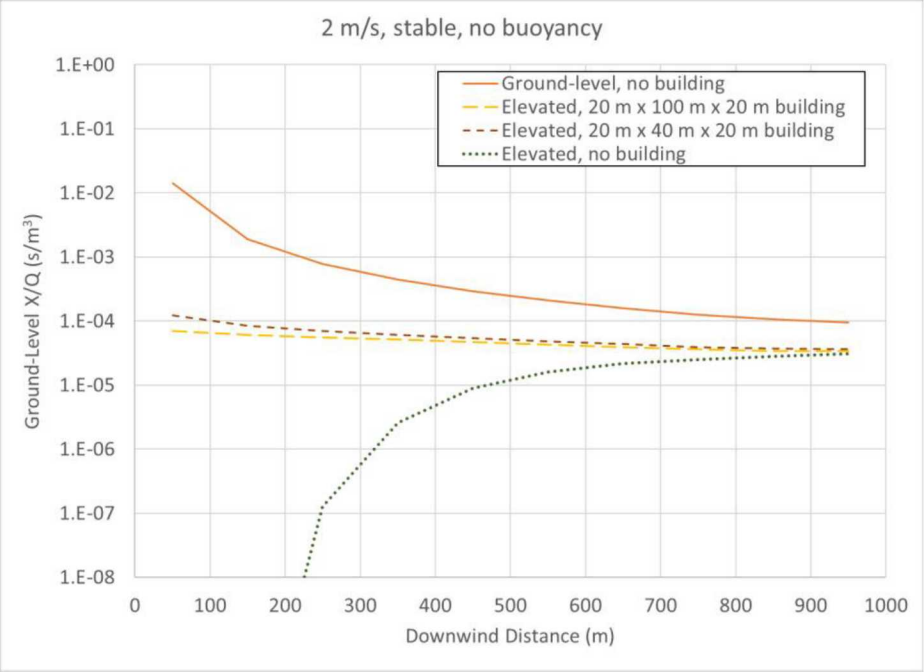

Figure 4-12. Ground-level, time-integrated X/Q versus distance for various release location/building configurations at the stable weather condition calculated with MACCS

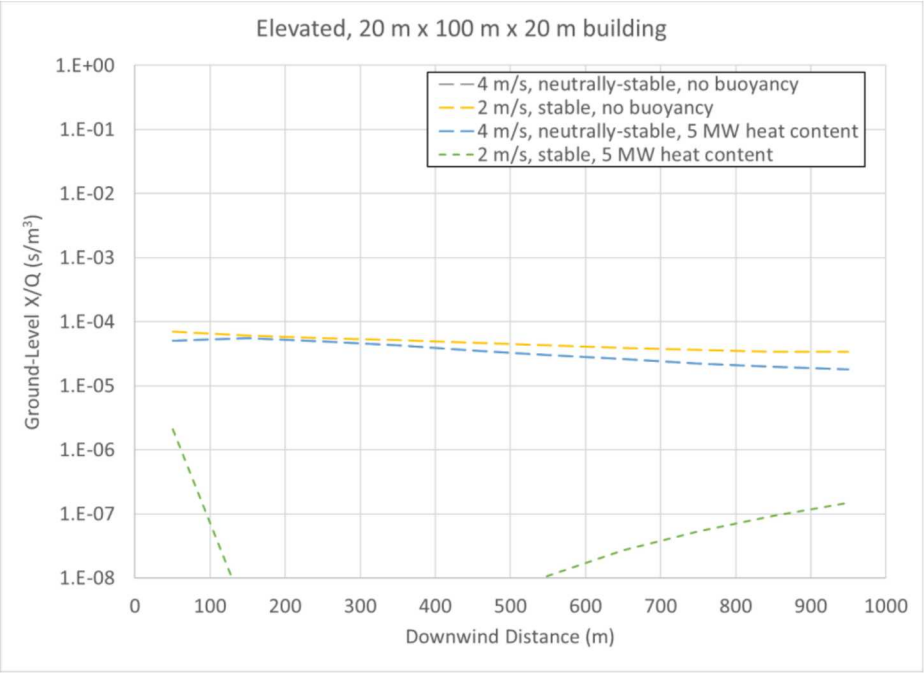

Figure 4-13. Ground-level, time-integrated X/Q versus distance for various weather and plume conditions with a 20 m x 100 m x 20 m building calculated with MACCS

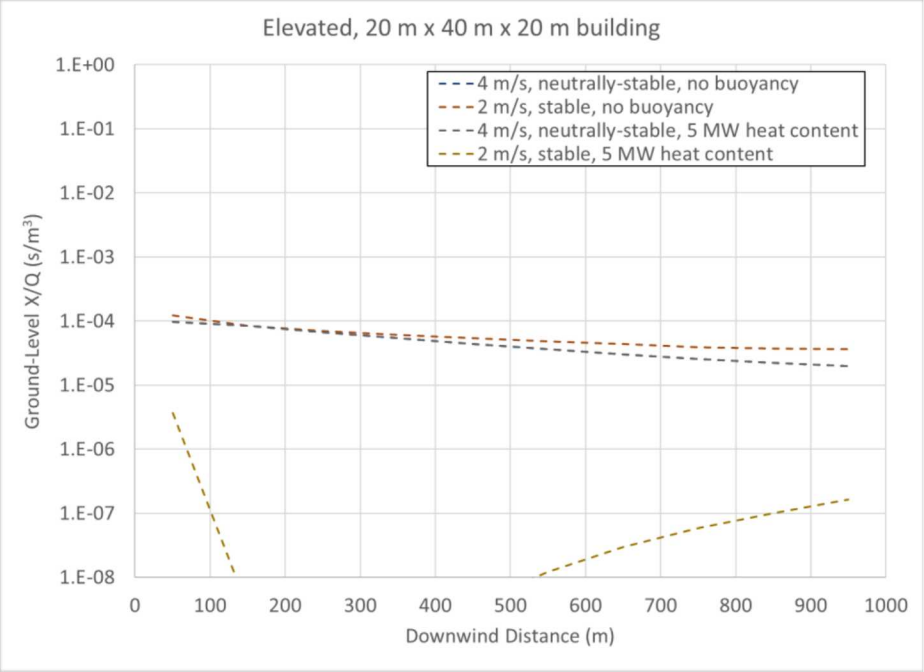

Figure 4-14. Ground-level, time-integrated X/Q versus distance for various weather and plume conditions with a 20 m x 40 m x 20 m building calculated with MACCS

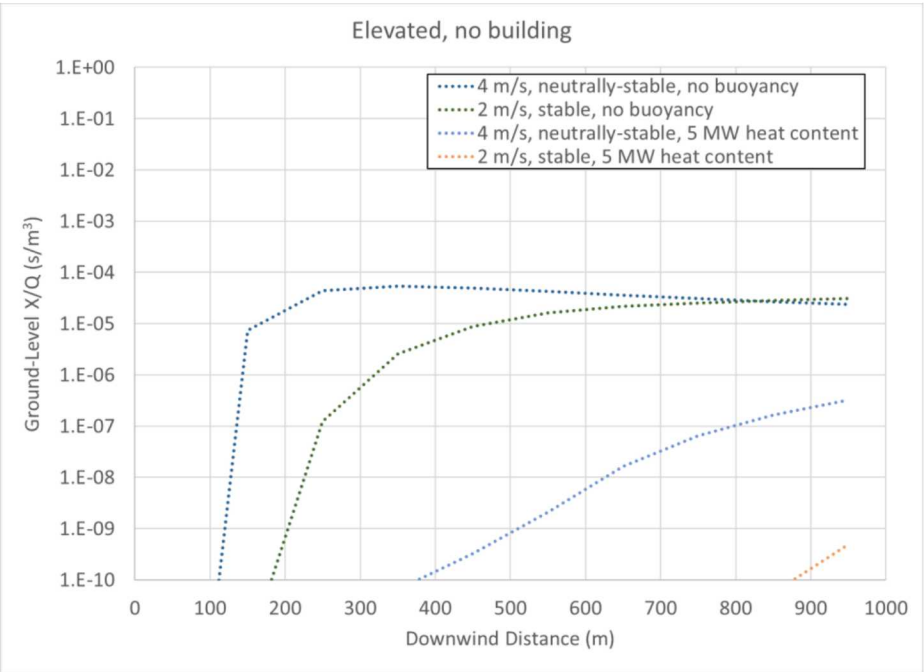

Figure 4-15. Ground-level, time-integrated X/Q versus distance from MACCS for various weather and plume conditions for an elevated release with no building

4.4. QUIC

Six of the twelve test cases were run with QUIC. The six test cases that included buoyant plumes were not run because QUIC does not include a method for continuously adding energy to the

plume. Comparing the results of these test cases run with QUIC shows the dependence on weather condition and building size in the QUIC models.

The results from the QUIC test cases with no buoyancy for the neutrally-stable and stable weather conditions are shown in Figure 4-16 and Figure 4-17, respectively. The observed trends for the two figures are as follows:

- The ground-level point release gives the highest ground-level X/Q values at all downwind distances, although the values for the other cases approach these values as distance increases.
- As expected, the curves for stability class F in Figure 4-17 are generally higher than the corresponding curves for stability class D in Figure 4-16, except for the elevated release with no building at shorter distances.
- The cases with elevated release (20 m) and no building have low concentrations at short distances but approach the curves for ground-level point sources as distance increases. For these cases, the ground-level X/Q initially rises as the plume content disperses toward the ground, then diminishes as further dispersion causes the plume to be diluted. For stability class F, this last feature occurs beyond 1000 m downwind.
- Adding a building significantly increases dispersion at short distances, but the building effects are greatly diminished at 1 km downwind.
- The effect of building size is not very significant except at very short distances.
- The effect of buildings on ground-level X/Q is greater when atmospheric stability is lower, even at short distances.

The results from the two test cases that included a 20 m x 100 m x 20 m building are shown in Figure 4-18. These results show that the QUIC models predict more dispersion under neutrally-stable conditions compared with stable conditions. Figure 4-19 shows that the trends for the two test cases that included a 20 m x 40 m x 20 m building are essentially the same as for the 20 m x 100 m x 20 m building.

The QUIC ground-level values of X/Q for an elevated release with no building are shown in Figure 4-20. Lower ground-level X/Q are observed near the release location under stable conditions relative to neutrally-stable conditions. However, the curves for the two cases cross at ~200 m. Based on these results, it appears that QUIC predicts more dispersion under a neutrally-stable condition compared with a stable condition when buildings are present. Higher values of X/Q at very short distances for D stability may arise because of the elevated release location.

The time average air concentrations for the horizontal plane at a height of 1 m and a vertical plane at the building centerline for the four test cases that include a building (Case 01, Case 02, Case 05 and Case 06) are shown in Figure 4-21, Figure 4-22, Figure 4-23, and Figure 4-24, respectively. The outline of the building is seen on the left side of each figure. The building wake in each case can be seen by examining the yellow contour just downstream of the building in both cross sections. These figures show a similar structure to the one in Figure 3-3 at downstream distances that are beyond the building wake.

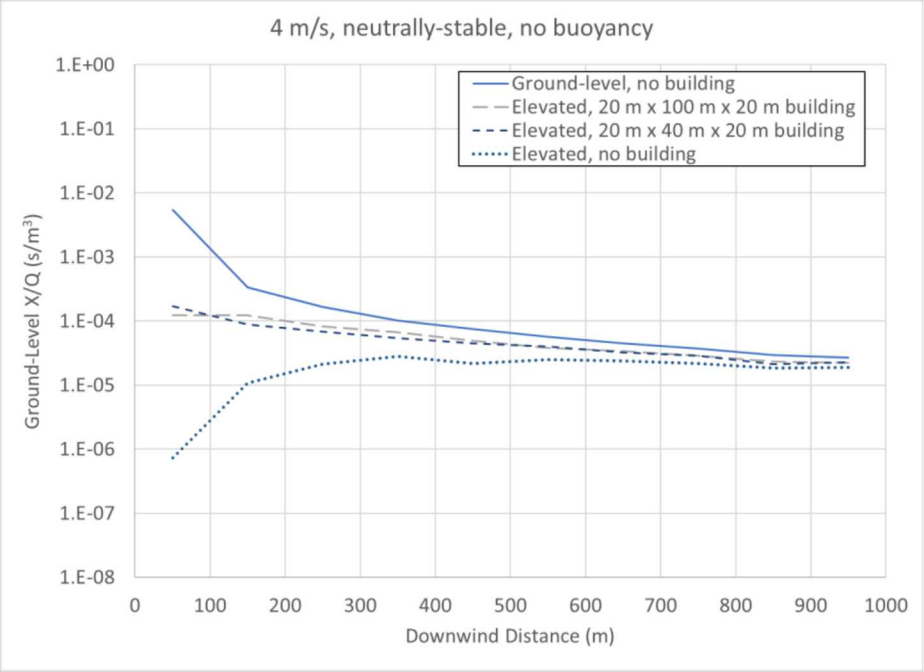

Figure 4-16. Ground-level, time-integrated X/Q versus distance for various release location/building configurations under the neutrally-stable weather condition calculated with QUIC

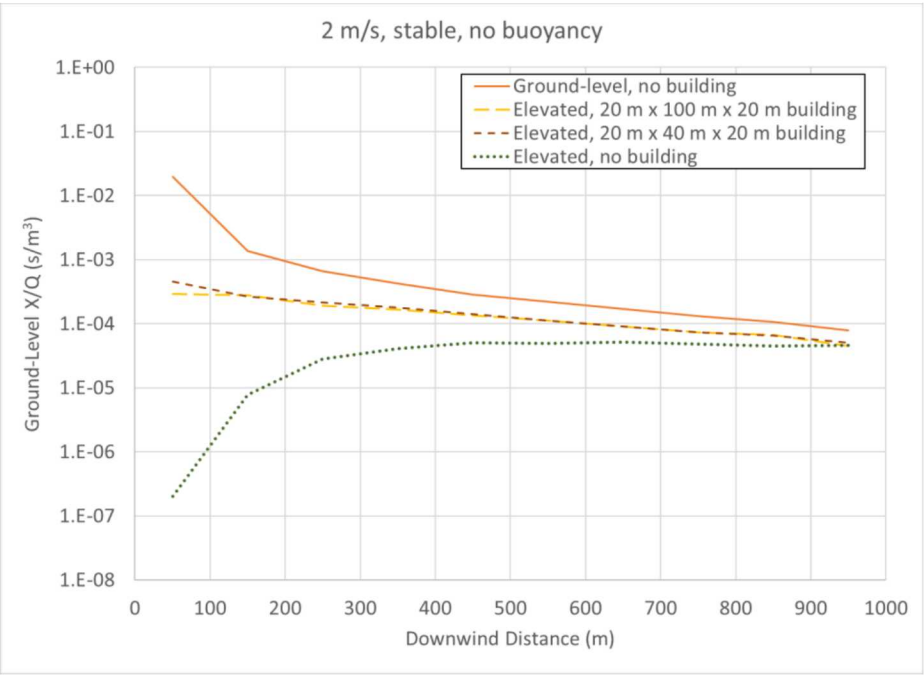

Figure 4-17. Ground-level, time-integrated X/Q versus distance for various release location/building configurations at the stable weather condition calculated with QUIC

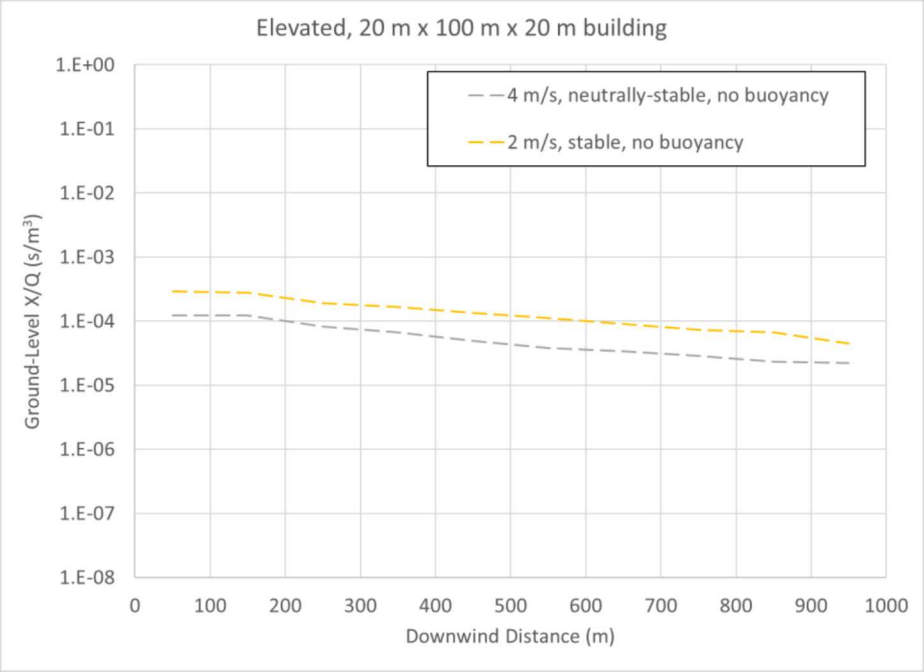

Figure 4-18. Ground-level, time-integrated X/Q versus distance for various weather conditions with a 20 m x 100 m x 20 m building calculated with QUIC

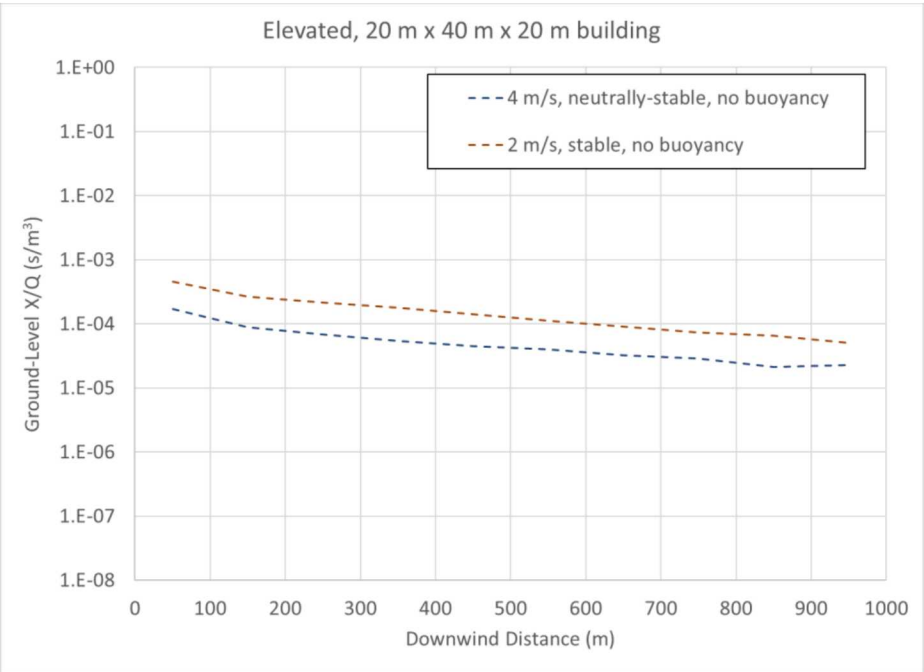

Figure 4-19. Ground-level, time-integrated X/Q versus distance for various weather conditions with a 20 m x 40 m x 20 m building calculated with QUIC

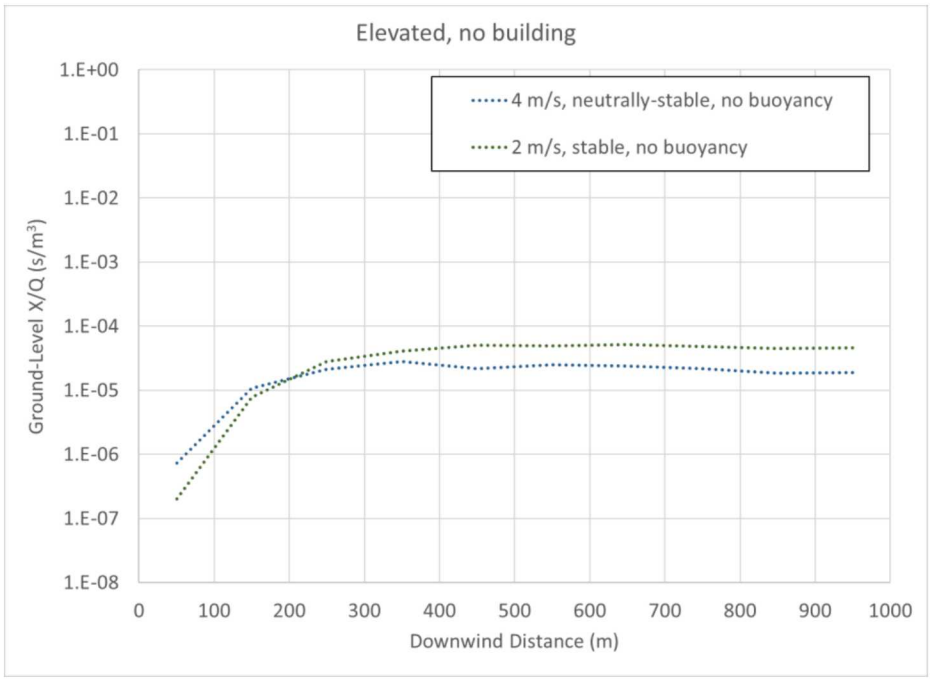

Figure 4-20. Ground-level, time-integrated X/Q versus distance from QUIC for various weather conditions for an elevated release with no building

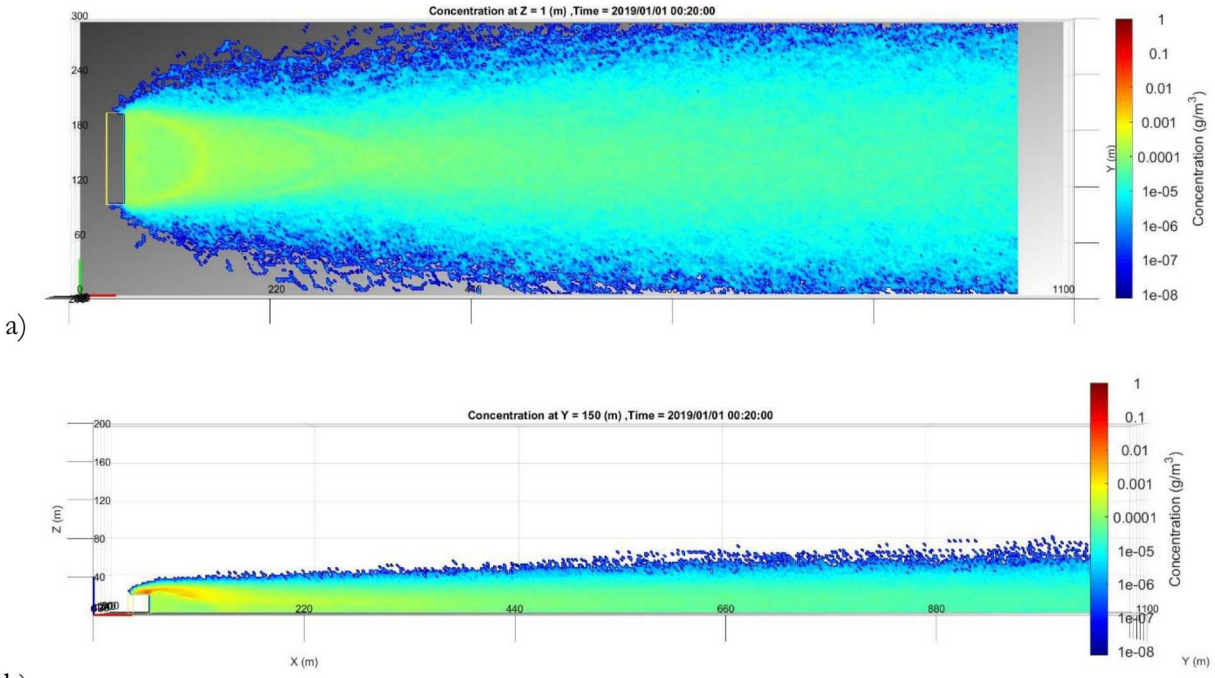

Figure 4-21. Time averaged air concentration for a) a horizontal plane at 1 m elevation and b) a vertical plane at building centerline for Case 01, (20 m x 100 m x 20 m, neutrally-stable weather condition) for QUIC.

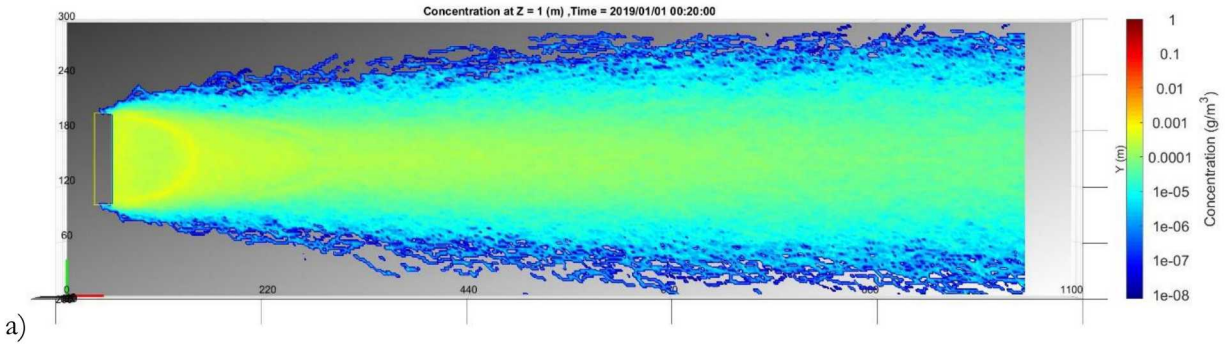

a)

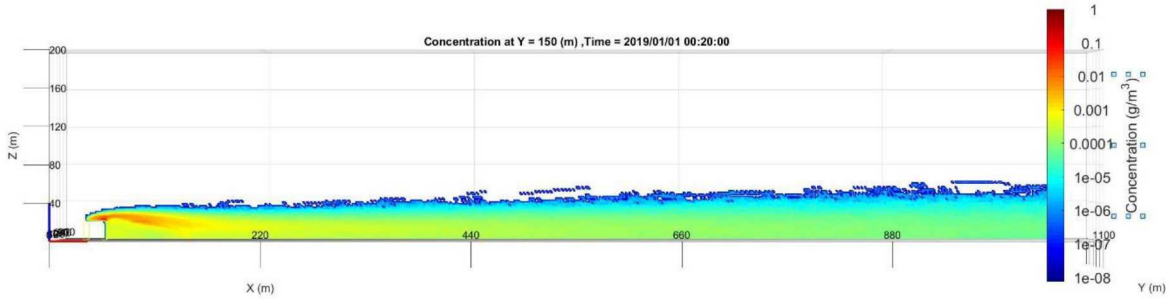

b)

Figure 4-22. Time averaged air concentration for a) a horizontal plane at 1 m elevation and b) a vertical plane at building centerline for Case 02, (20 m x 100 m x 20 m, stable weather condition) for QUIC.

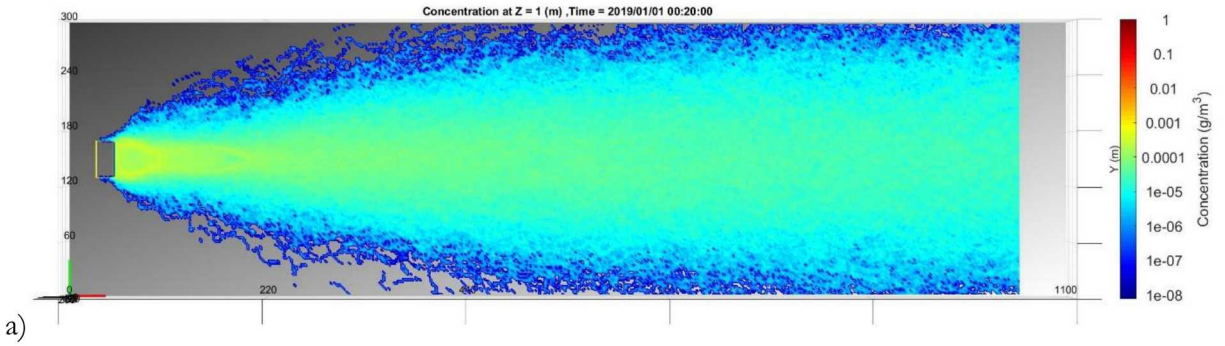

a)

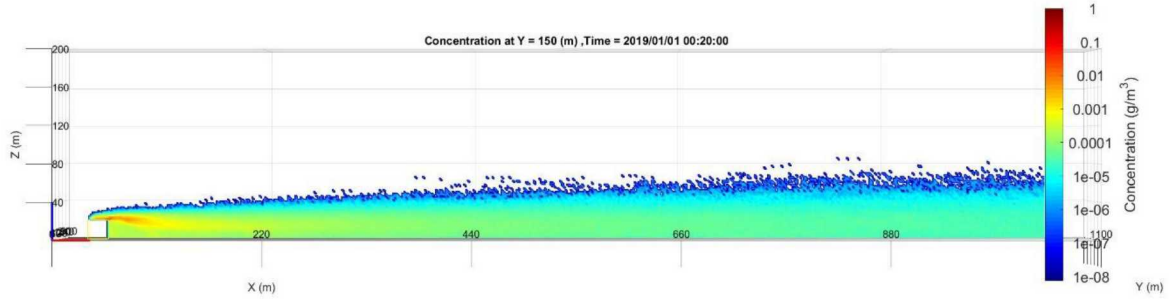

b)

Figure 4-23. Time averaged air concentration for a) a horizontal plane at 1 m elevation and b) a vertical plane at building centerline for Case 05, (20 m x 40 m x 20 m, neutrally-stable weather condition) for QUIC.

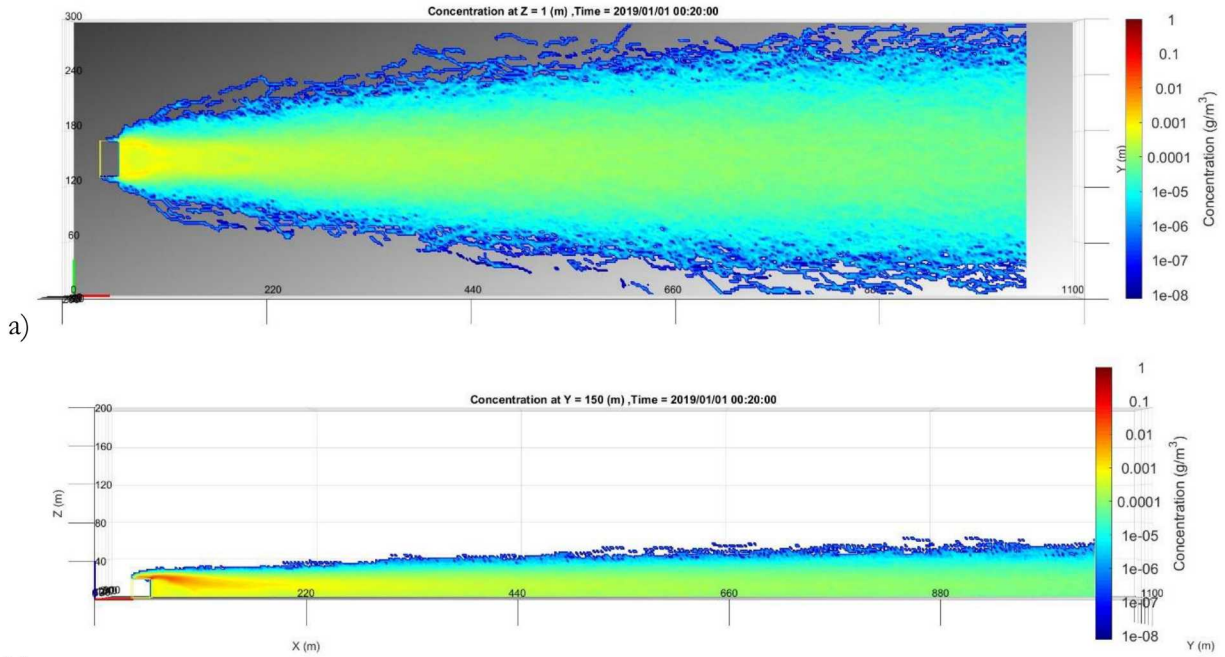

Figure 4-24. Time averaged air concentration for a) a horizontal plane at 1 m elevation and b) a vertical plane at building centerline for Case 06, (20 m x 40 m x 20 m, stable weather condition) for QUIC

5. CODE COMPARISONS

Four of the test cases include a building and no heat content in the plume, Case 01, Case 02, Case 05, and Case 06. The results from the AERMOD, ARCON96, QUIC and MACCS codes for those four test cases are shown in Figure 5-1, Figure 5-2, Figure 5-3, and Figure 5-4, respectively. In all four cases, the order from highest to lowest at 50 m is ARCON96, AERMOD, QUIC, MACCS. The order changes as distance increases. At 950 m, the order for the neutrally-stable cases (Case 01 and Case 05) is QUIC, MACCS, AERMOD, and ARCON96; for the stable cases (Case 02 and Case 06) the order is AERMOD, QUIC, MACCS, ARCON96. In all four cases ARCON96 transitions from predicting the highest ground-level, time-integrated values of X/Q to the lowest of the four codes. The relative order between QUIC and MACCS is consistent with distance; the location of AERMOD in the order changes between the neutrally-stable and stable conditions. Using these results, a strategy for modifying the input to the MACCS calculation to bound the results from the other three codes is developed.

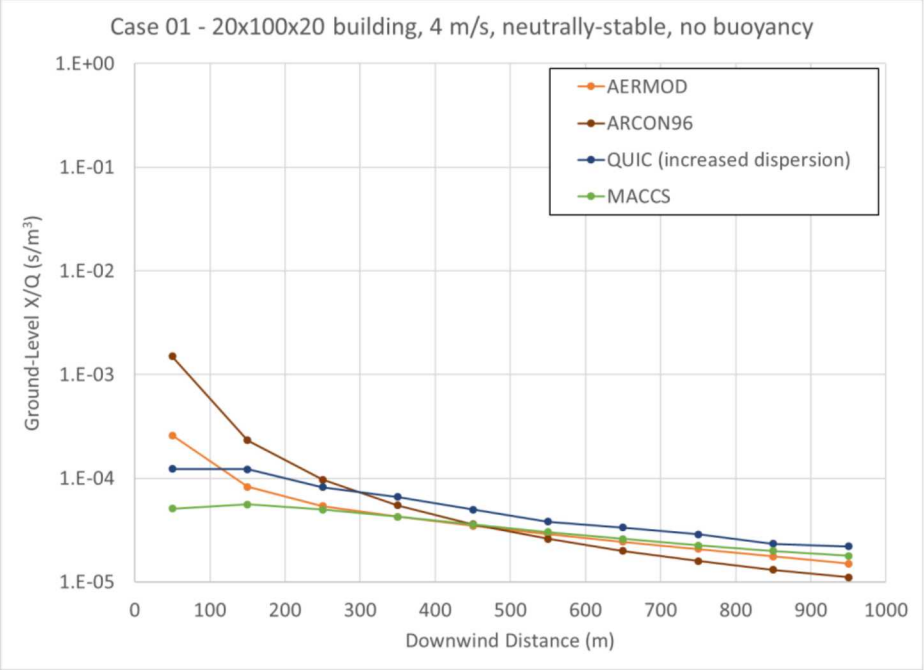

Figure 5-1. Ground-level, time-integrated X/Q versus distance for Case 01 for AERMOD, ARCON96, QUIC and MACCS

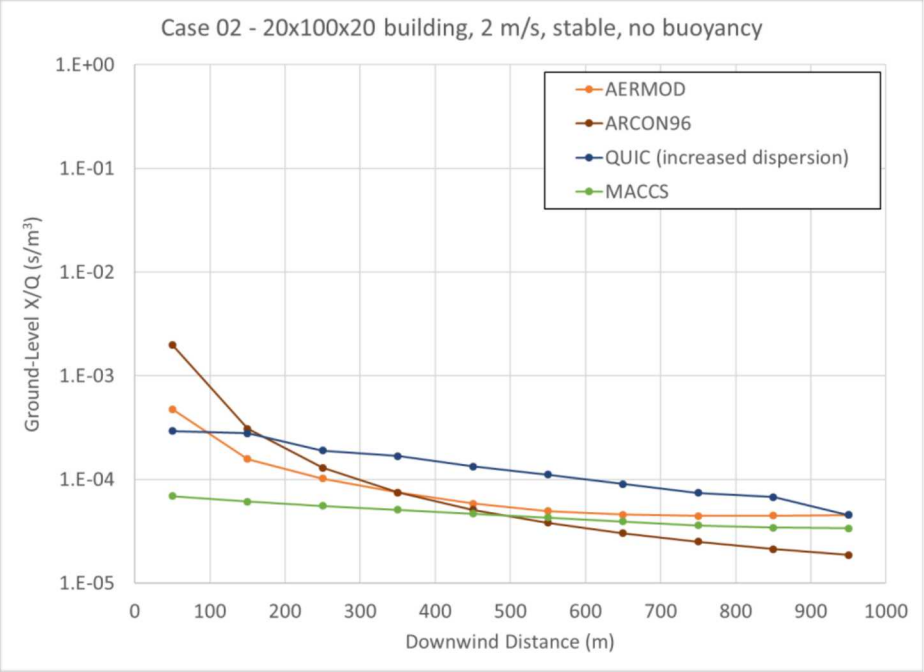

Figure 5-2. Ground-level, time-integrated X/Q versus distance for Case 02 for AERMOD, ARCON96, QUIC and MACCS

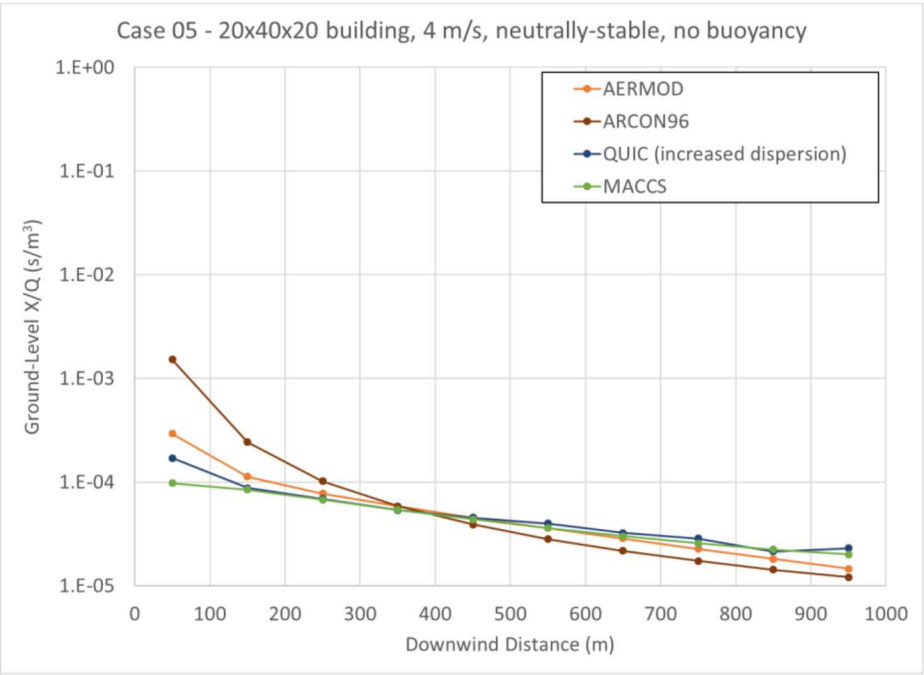

Figure 5-3. Ground-level, time-integrated X/Q versus distance for Case 05 for AERMOD, ARCON96, QUIC and MACCS

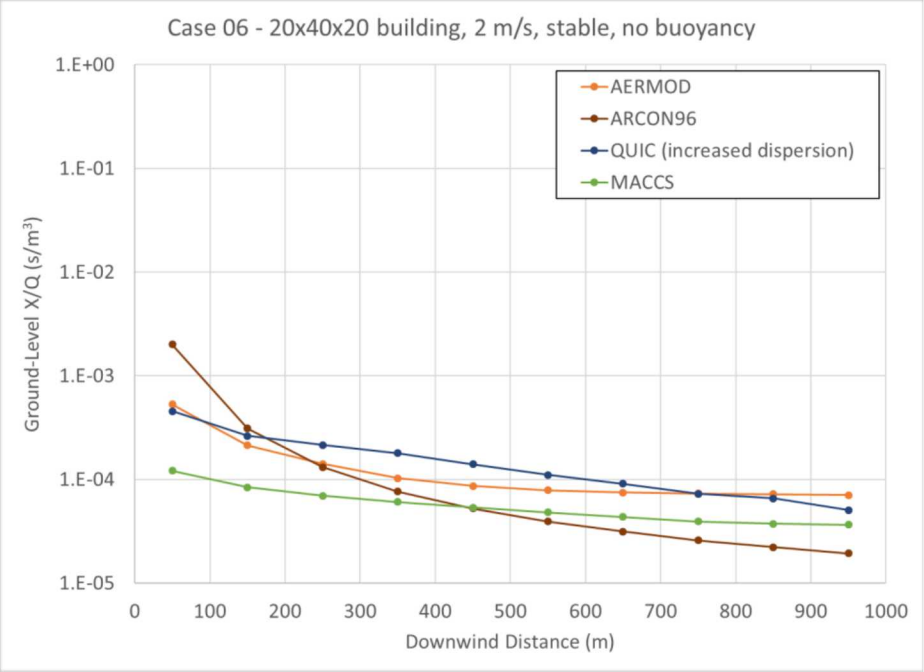

Figure 5-4. Ground-level, time-integrated X/Q versus distance for Case 06 for AERMOD, ARCON96, QUIC and MACCS

The first modification made to the MACCS input to bound the results from the other three codes is to specify a ground-level release, instead of a release at the height of the building. This is motivated by the Section 4.2 discussion of the ARCON96 model, which showed little to no dependence on elevation of the release or inclusion of the building, and the wake-induced building downwash observed in Figure 4-21, Figure 4-22, Figure 4-23, and Figure 4-24. Furthermore, Regulatory Guide 1.145 [10] discusses the modeling practice that release from sources with an elevation less than 2.5 times the building height should be modeled as ground-level releases. The results for Case 01, Case 02, Case 05, and Case 06 with the MACCS input modified to reflect a ground-level release (ground) compared with the AERMOD, ARCON96 and QUIC calculations are shown in Figure 5-5, Figure 5-6, Figure 5-7, and Figure 5-8, respectively. As seen in these figures, the modified MACCS results bound the results from AERMOD and QUIC for the entire 1000 m and the ARCON96 results from 150-250 m up to 1000 m. Based on these results, the modified ground MACCS inputs provide adequate nearfield results that are bounding.

If additional conservatism is needed or desired, a second modification can be made to the MACCS inputs. To mirror the ARCON96 model with no dependence on building size, the MACCS input can be modified to set the initial dispersion parameters to those used for a point-source (initial σ_y and σ_z = 0.1 m). This is the same as the DOE approach to conservatively estimate doses to collocated workers. The results for Case 01, Case 02, Case 05, and Case 06 with the MACCS inputs modified to reflect a point-source, ground-level release (ground, no area source) compared with the AERMOD, ARCON96 and QUIC calculations are shown in Figure 5-5, Figure 5-6, Figure 5-7, and Figure 5-8, respectively. These figures show that using a point-source in the MACCS calculations is enough to bound the other results over the entire distance range. If using a point-source is considered too bounding, another alternative is to use an intermediate area source between the standard values and a point-source. For example, area source parameters could be derived assuming concentrations at the ground-level building edges and top centerline locations less than 10% of the

ground-level centerline value, where 10% is the standard recommendation for defining an area source with MACCS [23].

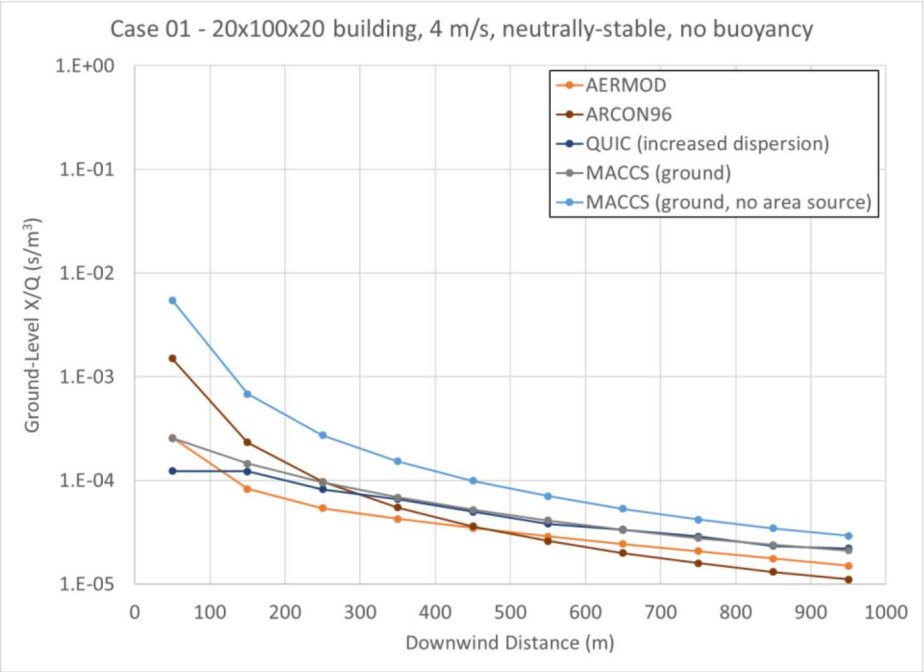

Figure 5-5. Ground-level, time-integrated X/Q versus distance for Case 01 for AERMOD, ARCON96, QUIC compared with modified MACCS calculations

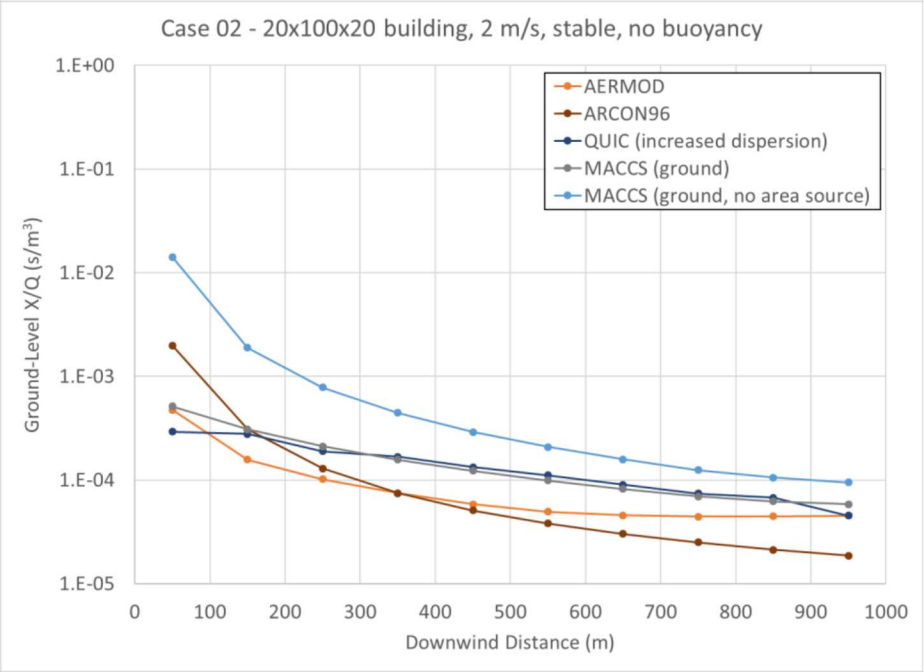

Figure 5-6. Ground-level, time-integrated X/Q versus distance for Case 02 for AERMOD, ARCON96, QUIC compared with modified MACCS calculations

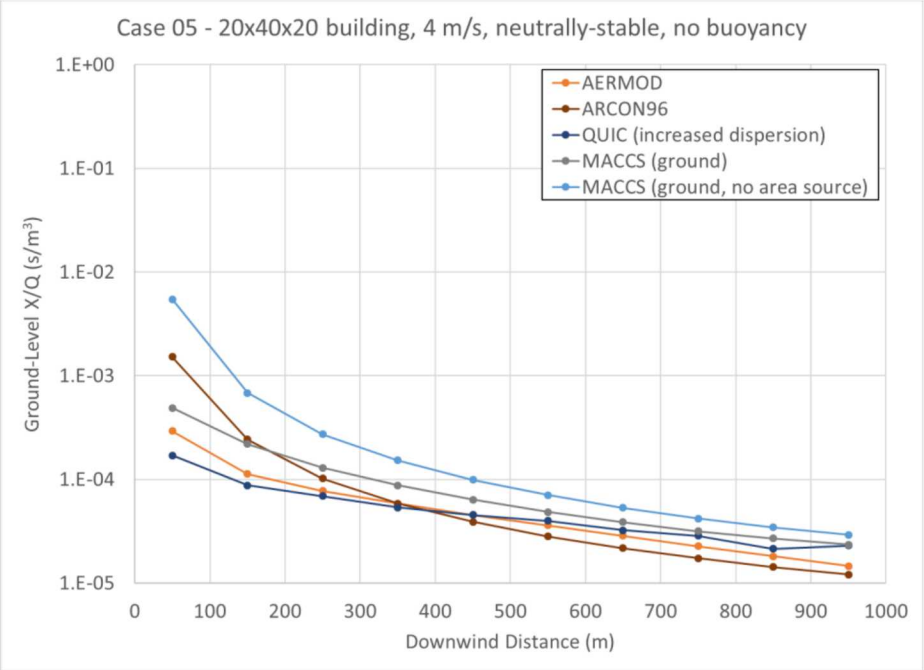

Figure 5-7. Ground-level, time-integrated X/Q versus distance for Case 05 for AERMOD, ARCON96, QUIC compared with modified MACCS calculations

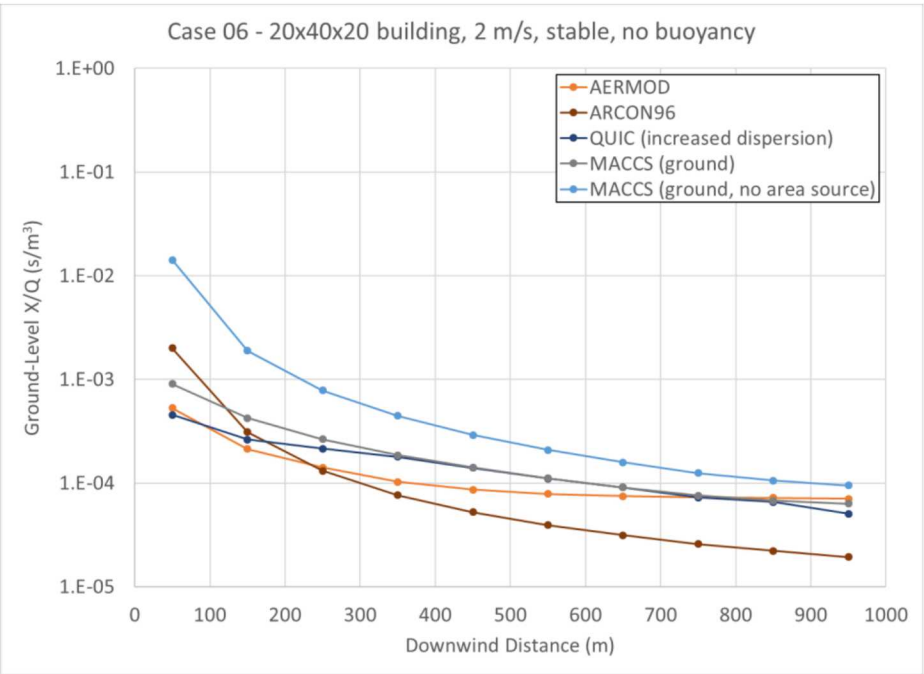

Figure 5-8. Ground-level, time-integrated X/Q versus distance for Case 06 for AERMOD, ARCON96, QUIC compared with modified MACCS calculations

Four of the test cases include a building and a buoyant plume, Case 03, Case 04, Case 07, and Case 08. The results from the AERMOD and MACCS codes for those four test cases are shown in Figure 5-9, Figure 5-10, Figure 5-11, and Figure 5-12, respectively. In all four cases, the AERMOD results for X/Q are higher over a significant portion of the distance range than the MACCS values. This is most evident for the stable cases (Case 04 and Case 08), where the AERMOD values of X/Q are higher over the entire range. Using these results, a strategy for modifying the input to the MACCS calculation to bound the results from AERMOD is developed.

As discussed above, the first modification made to the MACCS input to bound the results from the other three codes is to specify a ground-level release instead of a release at the height of the building. For the cases that include a buoyant plume, a similar modification is to ignore buoyancy. This is motivated by the Section 4.1 discussion that the AERMOD model showed very little dependence on the heat content of the plume. The results for Case 03, Case 04, Case 07, and Case 08 with the MACCS input modified to reflect a ground-level release with no buoyancy (ground, no heat) compared with the AERMOD calculations are shown in Figure 5-9, Figure 5-10, Figure 5-11, and Figure 5-12, respectively. These figures show that the modified MACCS results, assuming a ground release with no buoyancy (but still including an area source), bound the results from AERMOD for the entire 1000 m. Based on these results, the modified MACCS inputs provide adequate nearfield results that are bounding.

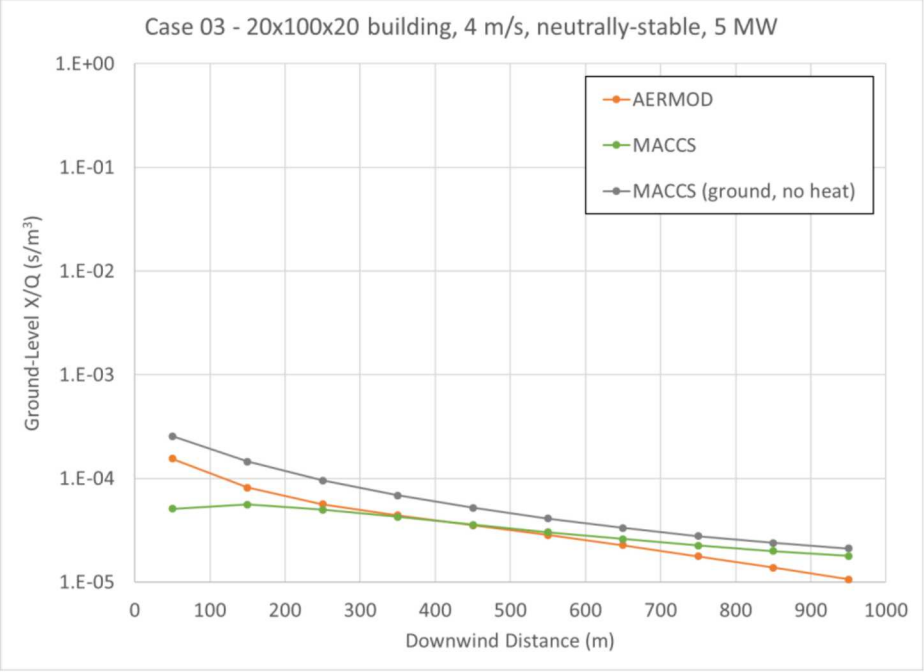

Figure 5-9. Ground-level, time-integrated X/Q versus distance for Case 03 for AERMOD and MACCS compared with modified MACCS calculations

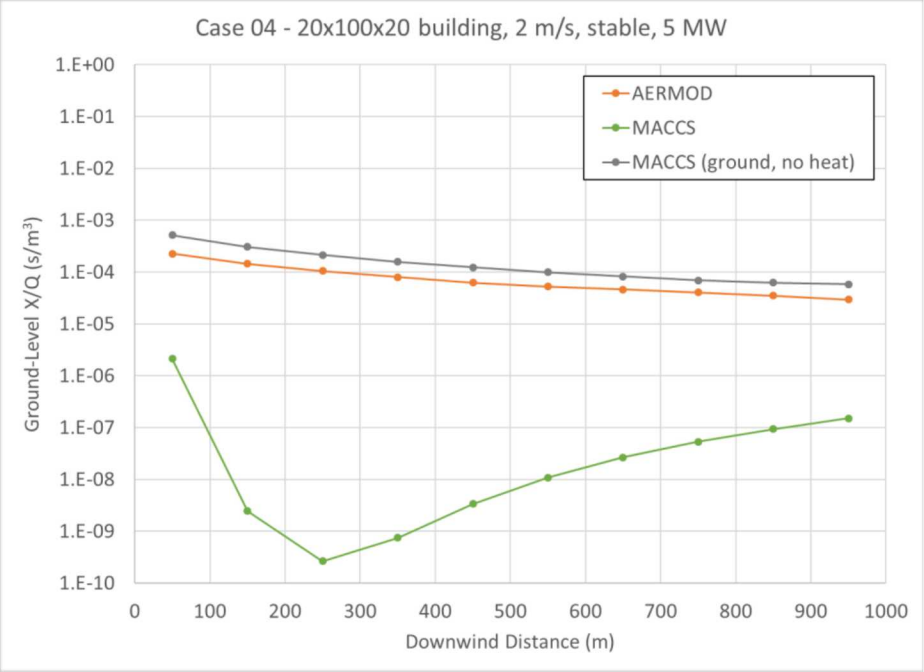

Figure 5-10. Ground-level, time-integrated X/Q versus distance for Case 04 for AERMOD and MACCS compared with modified MACCS calculations

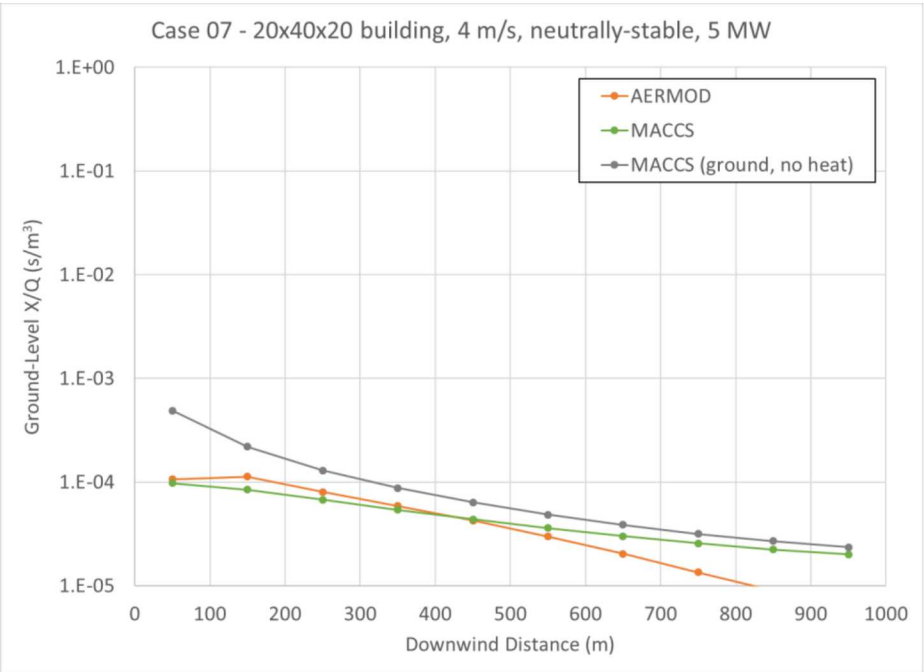

Figure 5-11. Ground-level, time-integrated X/Q versus distance for Case 07 for AERMOD and MACCS compared with modified MACCS calculations

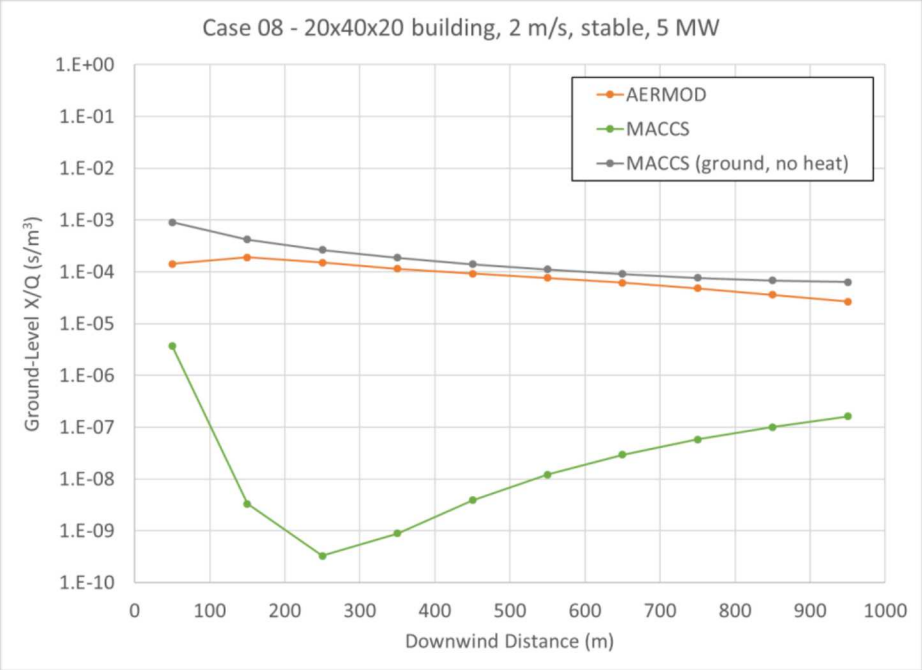

Figure 5-12. Ground-level, time-integrated X/Q versus distance for Case 08 for AERMOD and MACCS compared with modified MACCS calculations

6. SUMMARY

Three codes are used for comparisons in this report to evaluate the adequacy of MACCS in the nearfield; ARCON96, AERMOD and QUIC. In this evaluation, test cases were developed to give a broad range of weather conditions, building dimensions and plume buoyancy. The test cases are not intended to be exhaustive, but rather to represent the range of potential conditions.

Two weather conditions were chosen. The first condition is a constant wind field of 4 m/s with neutral stability (Pasquill-Gifford stability class D). This condition was selected as a typical weather condition for comparison. The second condition is a constant wind field of 2 m/s with stable conditions (Pasquill-Gifford stability class F). This weather condition was selected as a reduced dispersion condition that would result in higher ground-level concentrations and potentially highlight differences between models. Because nearfield doses are commonly evaluated at the 95th percentile for licensing applications, the weather conditions that were chosen are biased toward the stable end of the range to represent the ones more likely to represent a 95th percentile exposure.

For building dimensions, three configurations were chosen. The first configuration includes a building 20 m tall, 40 m wide and 20 m deep and was selected to represent a typical building size. The second configuration includes a building 20 m tall, 100 m wide and 20 m deep and was selected to represent a building with a more extreme width to height ratio. The third configuration has no building, but rather is an elevated point source and was selected to evaluate basic differences in dispersion models between the codes in the absence of confounding factors.

For the buoyancy condition, two variations were chosen, with and without buoyancy. For the cases with buoyancy, a plume energy content of 5 MW is used. These variations were chosen to evaluate the interactions between plume rise models and building wake models used in the four codes.

MACCS was run for the test cases with the Eimutis and Konicek dispersion parameter formulation [8] and the "NEW" meander model [9][10]. Based on the comparisons of MACCS with ARCON96, AERMOD and QUIC across the test cases, the following observations are made:

- MACCS calculations configured with point-source, ground-level, nonbuoyant plumes provide conservative nearfield results that bound the centerline, ground-level air concentrations from AERMOD, ARCON96, and QUIC.
- MACCS calculations with ground-level, nonbuoyant plumes that include the effects of the building wake (area source) provide nearfield results that bound the results from AERMOD and QUIC and the results from ARCON96 at distances >250 m.
- If using a point-source is too conservative and it is desired to bound the results from all three codes, another alternative is to use area source parameters in MACCS that are less than the standard values, i.e., an area source intermediate between the standard recommendation and a point source.

All of these options provide results from MACCS that are bounding for the test cases evaluated. Based on these observations, it appears that MACCS is adequate for use in nearfield calculations when using the following settings:

- The parameterization of Eimutis and Konicek [8] for the dispersion model.
- The plume meander model based on NUREG/CR-2260 [9] and Regulatory Guide 1.145 [10]. This model is selected by setting the value of the MACCS parameter MNDMOD to "NEW".

- The release modeled as a ground-level, nonbuoyant plume.
- The inclusion of the effects of the building wake (area source).

This report demonstrates that MACCS can be used at distances significantly shorter than 500 m downwind from a containment or reactor building (or other building from which a radioactive release occurs), contrary to the comment in Chanin and Young [4]. However, the MACCS user needs to select the MACCS input parameters appropriately to generate results that are adequately conservative for a specific application. Conservatism in the context of this report is based on centerline, ground-level air concentration, which translates to other results that are proportional to this concentration.

REFERENCES

[1] Y. Tominaga and T. Stathopoulos, 2016, "Ten Questions Concerning Modeling of Near-Field Pollutant Dispersion in the Built Environment," Building and Environment 105, 390-402.

[2] U.S. Nuclear Regulatory Commission (NRC), 2019, "NRC Non-Light Water Reactor (Non-LWR) Vision and Strategy, Volume 3: Computer Code Development Plans for Severe Accident Progression, Source Term, and Consequence Analysis," ML19093B404, US Nuclear Regulatory Commission, Washington D.C., April 2019. https://www.nrc.gov/docs/ML1909/ML19093B404.pdf

[3] N. Bixler, F. Walton, L. Eubanks, R. Haaker, and K. McFadden, to be published in 2020, "MELCOR Accident Consequence Analysis Code System (MACCS) – User's Guide and Reference Manual," NUREG/CR-XXXX Vol. 1, Nuclear Regulatory Commission, Washington, DC.

[4] D. Chanin and M.L. Young, 1998, "Code Manual for MACCS2 – User's Guide," NUREG/CR-6613 Vol. 1, Nuclear Regulatory Commission, Washington, DC.

[5] A.A. Simpkins, 2007, "Summary of Near-Field Methods for Atmospheric Release Modeling," ML072500257, Southwest Research Institute, San Antonio, TX, June 2007.

[6] U.S. Department of Energy (DOE), 2015, "Technical Report for Calculations of Atmospheric Dispersion at Onsite Locations for Department of Energy Nuclear Facilities," NSRD-2015-TD01, Nuclear Safety Research and Development, Washington D.C., April 2015.

[7] B.A. Napier, J.P. Rishel, and N.E. Bixler, 2011, "Final Review of Safety Assessment Issues at Savannah River Site, August 2011," PNNL-20990, Pacific Northwest National Laboratory, Richland, Washington.

[8] E.C. Eimutis, M.G. Konicek, 1972, "Derivations of Continuous Functions for the Lateral and Vertical Atmospheric Dispersion Coefficients," **Atmospheric Environment 6**, 859-863.

[9] W.G. Snell, and R.W. Jubach, 1981, "Technical Basis for Regulatory Guide 1.145, Atmospheric Dispersion Models for Potential Accident Consequence Assessments at Nuclear Power Plants," NUREG/CR-2260 / NUS-3854, NUS Corporation, October 1981.

[10] U.S. Nuclear Regulatory Commission (NRC), 1982, "Atmospheric Dispersion Models for Potential Accident Consequence Assessments at Nuclear Power Plants, Rev. 1," RG 1.145, US Nuclear Regulatory Commission, Washington D.C, November 1982 (reissued February 1983).

[11] CFD Direct, 2018, "OpenFOAM User Guide," https://cfd.direct/openfoam/user-guide/.

[12] M. Nelson and M. Brown, 2013, "The QUIC Start Guide (v 6.0.1)," LA-UR-13-27291, Los Alamos National Laboratory, Los Alamos, New Mexico.

[13] J.V. Ramsdell Jr. and C.A. Simonen, 1997, "Atmospheric Relative Concentrations in Building Wakes," NUREG/CR-6331 Rev. 1, Nuclear Regulatory Commission, Washington, DC.

[14] A.J. Cimorelli, S.G. Perry, A. Venkatram, J.C. Weil, R.J. Paine, R.B. Wilson, R.F. Lee, W.D. Peters, and R.W. Brode, 2005, "AERMOD: A Dispersion Model for Industrial Source Applications. Part I: General Model Formulation and Boundary Layer Characterization," American Meteorological Society, Journals Online, https://doi.org/10.1175/JAM2227.1.

[15] A. Gowardhan, M. Brown, M. Williams, E. Pardyjak, 2006, "Evaluation of the QUIC Urban Dispersion Model using the Salt Lake City URBAN 2000 Tracer Experiment Data - IOP 10," https://www.researchgate.net/publication/252751189.

[16] M. Brown, A. Gowardhan, M. Nelson, M. Williams, and E. Pardyjak, 2014, "Evaluation of the QUIC Wind and Dispersion Models Using the Joint Urban 2003 Field Experiment Dataset," https://www.researchgate.net/publication/255616796.

[17] J.V. Ramsdell Jr. and C.J. Fosmire, 1995, "Atmospheric Dispersion Estimates in the Vicinity of Buildings," PNL-10286, Pacific Northwest National Laboratory, Richland, Washington.

[18] L.L. Schulman, D.G. Strimaitis, and J.S. Scire, 2000, "Development and evaluation of the PRIME plume rise and building downwash model," **J. Air Waste Manage. Assoc. 50**, 378–390.

[19] A. Venkatram, V. Isakov, J. Yuan, and D. Pankratz, 2004, "Modeling Dispersion at Distances of Meters from Urban Sources," **Atmospheric Environment 38**, 4633-4641.

[20] R.P. Hosker and W.R. Pendergrass, "Flow and Dispersion near Clusters of Buildings," NUREG/CR-4113, Nuclear Regulatory Commission, Washington, DC.

[21] D. Golder, 1972, "Relations among Stability Parameters in the Surface Layer," Boundary-Layer Meteorology 3, 47-58.

[22] S.R. Hanna, G.A. Briggs, R.P. Hosker, Jr., 1982. "Handbook on Atmospheric Diffusion," DOE/TIC-11223.

[23] D.B. Turner 1970, "Workbook of Atmospheric Dispersion Estimates" (PSH-999-AP-26), US Department of Health, Education, and Welfare, Washington, DC, 32-34.

APPENDIX A. AERMOD INPUT FILES

Representative input files used in the evaluation of the test cases are shown below to illustrate implementation. The reader is directed to the code user manual to interpret the files.

A.1. Weather Input File – 4D.sfc

```
   41.3N    74.0W        UA_ID: 00014735  SF_ID:   14735  OS_ID:   99999    VERSION: 15181    CCVR_Sub
88  3  1  61  1  -3.7  0.275 -9.000 -9.000 -999. 2000.  500.0  0.0300  1.00  1.00   4.00 270.0  10.0 282.2  10.0    0 -9.00   50. 1005.   10 NAD-OS  NoSubs
88  3  1  61  2  -3.7  0.275 -9.000 -9.000 -999. 2000.  500.0  0.0300  1.00  1.00   4.00 270.0  10.0 282.2  10.0    0 -9.00   50. 1005.   10 NAD-OS  NoSubs
88  3  1  61  3  -3.7  0.275 -9.000 -9.000 -999. 2000.  500.0  0.0300  1.00  1.00   4.00 270.0  10.0 282.2  10.0    0 -9.00   50. 1005.   10 NAD-OS  NoSubs
88  3  1  61  4  -3.7  0.275 -9.000 -9.000 -999. 2000.  500.0  0.0300  1.00  1.00   4.00 270.0  10.0 282.2  10.0    0 -9.00   50. 1005.   10 NAD-OS  NoSubs
88  3  1  61  5  -3.7  0.275 -9.000 -9.000 -999. 2000.  500.0  0.0300  1.00  1.00   4.00 270.0  10.0 282.2  10.0    0 -9.00   50. 1005.   10 NAD-OS  NoSubs
88  3  1  61  6  -3.7  0.275 -9.000 -9.000 -999. 2000.  500.0  0.0300  1.00  1.00   4.00 270.0  10.0 282.2  10.0    0 -9.00   50. 1005.   10 NAD-OS  NoSubs
88  3  1  61  7  -3.7  0.275 -9.000 -9.000 -999. 2000.  500.0  0.0300  1.00  1.00   4.00 270.0  10.0 282.2  10.0    0 -9.00   50. 1005.   10 NAD-OS  NoSubs
88  3  1  61  8  -3.7  0.275 -9.000 -9.000 -999. 2000.  500.0  0.0300  1.00  1.00   4.00 270.0  10.0 282.2  10.0    0 -9.00   50. 1005.   10 NAD-OS  NoSubs
88  3  1  61  9  -3.7  0.275 -9.000 -9.000 -999. 2000.  500.0  0.0300  1.00  1.00   4.00 270.0  10.0 282.2  10.0    0 -9.00   50. 1005.   10 NAD-OS  NoSubs
88  3  1  61 10  -3.7  0.275 -9.000 -9.000 -999. 2000.  500.0  0.0300  1.00  1.00   4.00 270.0  10.0 282.2  10.0    0 -9.00   50. 1005.   10 NAD-OS  NoSubs
88  3  1  61 11  -3.7  0.275 -9.000 -9.000 -999. 2000.  500.0  0.0300  1.00  1.00   4.00 270.0  10.0 282.2  10.0    0 -9.00   50. 1005.   10 NAD-OS  NoSubs
88  3  1  61 12  -3.7  0.275 -9.000 -9.000 -999. 2000.  500.0  0.0300  1.00  1.00   4.00 270.0  10.0 282.2  10.0    0 -9.00   50. 1005.   10 NAD-OS  NoSubs
88  3  1  61 13  -3.7  0.275 -9.000 -9.000 -999. 2000.  500.0  0.0300  1.00  1.00   4.00 270.0  10.0 282.2  10.0    0 -9.00   50. 1005.   10 NAD-OS  NoSubs
88  3  1  61 14  -3.7  0.275 -9.000 -9.000 -999. 2000.  500.0  0.0300  1.00  1.00   4.00 270.0  10.0 282.2  10.0    0 -9.00   50. 1005.   10 NAD-OS  NoSubs
88  3  1  61 15  -3.7  0.275 -9.000 -9.000 -999. 2000.  500.0  0.0300  1.00  1.00   4.00 270.0  10.0 282.2  10.0    0 -9.00   50. 1005.   10 NAD-OS  NoSubs
88  3  1  61 16  -3.7  0.275 -9.000 -9.000 -999. 2000.  500.0  0.0300  1.00  1.00   4.00 270.0  10.0 282.2  10.0    0 -9.00   50. 1005.   10 NAD-OS  NoSubs
88  3  1  61 17  -3.7  0.275 -9.000 -9.000 -999. 2000.  500.0  0.0300  1.00  1.00   4.00 270.0  10.0 282.2  10.0    0 -9.00   50. 1005.   10 NAD-OS  NoSubs
88  3  1  61 18  -3.7  0.275 -9.000 -9.000 -999. 2000.  500.0  0.0300  1.00  1.00   4.00 270.0  10.0 282.2  10.0    0 -9.00   50. 1005.   10 NAD-OS  NoSubs
88  3  1  61 19  -3.7  0.275 -9.000 -9.000 -999. 2000.  500.0  0.0300  1.00  1.00   4.00 270.0  10.0 282.2  10.0    0 -9.00   50. 1005.   10 NAD-OS  NoSubs
88  3  1  61 20  -3.7  0.275 -9.000 -9.000 -999. 2000.  500.0  0.0300  1.00  1.00   4.00 270.0  10.0 282.2  10.0    0 -9.00   50. 1005.   10 NAD-OS  NoSubs
88  3  1  61 21  -3.7  0.275 -9.000 -9.000 -999. 2000.  500.0  0.0300  1.00  1.00   4.00 270.0  10.0 282.2  10.0    0 -9.00   50. 1005.   10 NAD-OS  NoSubs
88  3  1  61 22  -3.7  0.275 -9.000 -9.000 -999. 2000.  500.0  0.0300  1.00  1.00   4.00 270.0  10.0 282.2  10.0    0 -9.00   50. 1005.   10 NAD-OS  NoSubs
88  3  1  61 23  -3.7  0.275 -9.000 -9.000 -999. 2000.  500.0  0.0300  1.00  1.00   4.00 270.0  10.0 282.2  10.0    0 -9.00   50. 1005.   10 NAD-OS  NoSubs
88  3  1  61 24  -3.7  0.275 -9.000 -9.000 -999. 2000.  500.0  0.0300  1.00  1.00   4.00 270.0  10.0 282.2  10.0    0 -9.00   50. 1005.   10 NAD-OS  NoSubs
```

A.2. Weather Input File – 4D.pfl

```
88  3  1  1   10.0 0  270.0   4.00   9.00   99.00   99.00
88  3  1  1   100.0 1  270.0   4.00   8.00   99.00   99.00
88  3  1  2   10.0 0  270.0   4.00   9.00   99.00   99.00
88  3  1  2   100.0 1  270.0   4.00   8.00   99.00   99.00
88  3  1  3   10.0 0  270.0   4.00   9.00   99.00   99.00
88  3  1  3   100.0 1  270.0   4.00   8.00   99.00   99.00
88  3  1  4   10.0 0  270.0   4.00   9.00   99.00   99.00
88  3  1  4   100.0 1  270.0   4.00   8.00   99.00   99.00
88  3  1  5   10.0 0  270.0   4.00   9.00   99.00   99.00
88  3  1  5   100.0 1  270.0   4.00   8.00   99.00   99.00
88  3  1  6   10.0 0  270.0   4.00   9.00   99.00   99.00
88  3  1  6   100.0 1  270.0   4.00   8.00   99.00   99.00
88  3  1  7   10.0 0  270.0   4.00   9.00   99.00   99.00
88  3  1  7   100.0 1  270.0   4.00   8.00   99.00   99.00
88  3  1  8   10.0 0  270.0   4.00   9.00   99.00   99.00
88  3  1  8   100.0 1  270.0   4.00   8.00   99.00   99.00
88  3  1  9   10.0 0  270.0   4.00   9.00   99.00   99.00
88  3  1  9   100.0 1  270.0   4.00   8.00   99.00   99.00
88  3  1 10   10.0 0  270.0   4.00   9.00   99.00   99.00
88  3  1 10   100.0 1  270.0   4.00   8.00   99.00   99.00
88  3  1 11   10.0 0  270.0   4.00   9.00   99.00   99.00
88  3  1 11   100.0 1  270.0   4.00   8.00   99.00   99.00
88  3  1 12   10.0 0  270.0   4.00   9.00   99.00   99.00
88  3  1 12   100.0 1  270.0   4.00   8.00   99.00   99.00
88  3  1 13   10.0 0  270.0   4.00   9.00   99.00   99.00
88  3  1 13   100.0 1  270.0   4.00   8.00   99.00   99.00
88  3  1 14   10.0 0  270.0   4.00   9.00   99.00   99.00
88  3  1 14   100.0 1  270.0   4.00   8.00   99.00   99.00
88  3  1 15   10.0 0  270.0   4.00   9.00   99.00   99.00
88  3  1 15   100.0 1  270.0   4.00   8.00   99.00   99.00
88  3  1 16   10.0 0  270.0   4.00   9.00   99.00   99.00
88  3  1 16   100.0 1  270.0   4.00   8.00   99.00   99.00
88  3  1 17   10.0 0  270.0   4.00   9.00   99.00   99.00
88  3  1 17   100.0 1  270.0   4.00   8.00   99.00   99.00
88  3  1 18   10.0 0  270.0   4.00   9.00   99.00   99.00
88  3  1 18   100.0 1  270.0   4.00   8.00   99.00   99.00
88  3  1 19   10.0 0  270.0   4.00   9.00   99.00   99.00
88  3  1 19   100.0 1  270.0   4.00   8.00   99.00   99.00
88  3  1 20   10.0 0  270.0   4.00   9.00   99.00   99.00
88  3  1 20   100.0 1  270.0   4.00   8.00   99.00   99.00
88  3  1 21   10.0 0  270.0   4.00   9.00   99.00   99.00
88  3  1 21   100.0 1  270.0   4.00   8.00   99.00   99.00
88  3  1 22   10.0 0  270.0   4.00   9.00   99.00   99.00
88  3  1 22   100.0 1  270.0   4.00   8.00   99.00   99.00
88  3  1 23   10.0 0  270.0   4.00   9.00   99.00   99.00
88  3  1 23   100.0 1  270.0   4.00   8.00   99.00   99.00
88  3  1 24   10.0 0  270.0   4.00   9.00   99.00   99.00
88  3  1 24   100.0 1  270.0   4.00   8.00   99.00   99.00
```

A.3. Weather Input File – 2F.sfc

```
    41.3N    74.0W        UA_ID: 00014735  SF_ID:    14735  OS_ID:    99999    VERSION: 15181    CCVR_Sub
88  3  1  61  1  -4.0  0.082 -9.000 -9.000 -999. 2000.  12.5  0.0300  1.00  1.00  2.00 270.0  10.0 282.2  10.0  0 -9.00  50. 1005.  0 NAD-OS  NoSubs
88  3  1  61  2  -4.0  0.082 -9.000 -9.000 -999. 2000.  12.5  0.0300  1.00  1.00  2.00 270.0  10.0 282.2  10.0  0 -9.00  50. 1005.  0 NAD-OS  NoSubs
88  3  1  61  3  -4.0  0.082 -9.000 -9.000 -999. 2000.  12.5  0.0300  1.00  1.00  2.00 270.0  10.0 282.2  10.0  0 -9.00  50. 1005.  0 NAD-OS  NoSubs
88  3  1  61  4  -4.0  0.082 -9.000 -9.000 -999. 2000.  12.5  0.0300  1.00  1.00  2.00 270.0  10.0 282.2  10.0  0 -9.00  50. 1005.  0 NAD-OS  NoSubs
88  3  1  61  5  -4.0  0.082 -9.000 -9.000 -999. 2000.  12.5  0.0300  1.00  1.00  2.00 270.0  10.0 282.2  10.0  0 -9.00  50. 1005.  0 NAD-OS  NoSubs
88  3  1  61  6  -4.0  0.082 -9.000 -9.000 -999. 2000.  12.5  0.0300  1.00  1.00  2.00 270.0  10.0 282.2  10.0  0 -9.00  50. 1005.  0 NAD-OS  NoSubs
88  3  1  61  7  -4.0  0.082 -9.000 -9.000 -999. 2000.  12.5  0.0300  1.00  1.00  2.00 270.0  10.0 282.2  10.0  0 -9.00  50. 1005.  0 NAD-OS  NoSubs
88  3  1  61  8  -4.0  0.082 -9.000 -9.000 -999. 2000.  12.5  0.0300  1.00  1.00  2.00 270.0  10.0 282.2  10.0  0 -9.00  50. 1005.  0 NAD-OS  NoSubs
88  3  1  61  9  -4.0  0.082 -9.000 -9.000 -999. 2000.  12.5  0.0300  1.00  1.00  2.00 270.0  10.0 282.2  10.0  0 -9.00  50. 1005.  0 NAD-OS  NoSubs
88  3  1  61 10  -4.0  0.082 -9.000 -9.000 -999. 2000.  12.5  0.0300  1.00  1.00  2.00 270.0  10.0 282.2  10.0  0 -9.00  50. 1005.  0 NAD-OS  NoSubs
88  3  1  61 11  -4.0  0.082 -9.000 -9.000 -999. 2000.  12.5  0.0300  1.00  1.00  2.00 270.0  10.0 282.2  10.0  0 -9.00  50. 1005.  0 NAD-OS  NoSubs
88  3  1  61 12  -4.0  0.082 -9.000 -9.000 -999. 2000.  12.5  0.0300  1.00  1.00  2.00 270.0  10.0 282.2  10.0  0 -9.00  50. 1005.  0 NAD-OS  NoSubs
88  3  1  61 13  -4.0  0.082 -9.000 -9.000 -999. 2000.  12.5  0.0300  1.00  1.00  2.00 270.0  10.0 282.2  10.0  0 -9.00  50. 1005.  0 NAD-OS  NoSubs
88  3  1  61 14  -4.0  0.082 -9.000 -9.000 -999. 2000.  12.5  0.0300  1.00  1.00  2.00 270.0  10.0 282.2  10.0  0 -9.00  50. 1005.  0 NAD-OS  NoSubs
88  3  1  61 15  -4.0  0.082 -9.000 -9.000 -999. 2000.  12.5  0.0300  1.00  1.00  2.00 270.0  10.0 282.2  10.0  0 -9.00  50. 1005.  0 NAD-OS  NoSubs
88  3  1  61 16  -4.0  0.082 -9.000 -9.000 -999. 2000.  12.5  0.0300  1.00  1.00  2.00 270.0  10.0 282.2  10.0  0 -9.00  50. 1005.  0 NAD-OS  NoSubs
88  3  1  61 17  -4.0  0.082 -9.000 -9.000 -999. 2000.  12.5  0.0300  1.00  1.00  2.00 270.0  10.0 282.2  10.0  0 -9.00  50. 1005.  0 NAD-OS  NoSubs
88  3  1  61 18  -4.0  0.082 -9.000 -9.000 -999. 2000.  12.5  0.0300  1.00  1.00  2.00 270.0  10.0 282.2  10.0  0 -9.00  50. 1005.  0 NAD-OS  NoSubs
88  3  1  61 19  -4.0  0.082 -9.000 -9.000 -999. 2000.  12.5  0.0300  1.00  1.00  2.00 270.0  10.0 282.2  10.0  0 -9.00  50. 1005.  0 NAD-OS  NoSubs
88  3  1  61 20  -4.0  0.082 -9.000 -9.000 -999. 2000.  12.5  0.0300  1.00  1.00  2.00 270.0  10.0 282.2  10.0  0 -9.00  50. 1005.  0 NAD-OS  NoSubs
88  3  1  61 21  -4.0  0.082 -9.000 -9.000 -999. 2000.  12.5  0.0300  1.00  1.00  2.00 270.0  10.0 282.2  10.0  0 -9.00  50. 1005.  0 NAD-OS  NoSubs
88  3  1  61 22  -4.0  0.082 -9.000 -9.000 -999. 2000.  12.5  0.0300  1.00  1.00  2.00 270.0  10.0 282.2  10.0  0 -9.00  50. 1005.  0 NAD-OS  NoSubs
88  3  1  61 23  -4.0  0.082 -9.000 -9.000 -999. 2000.  12.5  0.0300  1.00  1.00  2.00 270.0  10.0 282.2  10.0  0 -9.00  50. 1005.  0 NAD-OS  NoSubs
88  3  1  61 24  -4.0  0.082 -9.000 -9.000 -999. 2000.  12.5  0.0300  1.00  1.00  2.00 270.0  10.0 282.2  10.0  0 -9.00  50. 1005.  0 NAD-OS  NoSubs
```

A.4. Weather Input File – 2F.pfl

```
88  3  1  1    10.0 0   270.0     2.00     9.00    99.00    99.00
88  3  1  1   100.0 1   270.0     2.00    12.00    99.00    99.00
88  3  1  2    10.0 0   270.0     2.00     9.00    99.00    99.00
88  3  1  2   100.0 1   270.0     2.00    12.00    99.00    99.00
88  3  1  3    10.0 0   270.0     2.00     9.00    99.00    99.00
88  3  1  3   100.0 1   270.0     2.00    12.00    99.00    99.00
88  3  1  4    10.0 0   270.0     2.00     9.00    99.00    99.00
88  3  1  4   100.0 1   270.0     2.00    12.00    99.00    99.00
88  3  1  5    10.0 0   270.0     2.00     9.00    99.00    99.00
88  3  1  5   100.0 1   270.0     2.00    12.00    99.00    99.00
88  3  1  6    10.0 0   270.0     2.00     9.00    99.00    99.00
88  3  1  6   100.0 1   270.0     2.00    12.00    99.00    99.00
88  3  1  7    10.0 0   270.0     2.00     9.00    99.00    99.00
88  3  1  7   100.0 1   270.0     2.00    12.00    99.00    99.00
88  3  1  8    10.0 0   270.0     2.00     9.00    99.00    99.00
88  3  1  8   100.0 1   270.0     2.00    12.00    99.00    99.00
88  3  1  9    10.0 0   270.0     2.00     9.00    99.00    99.00
88  3  1  9   100.0 1   270.0     2.00    12.00    99.00    99.00
88  3  1 10    10.0 0   270.0     2.00     9.00    99.00    99.00
88  3  1 10   100.0 1   270.0     2.00    12.00    99.00    99.00
88  3  1 11    10.0 0   270.0     2.00     9.00    99.00    99.00
88  3  1 11   100.0 1   270.0     2.00    12.00    99.00    99.00
88  3  1 12    10.0 0   270.0     2.00     9.00    99.00    99.00
88  3  1 12   100.0 1   270.0     2.00    12.00    99.00    99.00
88  3  1 13    10.0 0   270.0     2.00     9.00    99.00    99.00
88  3  1 13   100.0 1   270.0     2.00    12.00    99.00    99.00
88  3  1 14    10.0 0   270.0     2.00     9.00    99.00    99.00
88  3  1 14   100.0 1   270.0     2.00    12.00    99.00    99.00
88  3  1 15    10.0 0   270.0     2.00     9.00    99.00    99.00
88  3  1 15   100.0 1   270.0     2.00    12.00    99.00    99.00
88  3  1 16    10.0 0   270.0     2.00     9.00    99.00    99.00
88  3  1 16   100.0 1   270.0     2.00    12.00    99.00    99.00
88  3  1 17    10.0 0   270.0     2.00     9.00    99.00    99.00
88  3  1 17   100.0 1   270.0     2.00    12.00    99.00    99.00
88  3  1 18    10.0 0   270.0     2.00     9.00    99.00    99.00
88  3  1 18   100.0 1   270.0     2.00    12.00    99.00    99.00
88  3  1 19    10.0 0   270.0     2.00     9.00    99.00    99.00
88  3  1 19   100.0 1   270.0     2.00    12.00    99.00    99.00
88  3  1 20    10.0 0   270.0     2.00     9.00    99.00    99.00
88  3  1 20   100.0 1   270.0     2.00    12.00    99.00    99.00
88  3  1 21    10.0 0   270.0     2.00     9.00    99.00    99.00
88  3  1 21   100.0 1   270.0     2.00    12.00    99.00    99.00
88  3  1 22    10.0 0   270.0     2.00     9.00    99.00    99.00
88  3  1 22   100.0 1   270.0     2.00    12.00    99.00    99.00
88  3  1 23    10.0 0   270.0     2.00     9.00    99.00    99.00
88  3  1 23   100.0 1   270.0     2.00    12.00    99.00    99.00
88  3  1 24    10.0 0   270.0     2.00     9.00    99.00    99.00
88  3  1 24   100.0 1   270.0     2.00    12.00    99.00    99.00
```

A.5. Case01 Input File

```
**
**   AERMOD
**

CO STARTING
  TITLEONE  Case01 4D 0MW 20x100
  MODELOPT  FLAT CONC DDEP DRYDPLT
  AVERTIME  24  PERIOD
```

```
  POLLUTID  OTHER
  RUNORNOT  RUN
CO FINISHED

SO STARTING
  ELEVUNIT  METERS
  LOCATION  MAIN1   POINT  0.0  0.0  0.0

** Point Source       Mdot  Hgt   Temp  Vel   Diam
** Parameters:        ----  ----  ----  ----  ----
  SRCPARAM  MAIN1     1.0   20.0  0.0   0.0   3.0

  PARTDIAM  MAIN1 0.153 0.285 0.531 0.989  1.84  3.43  6.38  11.9  22.1  41.2
  MASSFRAX  MAIN1 0.092 0.146 0.141 0.144 0.112 0.080 0.072 0.071 0.071 0.071
  PARTDENS  MAIN1   1.0   1.0   1.0   1.0   1.0   1.0   1.0   1.0   1.0   1.0

  BUILDHGT Main1     20.00   20.00   20.00   20.00   20.00   20.00
  BUILDHGT Main1     20.00   20.00   20.00   20.00   20.00   20.00
  BUILDHGT Main1     20.00   20.00   20.00   20.00   20.00   20.00
  BUILDHGT Main1     20.00   20.00   20.00   20.00   20.00   20.00
  BUILDHGT Main1     20.00   20.00   20.00   20.00   20.00   20.00
  BUILDHGT Main1     20.00   20.00   20.00   20.00   20.00   20.00
  BUILDWID Main1     37.06   53.00   67.32   79.60   89.46   96.60
  BUILDWID Main1    100.81  101.95  100.00  101.95  100.81   96.60
  BUILDWID Main1     89.46   79.60   67.32   53.00   37.06   20.00
  BUILDWID Main1     37.06   53.00   67.32   79.60   89.46   96.60
  BUILDWID Main1    100.81  101.95  100.00  101.95  100.81   96.60
  BUILDWID Main1     89.46   79.60   67.32   53.00   37.06   20.00
  BUILDLEN Main1    101.95  100.81   96.60   89.46   79.60   67.32
  BUILDLEN Main1     53.00   37.06   20.00   37.06   53.00   67.32
  BUILDLEN Main1     79.60   89.46   96.60  100.81  101.95  100.00
  BUILDLEN Main1    101.95  100.81   96.60   89.46   79.60   67.32
  BUILDLEN Main1     53.00   37.06   20.00   37.06   53.00   67.32
  BUILDLEN Main1     79.60   89.46   96.60  100.81  101.95  100.00
  XBADJ    Main1    -52.71  -53.83  -53.30  -51.16  -47.46  -42.32
  XBADJ    Main1    -35.89  -28.38  -20.00  -28.38  -35.89  -42.32
  XBADJ    Main1    -47.46  -51.16  -53.30  -53.83  -52.71  -50.00
  XBADJ    Main1    -49.24  -46.98  -43.30  -38.30  -32.14  -25.00
  XBADJ    Main1    -17.10   -8.68    0.00   -8.68  -17.10  -25.00
  XBADJ    Main1    -32.14  -38.30  -43.30  -46.98  -49.24  -50.00
  YBADJ    Main1      9.85    9.40    8.66    7.66    6.43    5.00
  YBADJ    Main1      3.42    1.74    0.00   -1.74   -3.42   -5.00
  YBADJ    Main1     -6.43   -7.66   -8.66   -9.40   -9.85  -10.00
  YBADJ    Main1     -9.85   -9.40   -8.66   -7.66   -6.43   -5.00
  YBADJ    Main1     -3.42   -1.74    0.00    1.74    3.42    5.00
  YBADJ    Main1      6.43    7.66    8.66    9.40    9.85   10.00

  SRCGROUP  ALL
SO FINISHED

RE STARTING
RE GRIDCART CAR1 STA
            XYINC 50. 10 100. 0. 1 0.
RE GRIDCART CAR1 END
RE FINISHED

ME STARTING
  SURFFILE  4D_met\4D.sfc
  PROFFILE  4D_met\4D.pfl
  SURFDATA  14735  1988  ALBANY,NY
  UAIRDATA  14735  1988  ALBANY,NY
  SITEDATA  99999  1988  HUDSON
  PROFBASE  0.0  METERS
ME FINISHED

OU STARTING
  FILEFORM  EXP
  POSTFILE  24 ALL PLOT Case01\Case01.sum
OU FINISHED
```

A.6. Case08 Input File

```
**
**   AERMOD
**

CO STARTING
  TITLEONE  Case08 2F 5MW 20x40
  MODELOPT  FLAT CONC DDEP DRYDPLT
  AVERTIME  24  PERIOD
  POLLUTID  OTHER
  RUNORNOT  RUN
CO FINISHED

SO STARTING
  ELEVUNIT  METERS
  LOCATION  MAIN1   POINT  0.0  0.0  0.0

** Point Source       Mdot  Hgt   Temp  Vel   Diam
** Parameters:        ----  ----  ----  ----  ----
  SRCPARAM  MAIN1     1.0   20.0  -3700  0.5   6.22
```

```
  PARTDIAM  MAIN1 0.153 0.285 0.531 0.989  1.84  3.43  6.38  11.9  22.1  41.2
  MASSFRAX  MAIN1 0.092 0.146 0.141 0.144 0.112 0.080 0.072 0.071 0.071 0.071
  PARTDENS  MAIN1   1.0   1.0   1.0   1.0   1.0   1.0   1.0   1.0   1.0   1.0

  BUILDHGT Main1     20.00   20.00   20.00   20.00   20.00   20.00
  BUILDHGT Main1     20.00   20.00   20.00   20.00   20.00   20.00
  BUILDHGT Main1     20.00   20.00   20.00   20.00   20.00   20.00
  BUILDHGT Main1     20.00   20.00   20.00   20.00   20.00   20.00
  BUILDHGT Main1     20.00   20.00   20.00   20.00   20.00   20.00
  BUILDHGT Main1     20.00   20.00   20.00   20.00   20.00   20.00
  BUILDWID Main1     26.64   32.47   37.32   41.03   43.50   44.64
  BUILDWID Main1     44.43   42.87   40.00   42.87   44.43   44.64
  BUILDWID Main1     43.50   41.03   37.32   32.47   26.64   20.00
  BUILDWID Main1     26.64   32.47   37.32   41.03   43.50   44.64
  BUILDWID Main1     44.43   42.87   40.00   42.87   44.43   44.64
  BUILDWID Main1     43.50   41.03   37.32   32.47   26.64   20.00
  BUILDLEN Main1     42.87   44.43   44.64   43.50   41.03   37.32
  BUILDLEN Main1     32.47   26.64   20.00   26.64   32.47   37.32
  BUILDLEN Main1     41.03   43.50   44.64   44.43   42.87   40.00
  BUILDLEN Main1     42.87   44.43   44.64   43.50   41.03   37.32
  BUILDLEN Main1     32.47   26.64   20.00   26.64   32.47   37.32
  BUILDLEN Main1     41.03   43.50   44.64   44.43   42.87   40.00
  XBADJ    Main1    -23.17  -25.63  -27.32  -28.18  -28.18  -27.32
  XBADJ    Main1    -25.63  -23.17  -20.00  -23.17  -25.63  -27.32
  XBADJ    Main1    -28.18  -28.18  -27.32  -25.63  -23.17  -20.00
  XBADJ    Main1    -19.70  -18.79  -17.32  -15.32  -12.86  -10.00
  XBADJ    Main1     -6.84   -3.47    0.00   -3.47   -6.84  -10.00
  XBADJ    Main1    -12.86  -15.32  -17.32  -18.79  -19.70  -20.00
  YBADJ    Main1      9.85    9.40    8.66    7.66    6.43    5.00
  YBADJ    Main1      3.42    1.74    0.00   -1.74   -3.42   -5.00
  YBADJ    Main1     -6.43   -7.66   -8.66   -9.40   -9.85  -10.00
  YBADJ    Main1     -9.85   -9.40   -8.66   -7.66   -6.43   -5.00
  YBADJ    Main1     -3.42   -1.74    0.00    1.74    3.42    5.00
  YBADJ    Main1      6.43    7.66    8.66    9.40    9.85   10.00

  SRCGROUP  ALL
SO FINISHED

RE STARTING
RE GRIDCART CAR1 STA
            XYINC 50. 10 100. 0. 1 0.
RE GRIDCART CAR1 END
RE FINISHED

ME STARTING
  SURFFILE  2F_met\2F.sfc
  PROFFILE  2F_met\2F.pfl
  SURFDATA  14735  1988  ALBANY,NY
  UAIRDATA  14735  1988  ALBANY,NY
  SITEDATA  99999  1988  HUDSON
  PROFBASE  0.0  METERS
ME FINISHED

OU STARTING
  FILEFORM  EXP
  POSTFILE  24 ALL PLOT Case08\Case08.sum
OU FINISHED
```

APPENDIX B. ARCON96 INPUT FILES

Representative input files used in the evaluation of the test cases are shown below to illustrate implementation. The reader is directed to the code user manual to interpret the files.

B.1. Weather Input File – 4D.MET

```
4D      1 1   90  40  4   90  40
4D      1 2   90  40  4   90  40
4D      1 3   90  40  4   90  40
4D      1 4   90  40  4   90  40
4D      1 5   90  40  4   90  40
4D      1 6   90  40  4   90  40
4D      1 7   90  40  4   90  40
4D      1 8   90  40  4   90  40
4D      1 9   90  40  4   90  40
4D      110   90  40  4   90  40
4D      111   90  40  4   90  40
4D      112   90  40  4   90  40
4D      113   90  40  4   90  40
4D      114   90  40  4   90  40
4D      115   90  40  4   90  40
4D      116   90  40  4   90  40
4D      117   90  40  4   90  40
4D      118   90  40  4   90  40
4D      119   90  40  4   90  40
4D      120   90  40  4   90  40
4D      121   90  40  4   90  40
4D      122   90  40  4   90  40
4D      123   90  40  4   90  40
4D      124   90  40  4   90  40
4D      2 1   90  40  4   90  40
4D      2 2   90  40  4   90  40
...
4D    36514   90  40  4   90  40
4D    36515   90  40  4   90  40
4D    36516   90  40  4   90  40
4D    36517   90  40  4   90  40
4D    36518   90  40  4   90  40
4D    36519   90  40  4   90  40
4D    36520   90  40  4   90  40
4D    36521   90  40  4   90  40
4D    36522   90  40  4   90  40
4D    36523   90  40  4   90  40
4D    36524   90  40  4   90  40
```

B.2. Weather Input File – 2F.MET

```
2F      1 1   90  20  6   90  20
2F      1 2   90  20  6   90  20
2F      1 3   90  20  6   90  20
2F      1 4   90  20  6   90  20
2F      1 5   90  20  6   90  20
2F      1 6   90  20  6   90  20
2F      1 7   90  20  6   90  20
2F      1 8   90  20  6   90  20
2F      1 9   90  20  6   90  20
2F      110   90  20  6   90  20
2F      111   90  20  6   90  20
2F      112   90  20  6   90  20
2F      113   90  20  6   90  20
2F      114   90  20  6   90  20
2F      115   90  20  6   90  20
2F      116   90  20  6   90  20
2F      117   90  20  6   90  20
2F      118   90  20  6   90  20
2F      119   90  20  6   90  20
2F      120   90  20  6   90  20
2F      121   90  20  6   90  20
2F      122   90  20  6   90  20
2F      123   90  20  6   90  20
2F      124   90  20  6   90  20
2F      2 1   90  20  6   90  20
2F      2 2   90  20  6   90  20
...
2F    36514   90  20  6   90  20
2F    36515   90  20  6   90  20
2F    36516   90  20  6   90  20
2F    36517   90  20  6   90  20
2F    36518   90  20  6   90  20
2F    36519   90  20  6   90  20
2F    36520   90  20  6   90  20
2F    36521   90  20  6   90  20
2F    36522   90  20  6   90  20
2F    36523   90  20  6   90  20
2F    36524   90  20  6   90  20
```

B.3. Case 01 (50 m) Input File

```
1
4D.MET
    10.0
    50.0
   1
   2
    20.00
  2000.00
     0.00
     0.00
     0.00
  90  90
    50.00
     0.00
     0.00
Case01\CASE01_050.LOG
Case01\CASE01_050.CFD
 .03
     0.50
     4.00
   1   2   4   8  12  24  96 168 360 720
   1   2   4   8  11  22  87 152 324 648
     1.00    1.00
n
```

B.4. Case 06 (950 m) Input File

```
1
2F.MET
    10.0
    50.0
   1
   2
    20.00
   400.00
     0.00
     0.00
     0.00
  90  90
   950.00
     0.00
     0.00
Case06\CASE06_950.LOG
Case06\CASE06_950.CFD
 .03
     0.50
     4.00
   1   2   4   8  12  24  96 168 360 720
   1   2   4   8  11  22  87 152 324 648
     1.00    1.00
n
```

APPENDIX C. MACCS INPUT FILES

Representative input files used in the evaluation of the test cases are shown below to illustrate implementation. The reader is directed to the code user manual to interpret the files.

C.1. Case 01 Input File

```
* File created using WinMACCS version 3.11.6 SVN:6662 1/8/2020 5:47:10 PM
*
* MACCS Cyclical File: Case01.inp
*
* Form 'Atmos Description' Comment:
* Case 01
*
* ATNAM1, identifies this MACCS calculation
RIATNAM1001             '4D weather, 0 MW, 20x100 building'
*
* ACTIVITY_UNITS, model results are displayed in these units
UNITACTI001             Bq
*
* DIST_UNITS, model results are displayed in these units
UNITDIST001             km
*
* AREA_UNITS,  model results are displayed in these units
UNITAREA001             ha
*
* DOSE_UNITS,  model results are displayed in these units
UNITDOSE001             Sv
*
* NUMRAD, number of radial spatial elements
GENUMRAD001             10
*
* SPAEND, spatial endpoint distances (km)
GESPAEND001             0.1
GESPAEND002             0.2
GESPAEND003             0.3
GESPAEND004             0.4
GESPAEND005             0.5
GESPAEND006             0.6
GESPAEND007             0.7
GESPAEND008             0.8
GESPAEND009             0.9
GESPAEND010             1.
*
* NUMCOR, number of angular compass directions
GENUMCOR001             64
*
* NUMISO, number of nuclides
ISNUMISO001             1
*
* MAXGRP, number of chemical groups
ISMAXGRP001             1
*
* GRPNAM, chemical group names
ISGRPNAM001             Cesium
*
* MSMODL, multi source term model (TRUE, FALSE)
ISMSMODL001             .FALSE.
*
* WETDEP, DRYDEP, wet and dry deposition flags for each nuclide group
ISDEPFLA001             .FALSE.       .TRUE.
*
* NUMSTB, number of pseudostable radionuclides, always 0
ISNUMSTB001             0
*
* Form 'Pseudostable Radionuclides' Comment:
*
* NUMSTB, number of pseudostable radionuclides
ISNUMSTB001             1
*
* NAMSTB, list of pseudostable radionuclides
ISNAMSTB001             Ba-137m
*
* NUCNAM, IGROUP, chemical group associated with each nuclide
ISOTPGRP001             Cs-137        1
*
* CWASH1, washout coefficient number one, linear factor (1/s)
WDCWASH1001             1.E-04
*
* CWASH2, washout coefficient number two, exponential factor (1/s)
WDCWASH2001             0.8
*
* NPSGRP, number of particle size groups
DDNPSGRP001             10
*
* VDEPOS, dry deposition velocities for each particle size group (m/sec)
DDVDEPOS001             5.3471E-04
DDVDEPOS002             4.9073E-04
DDVDEPOS003             6.4289E-04
```

```
DDVDEPOS004             0.0010839
DDVDEPOS005             0.0021202
DDVDEPOS006             0.0043375
DDVDEPOS007             0.0083669
DDVDEPOS008             0.013719
DDVDEPOS009             0.016988
DDVDEPOS010             0.016988
*
* NUM_DIST, number of entries in the dispersion lookup table
NUM_DIST001             50
*
* DISTANCE, SIGMA_Y_A, SIGMA_Z_A, downwind distances (m), A-stability dispersion table
A-STB/DIS01             1.          0.366       0.192
A-STB/DIS02             1.4         0.496       0.263
A-STB/DIS03             2.          0.684       0.367
A-STB/DIS04             3.          0.987       0.537
A-STB/DIS05             4.          1.28        0.703
A-STB/DIS06             6.          1.84        1.03
A-STB/DIS07             8.          2.39        1.34
A-STB/DIS08             10.         2.93        1.66
A-STB/DIS09             14.         3.97        2.27
A-STB/DIS10             20.         5.47        3.17
A-STB/DIS11             30.         7.89        4.63
A-STB/DIS12             40.         10.2        6.06
A-STB/DIS13             60.         14.8        8.86
A-STB/DIS14             80.         19.1        11.6
A-STB/DIS15             100.        23.4        14.3
A-STB/DIS16             140.        31.7        18.9
A-STB/DIS17             200.        43.8        28.6
A-STB/DIS18             300.        63.1        51.7
A-STB/DIS19             400.        81.9        83.4
A-STB/DIS20             600.        118.        172.
A-STB/DIS21             800.        153.        294.
A-STB/DIS22             1000.       187.        448.
A-STB/DIS23             1400.       254.        920.
A-STB/DIS24             2000.       350.        1950.
A-STB/DIS25             3000.       505.        4580.
A-STB/DIS26             4000.       655.        8360.
A-STB/DIS27             6000.       945.        19600.
A-STB/DIS28             8000.       1220.       35700.
A-STB/DIS29             10000.      1500.       57000.
A-STB/DIS30             14000.      2030.       1.15000E+05
A-STB/DIS31             20000.      2800.       2.44000E+05
A-STB/DIS32             30000.      4040.       5.69000E+05
A-STB/DIS33             40000.      5240.       1.040000E+06
A-STB/DIS34             60000.      7560.       2.430000E+06
A-STB/DIS35             80000.      9800.       4.440000E+06
A-STB/DIS36             1.00000E+0512000.       7.080000E+06
A-STB/DIS37             1.40000E+0516200.       1.43E+07
A-STB/DIS38             2.00000E+0522400.       3.02E+07
A-STB/DIS39             3.00000E+0532300.       7.07E+07
A-STB/DIS40             4.00000E+0541900.       1.29E+08
A-STB/DIS41             6.00000E+0560500.       3.02E+08
A-STB/DIS42             8.00000E+0578400.       5.51E+08
A-STB/DIS43             1.000000E+06            95900.      8.79E+08
A-STB/DIS44             1.400000E+06            1.30000E+051.78E+09
A-STB/DIS45             2.000000E+06            1.79000E+053.75E+09
A-STB/DIS46             3.000000E+06            2.59000E+058.78E+09
A-STB/DIS47             4.000000E+06            3.35000E+051.6E+10
A-STB/DIS48             6.000000E+06            4.84000E+053.75E+10
A-STB/DIS49             8.000000E+06            6.27000E+056.84E+10
A-STB/DIS50             1.E+07      7.67000E+051.09E+11
*
* DISTANCE, SIGMA_Y_B, SIGMA_Z_B, downwind distances (m), B-stability dispersion table
B-STB/DIS01             1.          0.275       0.156
B-STB/DIS02             1.4         0.373       0.213
B-STB/DIS03             2.          0.514       0.296
B-STB/DIS04             3.          0.742       0.43
B-STB/DIS05             4.          0.962       0.56
B-STB/DIS06             6.          1.39        0.814
B-STB/DIS07             8.          1.8         1.06
B-STB/DIS08             10.         2.2         1.3
B-STB/DIS09             14.         2.98        1.78
B-STB/DIS10             20.         4.12        2.47
B-STB/DIS11             30.         5.94        3.59
B-STB/DIS12             40.         7.7         4.68
B-STB/DIS13             60.         11.1        6.8
B-STB/DIS14             80.         14.4        8.87
B-STB/DIS15             100.        17.6        10.9
B-STB/DIS16             140.        23.9        14.5
B-STB/DIS17             200.        32.9        20.1
B-STB/DIS18             300.        47.5        30.1
B-STB/DIS19             400.        61.6        40.6
B-STB/DIS20             600.        88.8        62.8
B-STB/DIS21             800.        115.        86.
B-STB/DIS22             1000.       141.        110.
B-STB/DIS23             1400.       191.        159.
B-STB/DIS24             2000.       263.        234.
B-STB/DIS25             3000.       380.        364.
B-STB/DIS26             4000.       493.        498.
B-STB/DIS27             6000.       710.        776.
B-STB/DIS28             8000.       921.        1060.
B-STB/DIS29             10000.      1130.       1360.
```

```
B-STB/DIS30     14000.      1530.       1960.
B-STB/DIS31     20000.      2110.       2910.
B-STB/DIS32     30000.      3040.       4530.
B-STB/DIS33     40000.      3940.       6220.
B-STB/DIS34     60000.      5680.       9700.
B-STB/DIS35     80000.      7370.       13300.
B-STB/DIS36     1.00000E+059020.        17000.
B-STB/DIS37     1.40000E+0512200.       24600.
B-STB/DIS38     2.00000E+0516900.       36400.
B-STB/DIS39     3.00000E+0524300.       56800.
B-STB/DIS40     4.00000E+0531500.       77900.
B-STB/DIS41     6.00000E+0545500.       1.22000E+05
B-STB/DIS42     8.00000E+0559000.       1.67000E+05
B-STB/DIS43     1.000000E+06            72100.      2.13000E+05
B-STB/DIS44     1.400000E+06            97700.      3.08000E+05
B-STB/DIS45     2.000000E+06            1.35000E+054.56000E+05
B-STB/DIS46     3.000000E+06            1.95000E+057.12000E+05
B-STB/DIS47     4.000000E+06            2.52000E+059.76000E+05
B-STB/DIS48     6.000000E+06            3.64000E+051.520000E+06
B-STB/DIS49     8.000000E+06            4.72000E+052.090000E+06
B-STB/DIS50     1.E+07      5.77000E+052.670000E+06
*
* DISTANCE, SIGMA_Y_C, SIGMA_Z_C, downwind distances (m), C-stability dispersion table
C-STB/DIS01     1.          0.209       0.116
C-STB/DIS02     1.4         0.283       0.157
C-STB/DIS03     2.          0.391       0.217
C-STB/DIS04     3.          0.563       0.314
C-STB/DIS05     4.          0.731       0.407
C-STB/DIS06     6.          1.05        0.587
C-STB/DIS07     8.          1.37        0.762
C-STB/DIS08     10.         1.67        0.932
C-STB/DIS09     14.         2.26        1.26
C-STB/DIS10     20.         3.13        1.75
C-STB/DIS11     30.         4.51        2.52
C-STB/DIS12     40.         5.84        3.27
C-STB/DIS13     60.         8.43        4.72
C-STB/DIS14     80.         10.9        6.12
C-STB/DIS15     100.        13.4        7.49
C-STB/DIS16     140.        18.1        10.2
C-STB/DIS17     200.        25.         14.1
C-STB/DIS18     300.        36.1        20.4
C-STB/DIS19     400.        46.8        26.5
C-STB/DIS20     600.        67.4        38.4
C-STB/DIS21     800.        87.4        49.9
C-STB/DIS22     1000.       107.        61.1
C-STB/DIS23     1400.       145.        83.
C-STB/DIS24     2000.       200.        115.
C-STB/DIS25     3000.       288.        166.
C-STB/DIS26     4000.       374.        216.
C-STB/DIS27     6000.       539.        313.
C-STB/DIS28     8000.       700.        406.
C-STB/DIS29     10000.      856.        498.
C-STB/DIS30     14000.      1160.       676.
C-STB/DIS31     20000.      1600.       936.
C-STB/DIS32     30000.      2310.       1350.
C-STB/DIS33     40000.      2990.       1760.
C-STB/DIS34     60000.      4320.       2550.
C-STB/DIS35     80000.      5600.       3310.
C-STB/DIS36     1.00000E+056850.        4060.
C-STB/DIS37     1.40000E+059280.        5510.
C-STB/DIS38     2.00000E+0512800.       7630.
C-STB/DIS39     3.00000E+0518500.       11000.
C-STB/DIS40     4.00000E+0523900.       14300.
C-STB/DIS41     6.00000E+0534500.       20700.
C-STB/DIS42     8.00000E+0544800.       27000.
C-STB/DIS43     1.000000E+06            54800.      33000.
C-STB/DIS44     1.400000E+06            74200.      44900.
C-STB/DIS45     2.000000E+06            1.02000E+0562100.
C-STB/DIS46     3.000000E+06            1.48000E+0589900.
C-STB/DIS47     4.000000E+06            1.92000E+051.17000E+05
C-STB/DIS48     6.000000E+06            2.76000E+051.69000E+05
C-STB/DIS49     8.000000E+06            3.58000E+052.20000E+05
C-STB/DIS50     1.E+07      4.38000E+052.69000E+05
*
* DISTANCE, SIGMA_Y_D, SIGMA_Z_D, downwind distances (m), D-stability dispersion table
D-STB/DIS01     1.          0.147       0.079
D-STB/DIS02     1.4         0.199       0.106
D-STB/DIS03     2.          0.275       0.145
D-STB/DIS04     3.          0.397       0.208
D-STB/DIS05     4.          0.514       0.268
D-STB/DIS06     6.          0.742       0.383
D-STB/DIS07     8.          0.962       0.493
D-STB/DIS08     10.         1.18        0.601
D-STB/DIS09     14.         1.59        0.808
D-STB/DIS10     20.         2.2         1.11
D-STB/DIS11     30.         3.17        1.58
D-STB/DIS12     40.         4.12        2.04
D-STB/DIS13     60.         5.94        2.91
D-STB/DIS14     80.         7.7         3.75
D-STB/DIS15     100.        9.41        4.57
D-STB/DIS16     140.        12.8        6.29
D-STB/DIS17     200.        17.6        8.64
D-STB/DIS18     300.        25.4        12.2
```

```
D-STB/DIS19     400.        32.9        15.4
D-STB/DIS20     600.        47.5        21.2
D-STB/DIS21     800.        61.6        26.6
D-STB/DIS22     1000.       75.3        31.5
D-STB/DIS23     1400.       102.        39.9
D-STB/DIS24     2000.       141.        50.6
D-STB/DIS25     3000.       203.        65.4
D-STB/DIS26     4000.       263.        78.
D-STB/DIS27     6000.       380.        99.2
D-STB/DIS28     8000.       493.        117.
D-STB/DIS29     10000.      603.        133.
D-STB/DIS30     14000.      817.        161.
D-STB/DIS31     20000.      1130.       196.
D-STB/DIS32     30000.      1630.       244.
D-STB/DIS33     40000.      2110.       286.
D-STB/DIS34     60000.      3040.       355.
D-STB/DIS35     80000.      3940.       414.
D-STB/DIS36     1.00000E+054820.        466.
D-STB/DIS37     1.40000E+056530.        557.
D-STB/DIS38     2.00000E+059020.        672.
D-STB/DIS39     3.00000E+0513000.       831.
D-STB/DIS40     4.00000E+0516900.       967.
D-STB/DIS41     6.00000E+0524300.       1190.
D-STB/DIS42     8.00000E+0531500.       1390.
D-STB/DIS43     1.000000E+06            38600.      1560.
D-STB/DIS44     1.400000E+06            52300.      1860.
D-STB/DIS45     2.000000E+06            72100.      2230.
D-STB/DIS46     3.000000E+06            1.04000E+052760.
D-STB/DIS47     4.000000E+06            1.35000E+053200.
D-STB/DIS48     6.000000E+06            1.95000E+053950.
D-STB/DIS49     8.000000E+06            2.52000E+054580.
D-STB/DIS50     1.E+07      3.09000E+055140.
*
* DISTANCE, SIGMA_Y_E, SIGMA_Z_E, downwind distances (m), E-stability dispersion table
E-STB/DIS01     1.          0.105       0.063
E-STB/DIS02     1.4         0.142       0.0845
E-STB/DIS03     2.          0.196       0.115
E-STB/DIS04     3.          0.282       0.164
E-STB/DIS05     4.          0.366       0.211
E-STB/DIS06     6.          0.528       0.3
E-STB/DIS07     8.          0.684       0.385
E-STB/DIS08     10.         0.837       0.468
E-STB/DIS09     14.         1.13        0.628
E-STB/DIS10     20.         1.56        0.856
E-STB/DIS11     30.         2.26        1.22
E-STB/DIS12     40.         2.93        1.57
E-STB/DIS13     60.         4.22        2.23
E-STB/DIS14     80.         5.47        2.86
E-STB/DIS15     100.        6.69        3.48
E-STB/DIS16     140.        9.07        4.72
E-STB/DIS17     200.        12.5        6.36
E-STB/DIS18     300.        18.1        8.79
E-STB/DIS19     400.        23.4        11.
E-STB/DIS20     600.        33.8        14.8
E-STB/DIS21     800.        43.8        18.3
E-STB/DIS22     1000.       53.6        21.5
E-STB/DIS23     1400.       72.6        27.3
E-STB/DIS24     2000.       100.        34.4
E-STB/DIS25     3000.       144.        43.4
E-STB/DIS26     4000.       187.        50.5
E-STB/DIS27     6000.       270.        61.6
E-STB/DIS28     8000.       350.        70.3
E-STB/DIS29     10000.      428.        77.7
E-STB/DIS30     14000.      581.        89.8
E-STB/DIS31     20000.      801.        104.
E-STB/DIS32     30000.      1160.       122.
E-STB/DIS33     40000.      1500.       136.
E-STB/DIS34     60000.      2160.       159.
E-STB/DIS35     80000.      2800.       177.
E-STB/DIS36     1.00000E+053430.        191.
E-STB/DIS37     1.40000E+054650.        216.
E-STB/DIS38     2.00000E+056410.        245.
E-STB/DIS39     3.00000E+059250.        281.
E-STB/DIS40     4.00000E+0512000.       310.
E-STB/DIS41     6.00000E+0517300.       355.
E-STB/DIS42     8.00000E+0522400.       391.
E-STB/DIS43     1.000000E+06            27400.      421.
E-STB/DIS44     1.400000E+06            37200.      470.
E-STB/DIS45     2.000000E+06            51300.      528.
E-STB/DIS46     3.000000E+06            74000.      602.
E-STB/DIS47     4.000000E+06            95900.      660.
E-STB/DIS48     6.000000E+06            1.38000E+05752.
E-STB/DIS49     8.000000E+06            1.79000E+05824.
E-STB/DIS50     1.E+07      2.19000E+05884.
*
* DISTANCE, SIGMA_Y_F, SIGMA_Z_F, downwind distances (m), F-stability dispersion table
F-STB/DIS011.   0.0722      0.053
F-STB/DIS021.4  0.0978      0.0697
F-STB/DIS032.   0.135       0.0932
F-STB/DIS043.   0.195       0.13
F-STB/DIS054.   0.252       0.164
F-STB/DIS066.   0.364       0.228
F-STB/DIS078.   0.472       0.288
```

```
F-STB/DIS0810.          0.578       0.345
F-STB/DIS0914.          0.783       0.454
F-STB/DIS1020.          1.08        0.607
F-STB/DIS1130.          1.56        0.845
F-STB/DIS1240.          2.02        1.07
F-STB/DIS1360.          2.91        1.48
F-STB/DIS1480.          3.78        1.88
F-STB/DIS15100.         4.62        2.25
F-STB/DIS16140.         6.26        2.98
F-STB/DIS17200.         8.64        3.99
F-STB/DIS18300.         12.5        5.51
F-STB/DIS19400.         16.2        6.89
F-STB/DIS20600.         23.3        9.43
F-STB/DIS21800.         30.2        11.7
F-STB/DIS221000.        37.         13.9
F-STB/DIS231400.        50.1        17.9
F-STB/DIS242000.        69.1        22.3
F-STB/DIS253000.        99.7        27.7
F-STB/DIS264000.        129.        31.7
F-STB/DIS276000.        186.        37.8
F-STB/DIS288000.        242.        42.4
F-STB/DIS2910000.       296.        46.1
F-STB/DIS3014000.       401.        52.
F-STB/DIS3120000.       553.        58.7
F-STB/DIS3230000.       798.        66.8
F-STB/DIS3340000.       1030.       73.
F-STB/DIS3460000.       1490.       82.2
F-STB/DIS3580000.       1930.       89.1
F-STB/DIS361.00000E+052370.         94.8
F-STB/DIS371.40000E+053210.         104.
F-STB/DIS382.00000E+054420.         114.
F-STB/DIS393.00000E+056380.         126.
F-STB/DIS404.00000E+058270.         135.
F-STB/DIS416.00000E+0511900.        149.
F-STB/DIS428.00000E+0515500.        160.
F-STB/DIS431.000000E+06             18900.      168.
F-STB/DIS441.400000E+06             25700.      182.
F-STB/DIS452.000000E+06             35400.      197.
F-STB/DIS463.000000E+06             51100.      216.
F-STB/DIS474.000000E+06             66200.      230.
F-STB/DIS486.000000E+06             95500.      251.
F-STB/DIS498.000000E+06             1.24000E+05267.
F-STB/DIS501.E+07       1.51000E+05280.
*
* YSCALE, linear scaling factor for sigma-y
DPYSCALE001             1.
*
* ZSCALE, linear scaling factor for sigma-z
DPZSCALE001             1.
*
* DISPMD,  dispersion long-range model
DPDISPMD001             LRDIST
*
* MNDMOD, plume meander model (OLD, NEW, OFF)
PMMNDMOD001             NEW
*
* Form 'Plume Rise Scale Factor' Comment:
*
* SCLCRW, scaling factor for entrainment of buoyant plume
PRSCLCRW001             1.
*
* SCLADP, scaling factor for the A through D stability plume rise formula
PRSCLADP001             1.
*
* SCLEFP, scaling factor for the E through F stability plume rise formula
PRSCLEFP001             1.
*
* BUILDH, building height (m)
WEBUILDH001             20.
*
* SIGYINIT, initial value of sigma-y for each of the plumes (m)
SIGYINIT00123.
*
* SIGZINIT, initial value of sigma-z for each of the plumes (m)
SIGZINIT0019.4
*
* ATNAM2, source term description
RDATNAM2001             '3600 Ci Cs-137 over 1 hour (1 Ci/s)'
*
* NUMREL, number of plumes
RDNUMREL001             1
*
* MAXRIS, index of risk-dominant plume segment
RDMAXRIS001             1
*
* REFTIM, representative time point for dispersion and radioactive decay
RDREFTIM001             0.5
*
* plume rise model  set to HEAT (DENSITY, HEAT)
RDPLMMOD001             HEAT
*
* PLHEAT, rate of heat release in each plume segment (W)
RDPLHEAT001             0.
```

```
*
* BRGSMD, Briggs plume rise model (ORIGINAL, IMPROVED)
RDBRGSMD001             IMPROVED
*
* PLHITE, height of each plume segment at release (m)
RDPLHITE001             20.
*
* PLUDUR, duration of each plume segment (s)
RDPLUDUR001             3600.
*
* PDELAY, start time of each plume segment from accident initiation (s)
RDPDELAY001             0.
*
* PSDIST, particle size distribution of each element group
RDPSDIST001             0.092       0.146       0.141       0.144       0.112       0.08        0.072       0.071       0.071       0.071
*
* CORINV, inventory of each radionuclide present at the time of accident initiation (Bq)
RDCORINV001             Cs-137      3600.
*
* Form 'Inventory Scale Factor' Comment:
*
* CORSCA, scaling factor to adjust the core inventory
RDCORSCA001             1.
*
* Form 'Daughter Ingrowth Flag' Comment:
*
* APLFRC, Specifies how release fractions are applied to daughter ingrowth products (PARENT, PROGENY)
RDAPLFRC001             PARENT
*
* Form 'Release Fractions' Comment:
*
* RELFRC, release fractions for each of the plume segments for each chemical group
RDRELFRC001             1.
*
* ENDAT1, set to TRUE if only running ATMOS
OCENDAT1001             .TRUE.
*
* Form 'Output Control' Comment:
*
* IDEBUG, specifies set of debug results to report
OCIDEBUG001             0
*
* NUCOUT, name of the nuclide to be listed on the dispersion listings
OCNUCOUT001             Cs-137
*
* ATDMODL, atmospheric transport model
ISATDMODL01             GAUSSIAN
*
* METCOD, meteorological sampling model (1, 2, 3, 4, or 5)
M1METCOD001             4
*
* BNDMXH, boundary weather mixing layer height (m)
M2BNDMXH001             1500.
*
* IBDSTB, boundary weather stability class index
M2IBDSTB001             4
*
* BNDRAN, boundary weather rain rate (mm/hr)
M2BNDRAN001             0.
*
* BNDWND, boundary weather wind speed (m/sec)
M2BNDWND001             4.
*
* ISTRDY, start day of the weather sequence
M3ISTRDY001             1
*
* ISTRHR, start hour of the weather sequence
M3ISTRHR001             1
*
* MAXHGT, determines mixing height model
M1MAXHGT001             DAY_ONLY
*
* NUM0,  used for no input, always 0
TYPE0NUMBER             0
*
* NUM0, number of results
TYPE0NUMBER             10
*
* INDREL, INDRAD, CCDF, ATMOS release and spatial interval
TYPE0OUT001             1           1           NONE
TYPE0OUT002             1           2           NONE
TYPE0OUT003             1           3           NONE
TYPE0OUT004             1           4           NONE
TYPE0OUT005             1           5           NONE
TYPE0OUT006             1           6           NONE
TYPE0OUT007             1           7           NONE
TYPE0OUT008             1           8           NONE
TYPE0OUT009             1           9           NONE
TYPE0OUT010             1           10          NONE
*
* NUM0_HY, used for no input, always 0
TYPE0_HYNUM             0
```

C.2. Case 08 Input File

```
* File created using WinMACCS version 3.11.6 SVN:6662 1/8/2020 5:47:23 PM
*
* MACCS Cyclical File: Case08.inp
*
* Form 'Atmos Description' Comment:
* Case 01
*
* ATNAM1, identifies this MACCS calculation
RIATNAM1001             '2F weather, 5 MW, 20x40 building'
*
* ACTIVITY_UNITS, model results are displayed in these units
UNITACTI001             Bq
*
* DIST_UNITS, model results are displayed in these units
UNITDIST001             km
*
* AREA_UNITS,  model results are displayed in these units
UNITAREA001             ha
*
* DOSE_UNITS,  model results are displayed in these units
UNITDOSE001             Sv
*
* NUMRAD, number of radial spatial elements
GENUMRAD001             10
*
* SPAEND, spatial endpoint distances (km)
GESPAEND001             0.1
GESPAEND002             0.2
GESPAEND003             0.3
GESPAEND004             0.4
GESPAEND005             0.5
GESPAEND006             0.6
GESPAEND007             0.7
GESPAEND008             0.8
GESPAEND009             0.9
GESPAEND010             1.
*
* NUMCOR, number of angular compass directions
GENUMCOR001             64
*
* NUMISO, number of nuclides
ISNUMISO001             1
*
* MAXGRP, number of chemical groups
ISMAXGRP001             1
*
* GRPNAM, chemical group names
ISGRPNAM001             Cesium
*
* MSMODL, multi source term model (TRUE, FALSE)
ISMSMODL001             .FALSE.
*
* WETDEP, DRYDEP, wet and dry deposition flags for each nuclide group
ISDEPFLA001             .FALSE.       .TRUE.
*
* NUMSTB, number of pseudostable radionuclides, always 0
ISNUMSTB001             0
*
* Form 'Pseudostable Radionuclides' Comment:
*
* NUMSTB, number of pseudostable radionuclides
ISNUMSTB001             1
*
* NAMSTB, list of pseudostable radionuclides
ISNAMSTB001             Ba-137m
*
* NUCNAM, IGROUP, chemical group associated with each nuclide
ISOTPGRP001             Cs-137        1
*
* CWASH1, washout coefficient number one, linear factor (1/s)
WDCWASH1001             1.E-04
*
* CWASH2, washout coefficient number two, exponential factor (1/s)
WDCWASH2001             0.8
*
* NPSGRP, number of particle size groups
DDNPSGRP001             10
*
* VDEPOS, dry deposition velocities for each particle size group (m/sec)
DDVDEPOS001             5.3471E-04
DDVDEPOS002             4.9073E-04
DDVDEPOS003             6.4289E-04
DDVDEPOS004             0.0010839
DDVDEPOS005             0.0021202
DDVDEPOS006             0.0043375
DDVDEPOS007             0.0083669
DDVDEPOS008             0.013719
DDVDEPOS009             0.016988
DDVDEPOS010             0.016988
*
* NUM_DIST, number of entries in the dispersion lookup table
```

NUM_DIST001 50
*
* DISTANCE, SIGMA_Y_A, SIGMA_Z_A, downwind distances (m), A-stability dispersion table
A-STB/DIS01 1. 0.366 0.192
A-STB/DIS02 1.4 0.496 0.263
A-STB/DIS03 2. 0.684 0.367
A-STB/DIS04 3. 0.987 0.537
A-STB/DIS05 4. 1.28 0.703
A-STB/DIS06 6. 1.84 1.03
A-STB/DIS07 8. 2.39 1.34
A-STB/DIS08 10. 2.93 1.66
A-STB/DIS09 14. 3.97 2.27
A-STB/DIS10 20. 5.47 3.17
A-STB/DIS11 30. 7.89 4.63
A-STB/DIS12 40. 10.2 6.06
A-STB/DIS13 60. 14.8 8.86
A-STB/DIS14 80. 19.1 11.6
A-STB/DIS15 100. 23.4 14.3
A-STB/DIS16 140. 31.7 18.9
A-STB/DIS17 200. 43.8 28.6
A-STB/DIS18 300. 63.1 51.7
A-STB/DIS19 400. 81.9 83.4
A-STB/DIS20 600. 118. 172.
A-STB/DIS21 800. 153. 294.
A-STB/DIS22 1000. 187. 448.
A-STB/DIS23 1400. 254. 920.
A-STB/DIS24 2000. 350. 1950.
A-STB/DIS25 3000. 505. 4580.
A-STB/DIS26 4000. 655. 8360.
A-STB/DIS27 6000. 945. 19600.
A-STB/DIS28 8000. 1220. 35700.
A-STB/DIS29 10000. 1500. 57000.
A-STB/DIS30 14000. 2030. 1.15000E+05
A-STB/DIS31 20000. 2800. 2.44000E+05
A-STB/DIS32 30000. 4040. 5.69000E+05
A-STB/DIS33 40000. 5240. 1.040000E+06
A-STB/DIS34 60000. 7560. 2.430000E+06
A-STB/DIS35 80000. 9800. 4.440000E+06
A-STB/DIS36 1.00000E+0512000. 7.080000E+06
A-STB/DIS37 1.40000E+0516200. 1.43E+07
A-STB/DIS38 2.00000E+0522400. 3.02E+07
A-STB/DIS39 3.00000E+0532300. 7.07E+07
A-STB/DIS40 4.00000E+0541900. 1.29E+08
A-STB/DIS41 6.00000E+0560500. 3.02E+08
A-STB/DIS42 8.00000E+0578400. 5.51E+08
A-STB/DIS43 1.000000E+06 95900. 8.79E+08
A-STB/DIS44 1.400000E+06 1.30000E+051.78E+09
A-STB/DIS45 2.000000E+06 1.79000E+053.75E+09
A-STB/DIS46 3.000000E+06 2.59000E+058.78E+09
A-STB/DIS47 4.000000E+06 3.35000E+051.6E+10
A-STB/DIS48 6.000000E+06 4.84000E+053.75E+10
A-STB/DIS49 8.000000E+06 6.27000E+056.84E+10
A-STB/DIS50 1.E+07 7.67000E+051.09E+11
*
* DISTANCE, SIGMA_Y_B, SIGMA_Z_B, downwind distances (m), B-stability dispersion table
B-STB/DIS01 1. 0.275 0.156
B-STB/DIS02 1.4 0.373 0.213
B-STB/DIS03 2. 0.514 0.296
B-STB/DIS04 3. 0.742 0.43
B-STB/DIS05 4. 0.962 0.56
B-STB/DIS06 6. 1.39 0.814
B-STB/DIS07 8. 1.8 1.06
B-STB/DIS08 10. 2.2 1.3
B-STB/DIS09 14. 2.98 1.78
B-STB/DIS10 20. 4.12 2.47
B-STB/DIS11 30. 5.94 3.59
B-STB/DIS12 40. 7.7 4.68
B-STB/DIS13 60. 11.1 6.8
B-STB/DIS14 80. 14.4 8.87
B-STB/DIS15 100. 17.6 10.9
B-STB/DIS16 140. 23.9 14.5
B-STB/DIS17 200. 32.9 20.1
B-STB/DIS18 300. 47.5 30.1
B-STB/DIS19 400. 61.6 40.6
B-STB/DIS20 600. 88.8 62.8
B-STB/DIS21 800. 115. 86.
B-STB/DIS22 1000. 141. 110.
B-STB/DIS23 1400. 191. 159.
B-STB/DIS24 2000. 263. 234.
B-STB/DIS25 3000. 380. 364.
B-STB/DIS26 4000. 493. 498.
B-STB/DIS27 6000. 710. 776.
B-STB/DIS28 8000. 921. 1060.
B-STB/DIS29 10000. 1130. 1360.
B-STB/DIS30 14000. 1530. 1960.
B-STB/DIS31 20000. 2110. 2910.
B-STB/DIS32 30000. 3040. 4530.
B-STB/DIS33 40000. 3940. 6220.
B-STB/DIS34 60000. 5680. 9700.
B-STB/DIS35 80000. 7370. 13300.
B-STB/DIS36 1.00000E+059020. 17000.
B-STB/DIS37 1.40000E+0512200. 24600.
B-STB/DIS38 2.00000E+0516900. 36400.

```
B-STB/DIS39     3.00000E+0524300.   56800.
B-STB/DIS40     4.00000E+0531500.   77900.
B-STB/DIS41     6.00000E+0545500.   1.22000E+05
B-STB/DIS42     8.00000E+0559000.   1.67000E+05
B-STB/DIS43     1.000000E+06        72100.      2.13000E+05
B-STB/DIS44     1.400000E+06        97700.      3.08000E+05
B-STB/DIS45     2.000000E+06        1.35000E+054.56000E+05
B-STB/DIS46     3.000000E+06        1.95000E+057.12000E+05
B-STB/DIS47     4.000000E+06        2.52000E+059.76000E+05
B-STB/DIS48     6.000000E+06        3.64000E+051.520000E+06
B-STB/DIS49     8.000000E+06        4.72000E+052.090000E+06
B-STB/DIS50     1.E+07      5.77000E+052.670000E+06
*
* DISTANCE, SIGMA_Y_C, SIGMA_Z_C, downwind distances (m), C-stability dispersion table
C-STB/DIS01     1.          0.209       0.116
C-STB/DIS02     1.4         0.283       0.157
C-STB/DIS03     2.          0.391       0.217
C-STB/DIS04     3.          0.563       0.314
C-STB/DIS05     4.          0.731       0.407
C-STB/DIS06     6.          1.05        0.587
C-STB/DIS07     8.          1.37        0.762
C-STB/DIS08     10.         1.67        0.932
C-STB/DIS09     14.         2.26        1.26
C-STB/DIS10     20.         3.13        1.75
C-STB/DIS11     30.         4.51        2.52
C-STB/DIS12     40.         5.84        3.27
C-STB/DIS13     60.         8.43        4.72
C-STB/DIS14     80.         10.9        6.12
C-STB/DIS15     100.        13.4        7.49
C-STB/DIS16     140.        18.1        10.2
C-STB/DIS17     200.        25.         14.1
C-STB/DIS18     300.        36.1        20.4
C-STB/DIS19     400.        46.8        26.5
C-STB/DIS20     600.        67.4        38.4
C-STB/DIS21     800.        87.4        49.9
C-STB/DIS22     1000.       107.        61.1
C-STB/DIS23     1400.       145.        83.
C-STB/DIS24     2000.       200.        115.
C-STB/DIS25     3000.       288.        166.
C-STB/DIS26     4000.       374.        216.
C-STB/DIS27     6000.       539.        313.
C-STB/DIS28     8000.       700.        406.
C-STB/DIS29     10000.      856.        498.
C-STB/DIS30     14000.      1160.       676.
C-STB/DIS31     20000.      1600.       936.
C-STB/DIS32     30000.      2310.       1350.
C-STB/DIS33     40000.      2990.       1760.
C-STB/DIS34     60000.      4320.       2550.
C-STB/DIS35     80000.      5600.       3310.
C-STB/DIS36     1.00000E+056850.        4060.
C-STB/DIS37     1.40000E+059280.        5510.
C-STB/DIS38     2.00000E+0512800.       7630.
C-STB/DIS39     3.00000E+0518500.       11000.
C-STB/DIS40     4.00000E+0523900.       14300.
C-STB/DIS41     6.00000E+0534500.       20700.
C-STB/DIS42     8.00000E+0544800.       27000.
C-STB/DIS43     1.000000E+06            54800.      33000.
C-STB/DIS44     1.400000E+06            74200.      44900.
C-STB/DIS45     2.000000E+06            1.02000E+0562100.
C-STB/DIS46     3.000000E+06            1.48000E+0589900.
C-STB/DIS47     4.000000E+06            1.92000E+051.17000E+05
C-STB/DIS48     6.000000E+06            2.76000E+051.69000E+05
C-STB/DIS49     8.000000E+06            3.58000E+052.20000E+05
C-STB/DIS50     1.E+07      4.38000E+052.69000E+05
*
* DISTANCE, SIGMA_Y_D, SIGMA_Z_D, downwind distances (m), D-stability dispersion table
D-STB/DIS01     1.          0.147       0.079
D-STB/DIS02     1.4         0.199       0.106
D-STB/DIS03     2.          0.275       0.145
D-STB/DIS04     3.          0.397       0.208
D-STB/DIS05     4.          0.514       0.268
D-STB/DIS06     6.          0.742       0.383
D-STB/DIS07     8.          0.962       0.493
D-STB/DIS08     10.         1.18        0.601
D-STB/DIS09     14.         1.59        0.808
D-STB/DIS10     20.         2.2         1.11
D-STB/DIS11     30.         3.17        1.58
D-STB/DIS12     40.         4.12        2.04
D-STB/DIS13     60.         5.94        2.91
D-STB/DIS14     80.         7.7         3.75
D-STB/DIS15     100.        9.41        4.57
D-STB/DIS16     140.        12.8        6.29
D-STB/DIS17     200.        17.6        8.64
D-STB/DIS18     300.        25.4        12.2
D-STB/DIS19     400.        32.9        15.4
D-STB/DIS20     600.        47.5        21.2
D-STB/DIS21     800.        61.6        26.6
D-STB/DIS22     1000.       75.3        31.5
D-STB/DIS23     1400.       102.        39.9
D-STB/DIS24     2000.       141.        50.6
D-STB/DIS25     3000.       203.        65.4
D-STB/DIS26     4000.       263.        78.
D-STB/DIS27     6000.       380.        99.2
```

```
D-STB/DIS28             8000.           493.            117.
D-STB/DIS29             10000.          603.            133.
D-STB/DIS30             14000.          817.            161.
D-STB/DIS31             20000.          1130.           196.
D-STB/DIS32             30000.          1630.           244.
D-STB/DIS33             40000.          2110.           286.
D-STB/DIS34             60000.          3040.           355.
D-STB/DIS35             80000.          3940.           414.
D-STB/DIS36             1.00000E+054820.        466.
D-STB/DIS37             1.40000E+056530.        557.
D-STB/DIS38             2.00000E+059020.        672.
D-STB/DIS39             3.00000E+0513000.       831.
D-STB/DIS40             4.00000E+0516900.       967.
D-STB/DIS41             6.00000E+0524300.       1190.
D-STB/DIS42             8.00000E+0531500.       1390.
D-STB/DIS43             1.000000E+06            38600.          1560.
D-STB/DIS44             1.400000E+06            52300.          1860.
D-STB/DIS45             2.000000E+06            72100.          2230.
D-STB/DIS46             3.000000E+06            1.04000E+052760.
D-STB/DIS47             4.000000E+06            1.35000E+053200.
D-STB/DIS48             6.000000E+06            1.95000E+053950.
D-STB/DIS49             8.000000E+06            2.52000E+054580.
D-STB/DIS50             1.E+07          3.09000E+055140.
*
* DISTANCE, SIGMA_Y_E, SIGMA_Z_E, downwind distances (m), E-stability dispersion table
E-STB/DIS01             1.              0.105           0.063
E-STB/DIS02             1.4             0.142           0.0845
E-STB/DIS03             2.              0.196           0.115
E-STB/DIS04             3.              0.282           0.164
E-STB/DIS05             4.              0.366           0.211
E-STB/DIS06             6.              0.528           0.3
E-STB/DIS07             8.              0.684           0.385
E-STB/DIS08             10.             0.837           0.468
E-STB/DIS09             14.             1.13            0.628
E-STB/DIS10             20.             1.56            0.856
E-STB/DIS11             30.             2.26            1.22
E-STB/DIS12             40.             2.93            1.57
E-STB/DIS13             60.             4.22            2.23
E-STB/DIS14             80.             5.47            2.86
E-STB/DIS15             100.            6.69            3.48
E-STB/DIS16             140.            9.07            4.72
E-STB/DIS17             200.            12.5            6.36
E-STB/DIS18             300.            18.1            8.79
E-STB/DIS19             400.            23.4            11.
E-STB/DIS20             600.            33.8            14.8
E-STB/DIS21             800.            43.8            18.3
E-STB/DIS22             1000.           53.6            21.5
E-STB/DIS23             1400.           72.6            27.3
E-STB/DIS24             2000.           100.            34.4
E-STB/DIS25             3000.           144.            43.4
E-STB/DIS26             4000.           187.            50.5
E-STB/DIS27             6000.           270.            61.6
E-STB/DIS28             8000.           350.            70.3
E-STB/DIS29             10000.          428.            77.7
E-STB/DIS30             14000.          581.            89.8
E-STB/DIS31             20000.          801.            104.
E-STB/DIS32             30000.          1160.           122.
E-STB/DIS33             40000.          1500.           136.
E-STB/DIS34             60000.          2160.           159.
E-STB/DIS35             80000.          2800.           177.
E-STB/DIS36             1.00000E+053430.        191.
E-STB/DIS37             1.40000E+054650.        216.
E-STB/DIS38             2.00000E+056410.        245.
E-STB/DIS39             3.00000E+059250.        281.
E-STB/DIS40             4.00000E+0512000.       310.
E-STB/DIS41             6.00000E+0517300.       355.
E-STB/DIS42             8.00000E+0522400.       391.
E-STB/DIS43             1.000000E+06            27400.          421.
E-STB/DIS44             1.400000E+06            37200.          470.
E-STB/DIS45             2.000000E+06            51300.          528.
E-STB/DIS46             3.000000E+06            74000.          602.
E-STB/DIS47             4.000000E+06            95900.          660.
E-STB/DIS48             6.000000E+06            1.38000E+05752.
E-STB/DIS49             8.000000E+06            1.79000E+05824.
E-STB/DIS50             1.E+07          2.19000E+05884.
*
* DISTANCE, SIGMA_Y_F, SIGMA_Z_F, downwind distances (m), F-stability dispersion table
F-STB/DIS011.           0.0722          0.053
F-STB/DIS021.4          0.0978          0.0697
F-STB/DIS032.           0.135           0.0932
F-STB/DIS043.           0.195           0.13
F-STB/DIS054.           0.252           0.164
F-STB/DIS066.           0.364           0.228
F-STB/DIS078.           0.472           0.288
F-STB/DIS0810.          0.578           0.345
F-STB/DIS0914.          0.783           0.454
F-STB/DIS1020.          1.08            0.607
F-STB/DIS1130.          1.56            0.845
F-STB/DIS1240.          2.02            1.07
F-STB/DIS1360.          2.91            1.48
F-STB/DIS1480.          3.78            1.88
F-STB/DIS15100.         4.62            2.25
F-STB/DIS16140.         6.26            2.98
```

```
F-STB/DIS17200.          8.64          3.99
F-STB/DIS18300.          12.5          5.51
F-STB/DIS19400.          16.2          6.89
F-STB/DIS20600.          23.3          9.43
F-STB/DIS21800.          30.2          11.7
F-STB/DIS221000.         37.           13.9
F-STB/DIS231400.         50.1          17.9
F-STB/DIS242000.         69.1          22.3
F-STB/DIS253000.         99.7          27.7
F-STB/DIS264000.         129.          31.7
F-STB/DIS276000.         186.          37.8
F-STB/DIS288000.         242.          42.4
F-STB/DIS2910000.        296.          46.1
F-STB/DIS3014000.        401.          52.
F-STB/DIS3120000.        553.          58.7
F-STB/DIS3230000.        798.          66.8
F-STB/DIS3340000.        1030.         73.
F-STB/DIS3460000.        1490.         82.2
F-STB/DIS3580000.        1930.         89.1
F-STB/DIS361.00000E+052370.            94.8
F-STB/DIS371.40000E+053210.            104.
F-STB/DIS382.00000E+054420.            114.
F-STB/DIS393.00000E+056380.            126.
F-STB/DIS404.00000E+058270.            135.
F-STB/DIS416.00000E+0511900.           149.
F-STB/DIS428.00000E+0515500.           160.
F-STB/DIS431.000000E+06                18900.        168.
F-STB/DIS441.400000E+06                25700.        182.
F-STB/DIS452.000000E+06                35400.        197.
F-STB/DIS463.000000E+06                51100.        216.
F-STB/DIS474.000000E+06                66200.        230.
F-STB/DIS486.000000E+06                95500.        251.
F-STB/DIS498.000000E+06                1.24000E+05267.
F-STB/DIS501.E+07        1.51000E+05280.
*
* YSCALE, linear scaling factor for sigma-y
DPYSCALE001              1.
*
* ZSCALE, linear scaling factor for sigma-z
DPZSCALE001              1.
*
* DISPMD,  dispersion long-range model
DPDISPMD001              LRDIST
*
* MNDMOD, plume meander model (OLD, NEW, OFF)
PMMNDMOD001              NEW
*
* Form 'Plume Rise Scale Factor' Comment:
*
* SCLCRW, scaling factor for entrainment of buoyant plume
PRSCLCRW001              1.
*
* SCLADP, scaling factor for the A through D stability plume rise formula
PRSCLADP001              1.
*
* SCLEFP, scaling factor for the E through F stability plume rise formula
PRSCLEFP001              1.
*
* BUILDH, building height (m)
WEBUILDH001              20.
*
* SIGYINIT, initial value of sigma-y for each of the plumes (m)
SIGYINIT0019.2
*
* SIGZINIT, initial value of sigma-z for each of the plumes (m)
SIGZINIT0019.4
*
* ATNAM2, source term description
RDATNAM2001              '3600 Ci Cs-137 over 1 hour (1 Ci/s)'
*
* NUMREL, number of plumes
RDNUMREL001              1
*
* MAXRIS, index of risk-dominant plume segment
RDMAXRIS001              1
*
* REFTIM, representative time point for dispersion and radioactive decay
RDREFTIM001              0.5
*
* plume rise model  set to HEAT (DENSITY, HEAT)
RDPLMMOD001              HEAT
*
* PLHEAT, rate of heat release in each plume segment (W)
RDPLHEAT001              5.000000E+06
*
* BRGSMD, Briggs plume rise model (ORIGINAL, IMPROVED)
RDBRGSMD001              IMPROVED
*
* PLHITE, height of each plume segment at release (m)
RDPLHITE001              20.
*
* PLUDUR, duration of each plume segment (s)
RDPLUDUR001              3600.
```

```
*
* PDELAY, start time of each plume segment from accident initiation (s)
RDPDELAY001             0.
*
* PSDIST, particle size distribution of each element group
RDPSDIST001             0.092       0.146       0.141       0.144       0.112       0.08        0.072       0.071       0.071       0.071
*
* CORINV, inventory of each radionuclide present at the time of accident initiation (Bq)
RDCORINV001             Cs-137      3600.
*
* Form 'Inventory Scale Factor' Comment:
*
* CORSCA, scaling factor to adjust the core inventory
RDCORSCA001             1.
*
* Form 'Daughter Ingrowth Flag' Comment:
*
* APLFRC, Specifies how release fractions are applied to daughter ingrowth products (PARENT, PROGENY)
RDAPLFRC001             PARENT
*
* Form 'Release Fractions' Comment:
*
* RELFRC, release fractions for each of the plume segments for each chemical group
RDRELFRC001             1.
*
* ENDAT1, set to TRUE if only running ATMOS
OCENDAT1001             .TRUE.
*
* Form 'Output Control' Comment:
*
* IDEBUG, specifies set of debug results to report
OCIDEBUG001             0
*
* NUCOUT, name of the nuclide to be listed on the dispersion listings
OCNUCOUT001             Cs-137
*
* ATDMODL, atmospheric transport model
ISATDMODL01             GAUSSIAN
*
* METCOD, meteorological sampling model (1, 2, 3, 4, or 5)
M1METCOD001             4
*
* BNDMXH, boundary weather mixing layer height (m)
M2BNDMXH001             1500.
*
* IBDSTB, boundary weather stability class index
M2IBDSTB001             6
*
* BNDRAN, boundary weather rain rate (mm/hr)
M2BNDRAN001             0.
*
* BNDWND, boundary weather wind speed (m/sec)
M2BNDWND001             2.
*
* ISTRDY, start day of the weather sequence
M3ISTRDY001             1
*
* ISTRHR, start hour of the weather sequence
M3ISTRHR001             1
*
* MAXHGT, determines mixing height model
M1MAXHGT001             DAY_ONLY
*
* NUM0,  used for no input, always 0
TYPE0NUMBER             0
*
* NUM0, number of results
TYPE0NUMBER             10
*
* INDREL, INDRAD, CCDF, ATMOS release and spatial interval
TYPE0OUT001             1           1           NONE
TYPE0OUT002             1           2           NONE
TYPE0OUT003             1           3           NONE
TYPE0OUT004             1           4           NONE
TYPE0OUT005             1           5           NONE
TYPE0OUT006             1           6           NONE
TYPE0OUT007             1           7           NONE
TYPE0OUT008             1           8           NONE
TYPE0OUT009             1           9           NONE
TYPE0OUT010             1           10          NONE
*
* NUM0_HY, used for no input, always 0
TYPE0_HYNUM             0
```

APPENDIX D. QUIC INPUT FILES

Representative input files used in the evaluation of the test cases are shown below to illustrate implementation. The reader is directed to the code user manual to interpret the files.

D.1. Weather Input

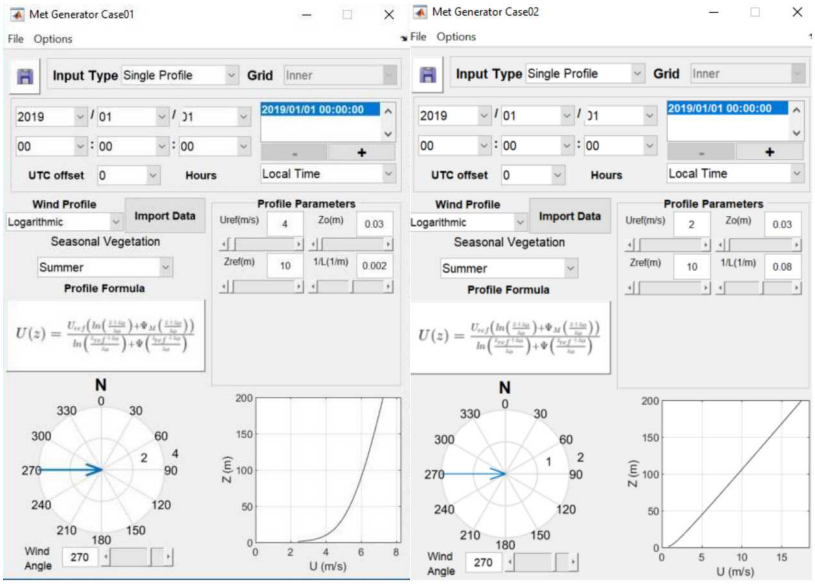

D.2. Weather Input – Increased Dispersion

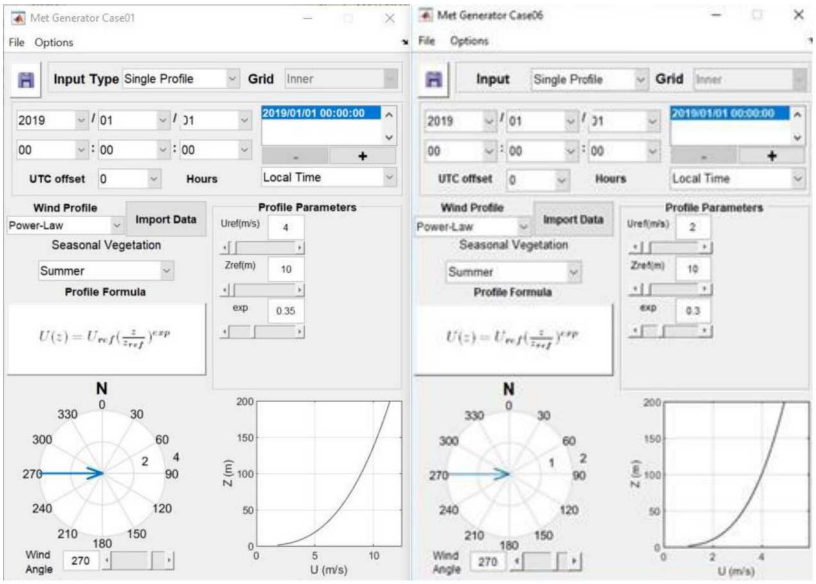

D.3. Simulation Parameters

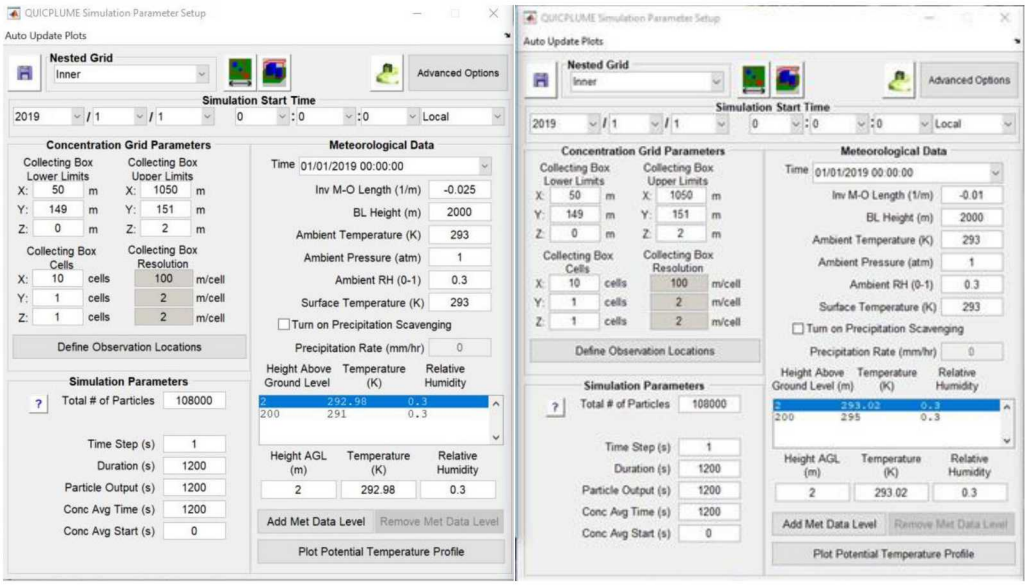

D.4. Source Parameters

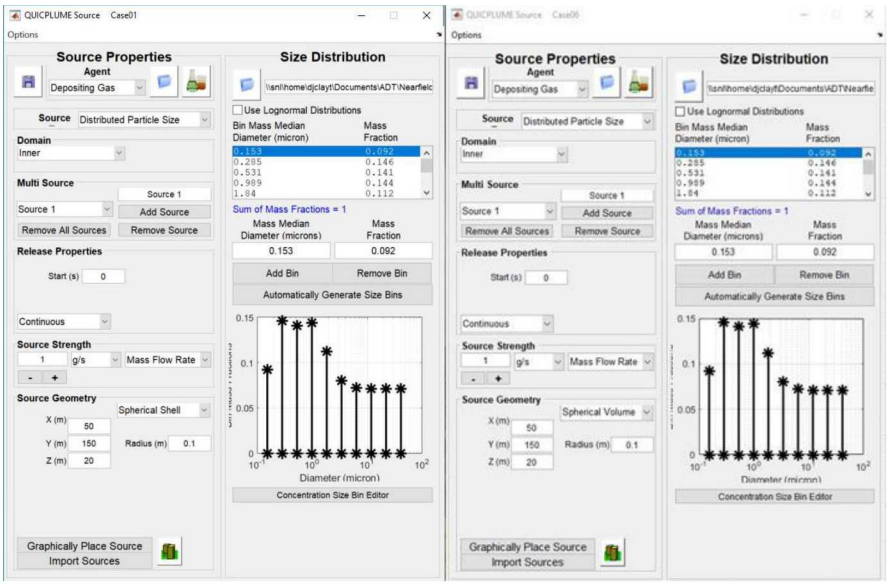

DISTRIBUTION

Email—External

Name	Company Email Address	Company Name
Jon Barr	Jonathan.Barr@nrc.gov	U.S. NRC
Keith Compton	Keith.Compton@nrc.gov	U.S. NRC
Salman Haq	Salman.Haq@nrc.gov	U.S. NRC

Email—Internal

Name	Org.	Sandia Email Address
Daniel Clayton	08843	djclayt@sandia.gov
Nathan Bixler	08855	nbixler@sandia.gov
John Fulton	08855	jdfulto@sandia.gov
Technical Library	01177	libref@sandia.gov

This page left blank

This page left blank

Sandia National Laboratories

Sandia National Laboratories is a multimission laboratory managed and operated by National Technology & Engineering Solutions of Sandia LLC, a wholly owned subsidiary of Honeywell International Inc. for the U.S. Department of Energy's National Nuclear Security Administration under contract DE-NA0003525.